Thin Film Materials and their Applications

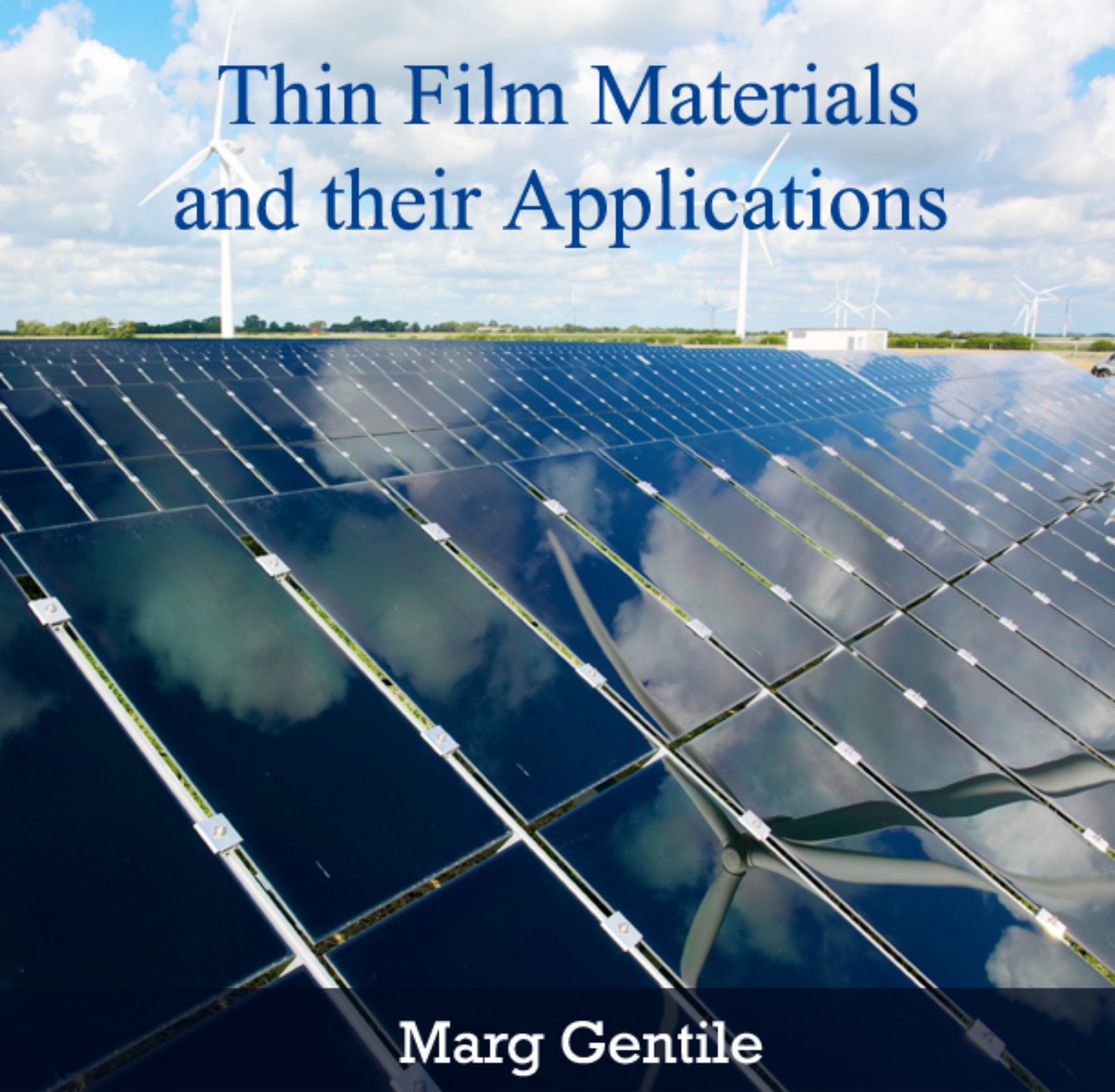

Marg Gentile

First Edition, 2012

ISBN 978-81-323-2907-7

Published by:
Orange Apple
4735/22 Prakashdeep Bldg,
Ansari Road, Darya Ganj,
Delhi - 110002
Email: info@wtbooks.com

Table of Contents

Chapter- 1

Thin Film

A **thin film** is a layer of material ranging from fractions of a nanometre (monolayer) to several micrometres in thickness. Electronic semiconductor devices and optical coatings are the main applications benefiting from thin film construction.

A familiar application of thin films is the household mirror which typically has a thin metal coating on the back of a sheet of glass to form a reflective interface. The process of silvering was once commonly used to produce mirrors. A very thin film coating (less than a nanometre) is used to produce two-way mirrors.

The performance of optical coatings (e.g. antireflective, or AR, coatings) are typically enhanced when the thin film coating consists of multiple layers having varying thicknesses and refractive indices. Similarly, a periodic structure of alternating thin films of different materials may collectively form a so-called superlattice which exploits the phenomenon of quantum confinement by restricting electronic phenomena to two-dimensions.

Work is being done with ferromagnetic and ferroelectric thin films for use as computer memory. It is also being applied to pharmaceuticals, via thin film drug delivery. Thin-films are used to produce thin-film batteries. Thin film application also be adopted on Dye-sensitized solar cell.

Ceramic thin films are in wide use. The relatively high hardness and inertness of ceramic materials make this type of thin coating of interest for protection of substrate materials against corrosion, oxidation and wear. In particular, the use of such coatings on cutting tools can extend the life of these items by several orders of magnitude.

Research is being done on a new class of thin film inorganic oxide materials, called amorphous heavy-metal cation multicomponent oxide, which could be used to make transparent transistors that are inexpensive, stable, and environmentally benign.

Deposition

The act of applying a thin film to a surface is *thin-film deposition* - any technique for depositing a thin film of material onto a substrate or onto previously deposited layers. "Thin" is a relative term, but most deposition techniques control layer thickness within a few tens of nanometres. Molecular beam epitaxy allows a single layer of atoms to be deposited at a time.

It is useful in the manufacture of optics (for reflective, anti-reflective coatings or self-cleaning glass, for instance), electronics (layers of insulators, semiconductors, and conductors form integrated circuits), packaging (i.e., aluminium-coated PET film), and in contemporary art. Similar processes are sometimes used where thickness is not important: for instance, the purification of copper by electroplating, and the deposition of silicon and enriched uranium by a CVD-like process after gas-phase processing.

Deposition techniques fall into two broad categories, depending on whether the process is primarily chemical or physical.

Chemical deposition

Here, a fluid precursor undergoes a chemical change at a solid surface, leaving a solid layer. An everyday example is the formation of soot on a cool object when it is placed inside a flame. Since the fluid surrounds the solid object, deposition happens on every surface, with little regard to direction; thin films from chemical deposition techniques tend to be *conformal*, rather than *directional*.

Chemical deposition is further categorized by the phase of the precursor:

- **Plating** relies on liquid precursors, often a solution of water with a salt of the metal to be deposited. Some plating processes are driven entirely by reagents in the solution (usually for noble metals), but by far the most commercially important process is electroplating. It was not commonly used in semiconductor processing for many years, but has seen a resurgence with more widespread use of chemical-mechanical polishing techniques.

- **Chemical solution deposition** (CSD) uses a liquid precursor, usually a solution of organometallic powders dissolved in an organic solvent. This is a relatively inexpensive, simple thin film process that is able to produce stoichiometrically accurate crystalline phases. This technique is also known as **Sol-Gel** because the 'sol' (or solution) gradually evolves towards the formation of a gel-like diphasic system.

- **Chemical vapor deposition** (CVD) generally uses a gas-phase precursor, often a halide or hydride of the element to be deposited. In the case of **MOCVD**, an organometallic gas is used. Commercial techniques often use very low pressures of precursor gas.

- **Plasma enhanced CVD** (PECVD) uses an ionized vapor, or plasma, as a precursor. Unlike the soot example above, commercial PECVD relies on electromagnetic means (electric current, microwave excitation), rather than a chemical reaction, to produce a plasma.

Physical deposition

Physical deposition uses mechanical, electromechanical or thermodynamic means to produce a thin film of solid. An everyday example is the formation of frost. Since most engineering materials are held together by relatively high energies, and chemical reactions are not used to store these energies, commercial physical deposition systems tend to require a low-pressure vapor environment to function properly; most can be classified as **physical vapor deposition** (PVD).

The material to be deposited is placed in an energetic, entropic environment, so that particles of material escape its surface. Facing this source is a cooler surface which draws energy from these particles as they arrive, allowing them to form a solid layer. The whole system is kept in a vacuum deposition chamber, to allow the particles to travel as freely as possible. Since particles tend to follow a straight path, films deposited by physical means are commonly *directional*, rather than *conformal*.

Examples of physical deposition include:

- A **thermal evaporator** uses an electric resistance heater to melt the material and raise its vapor pressure to a useful range. This is done in a high vacuum, both to allow the vapor to reach the substrate without reacting with or scattering against other gas-phase atoms in the chamber, and reduce the incorporation of impurities from the residual gas in the vacuum chamber. Obviously, only materials with a much higher vapor pressure than the heating element can be deposited without contamination of the film. Molecular beam epitaxy is a particularly sophisticated form of thermal evaporation.
    - An **electron beam evaporator** fires a high-energy beam from an electron gun to boil a small spot of material; since the heating is not uniform, lower vapor pressure materials can be deposited. The beam is usually bent through an angle of 270° in order to ensure that the gun filament is not directly exposed to the evaporant flux. Typical deposition rates for electron beam evaporation range from 1 to 10 nanometres per second.

- **Sputtering** relies on a plasma (usually a noble gas, such as argon) to knock material from a "target" a few atoms at a time. The target can be kept at a relatively low temperature, since the process is not one of evaporation, making this one of the most flexible deposition techniques. It is especially useful for compounds or mixtures, where different components would otherwise tend to evaporate at different rates. Note, sputtering's step coverage is more or less conformal.It is also widely used in the optical media. The manufacturing of all formats of CD, DVD, and BD are done with the help of this technique. It is a fast

technique and also it provides a good thickness control. Presently, nitrogen and oxygen gases are also being used in sputtering.

- **Pulsed laser deposition** systems work by an ablation process. Pulses of focused laser light vaporize the surface of the target material and convert it to plasma; this plasma usually reverts to a gas before it reaches the substrate.

- **Cathodic arc deposition** (arc-PVD) which is a kind of ion beam deposition where an electrical arc is created that literally blasts ions from the cathode. The arc has an extremely high power density resulting in a high level of ionization (30-100%), multiply charged ions, neutral particles, clusters and macro-particles (droplets). If a reactive gas is introduced during the evaporation process, dissociation, ionization and excitation can occur during interaction with the ion flux and a compound film will be deposited.

- **Electrohydrodynamic deposition (Electrospray deposition)** is a relatively new process of thin film deposition. The liquid to be deposited, either in the form of nano-particle solution or simply a solution, is fed to a small capillary nozzle (usually metallic) which is connected to a high power source. The substrate on which the film has to be deposited is connected to the ground terminal of the power source. Through the influence of electric field, the liquid coming out of the nozzle takes a conical shape (Taylor cone) and at the apex of the cone a thin jet emanates which disintegrates into very fine and small positively charged droplets under the influence of Rayleigh charge limt. The droplets keep getting smaller and smaller and ultimately get deposited on the substrate as a uniform thin layer.

Other deposition processes

Some methods fall outside these two categories, relying on a mixture of chemical and physical means:

- In **reactive sputtering**, a small amount of some non-noble gas such as oxygen or nitrogen is mixed with the plasma-forming gas. After the material is sputtered from the target, it reacts with this gas, so that the deposited film is a different material, i.e. an oxide or nitride of the target material.

- In **molecular beam epitaxy** (MBE), slow streams of an element can be directed at the substrate, so that material deposits one atomic layer at a time. Compounds such as gallium arsenide are usually deposited by repeatedly applying a layer of one element (i.e., gallium), then a layer of the other (i.e., As), so that the process is chemical, as well as physical. The beam of material can be generated by either physical means (that is, by a furnace) or by a chemical reaction (chemical beam epitaxy).

- In **topotaxy**, a specialized technique similar to epitaxy, thin film crystal growth occurs in three dimensions due to the crystal structure similarities (either

heterotopotaxy or homotopotaxy) between the substrate crystal and the growing thin film material.

Thin-film photovoltaic cells

Thin-film technologies are also being developed as a means of substantially reducing the cost of photovoltaic (PV) systems. The rationale for this is that thin-film modules are cheaper to manufacture owing to their reduced material costs, energy costs, handling costs and capital costs. This is especially represented in the use of printed electronics (roll-to-roll) processes.

Thin films belong to the second and third photovoltaic cell generations.

Thin-film batteries

Thin-film printing technology is being used to apply solid-state lithium polymers to a variety of substrates to create unique batteries for specialized applications. Thin-film batteries can be deposited directly onto chips or chip packages in any shape or size. Flexible batteries can be made by printing onto plastic, thin metal foil, or paper.

Chapter- 2

Thin Film Solar Cell

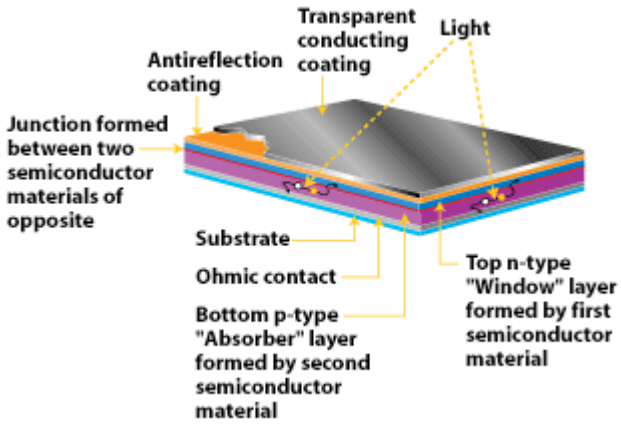

Cross-section of thin film polycrystalline solar cell.

A **thin-film solar cell** (TFSC), also called a **thin-film photovoltaic cell** (TFPV), is a solar cell that is made by depositing one or more thin layers (thin film) of photovoltaic material on a substrate. The thickness range of such a layer is wide and varies from a few nanometers to tens of micrometers.

Many different photovoltaic materials are deposited with various deposition methods on a variety of substrates. Thin-film solar cells are usually categorized according to the photovoltaic material used:

- Amorphous silicon (a-Si) and other thin-film silicon (TF-Si)
- Cadmium Telluride (CdTe)
- Copper indium gallium selenide (CIS or CIGS)
- Dye-sensitized solar cell (DSC) and other organic solar cells

$$\begin{pmatrix}\mathrm{Cu}\\ \mathrm{Ag}\\ \mathrm{Au}\end{pmatrix}\begin{pmatrix}\mathrm{Al}\\ \mathrm{Ga}\\ \mathrm{In}\end{pmatrix}\begin{pmatrix}\mathrm{S}\\ \mathrm{Se}\\ \mathrm{Te}\end{pmatrix}_2$$

Possible combinations of Group-(I, III, VI) elements in the periodic table that yield a compound showing photovoltaic effect (*Cu, Ag, Au* | *Al, Ga, In* | *S, Se, Te*).

History

Initially appearing as small strips powering hand-held calculators, thin-film PV is now available in very large modules used in sophisticated building-integrated installations and vehicle charging systems. GBI Research projects thin film production to grow 24% from 2009 levels and to reach 22,214 MW in 2020. "Expectations are that in the long-term, thin-film solar PV technology would surpass dominating conventional solar PV technology, thus enabling the long sought-after grid parity objective."

Thin-film silicon

A silicon thin-film cell uses amorphous (a-Si or a-Si:H), protocrystalline, nanocrystalline (nc-Si or nc-Si:H) or black silicon. Thin-film silicon is opposed to *wafer* (or *bulk*) silicon (monocrystalline or polycrystalline).

Design and fabrication

The silicon is mainly deposited by chemical vapor deposition, typically plasma-enhanced (PE-CVD), from silane gas and hydrogen gas. Other deposition techniques being investigated include sputtering and hot wire techniques.

The silicon is deposited on glass, plastic or metal which has been coated with a layer of transparent conducting oxide (TCO).

A p-i-n structure is usually used, as opposed to an n-i-p structure. This is because the mobility of electrons in a-Si:H is roughly 1 or 2 orders of magnitude larger than that of holes, and thus the collection rate of electrons moving from the p- to n-type contact is better than holes moving from p- to n-type contact. Therefore, the p-type layer should be placed at the top where the light intensity is stronger, so that the majority of the charge carriers crossing the junction would be electrons..

Micromorphous silicon

Micromorphous silicon module technology combines two different types of silicon, amorphous and microcrystalline, in a top and a bottom photovoltaic cell. Use of

protocrystalline silicon for the intrinsic layer has shown to optimize the open circuit voltage of an a-Si photovoltaic cell.

Efficiency

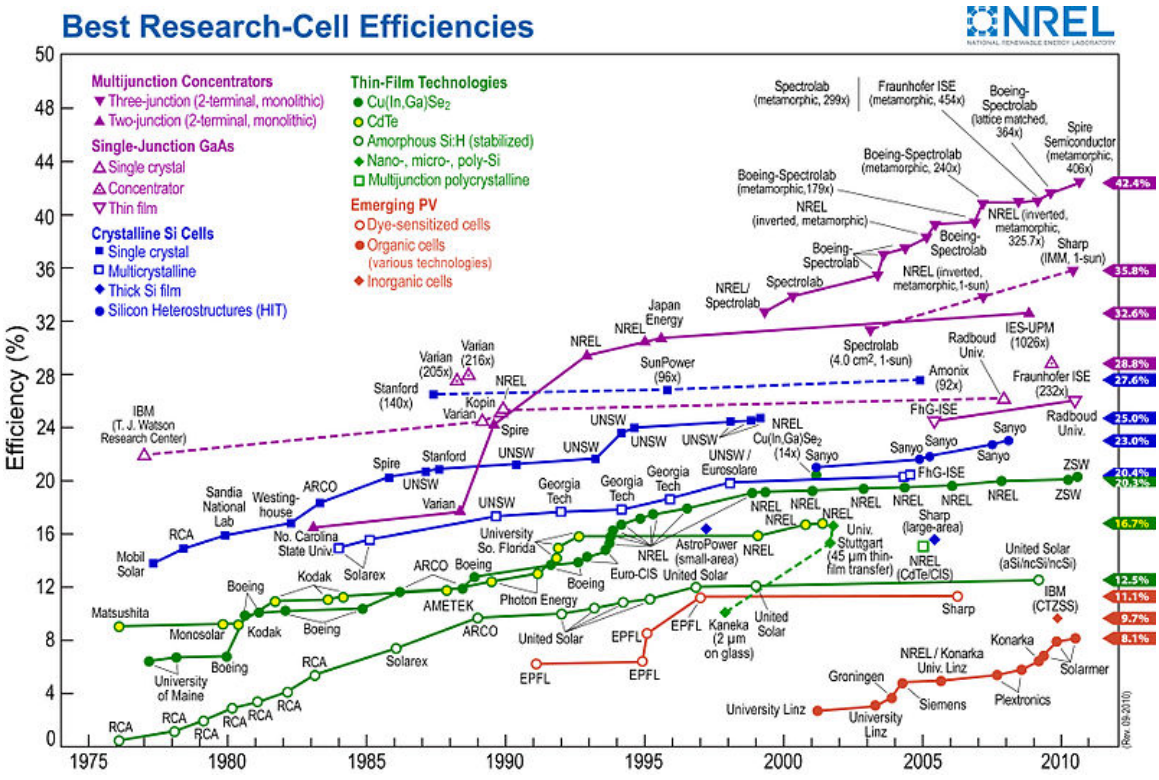

Solar Cell Efficiencies

These types of silicon present dangling and twisted bonds, which results in deep defects (energy levels in the bandgap) as well as deformation of the valence and conduction bands (band tails). The solar cells made from these materials tend to have lower energy conversion efficiency than bulk silicon (also called crystalline or wafer silicon), but are also less expensive to produce. The quantum efficiency of thin-film solar cells is also lower due to reduced number of collected charge carriers per incident photon.

Amorphous silicon has a higher bandgap (1.7 eV) than crystalline silicon (c-Si) (1.1 eV), which means it absorbs the visible part of the solar spectrum more strongly than the infrared portion of the spectrum. As nc-Si has about the same bandgap as c-Si, the nc-Si and a-Si can advantageously be combined in thin layers, creating a layered cell called a *tandem cell*. The top cell in a-Si absorbs the visible light and leaves the infrared part of the spectrum for the bottom cell in nc-Si.

Recently, solutions to overcome the limitations of thin-film silicon have been developed. Light trapping schemes where the incoming light is obliquely coupled into the silicon and the light traverses the film several times enhance the absorption of sunlight in the films.

Thermal processing techniques enhance the crystallinity of the silicon and pacify electronic defects.

Building integrated photovoltaics

Thin film photovoltaic panels being installed onto a roof

Thin film solar panels are commercially available for installation onto the roofs of buildings, either applied onto the finished roof, or integrated into the roof covering. The advantage over tradition PV panels is that they are very low in weight, are not subject to wind lifting, and can be walked on (with care). The comparable disadvantages are increased cost and reduced efficiency.

A silicon thin film technology is being developed for building integrated photovoltaics (BIPV) in the form of semitransparent solar cells which can be applied as window glazing. These cells function as window tinting while generating electricity.

Organic solar cells

The Organic solar cell is another alternative to the more conventional materials used to make photovoltaics. Although a very novel technology it is promising since it offers a very low cost solution.

Efficiencies, volumes and prices

Since the invention of the first modern silicon solar cell in 1954, incremental improvements have resulted in modules capable of converting 12 to 18 percent of solar radiation into electricity. The performance and potential of thin-film materials are high, reaching cell efficiencies of 12%-20%; prototype module efficiencies of 7%-13%; and production modules in the range of 9%. Future module efficiencies are expected to climb close to the state-of-the-art of today's best cells, or to about 10-16%.

Annual manufacturing volume in the United States has grown from about 12 megawatts (MW) per year in 2003 to more than 20 MW/yr in 2004; 40-50 MW/yr production levels are expected in 2005 with continued rapid growth in the years after that.

Costs are expected to drop to below $\$100/m^2$ in volume production, and could reach even lower levels—well under $\$50/m^2$, the DOE/NREL goal for thin films—when fully optimized. At these levels, thin-film modules will cost less than fifty cents per watt to manufacture, opening new markets such as cost-effective distributed power and utility production to thin-film electricity generation.

As crystalline silicon price rose, the production cost of silicon-based solar cell module in 2008 was at some point 4-5 times higher than that of thin film modules. Thin-film producers still enjoy in 2009 price advantage as its production cost is 20% less than that of silicon modules.It is expected that the production cost of thin-film will continue dropping (40% less than silicon), as Chinese producers are now putting more resources into R&D and partnering with manufacturing equipment suppliers

Production, cost and market

In recent years, the manufacturers of thin-film solar modules are bringing costs down and gaining in competitive strength through advanced thin film technology. However, the traditional crystalline silicon technologies will not give up their market positions for a few years because they still hold considerable development potential in terms of the cost. Efficiency of thin film solar is considerably lower and thin film solar manufacturing equipment suppliers intend to score costs of below USD 1/W, and Anwell Technologies Limited claimed that they intend to bring it down further to USD 0.5/W. Those equipment suppliers have been doing R&D for micro-morphous silicon modules since 2008. This technology represents a development based on the thin-film panels made of ordinary amorphous silicon marketed at present that brings higher cell efficiency by depositing an additional absorber layer made of micro crystalline silicon on the amorphous layer. Some equipment suppliers even claim that there will be machinery in

market to manufacture these new modules at $0.70. With such potential of further development of thin film solar technology, the European Photovoltaic Industry Association (EPIA) expects that manufacturing capacities for these technologies will double to over 4GW by 2010 representing a market share of around 20%.

Installations

First Solar, the CdTe thin-film manufacturer stated that "at the end of 2007, over 300 MW of First Solar PV modules had been installed worldwide." Below is a list of several recent installations:

- Since 16 October 2008, Germany's largest thin-film pitched roof system, constructed by Riedel Recycling, has been in operation and producing solar power in Moers near Duisburg. Over eleven thousand cadmium telluride modules, from First Solar, deliver a total of 837 kW.
- First Solar recently completed a 2.4 MW rooftop installation as part of Southern California Edison program to install 250 MW of rooftop solar panels throughout Southern California over by 2013.
- First Solar announced a 7.5 MW system to be installed in Blythe, CA, where the California Public Utilities Commission has accepted a 12 ¢/kWh power purchase agreement with First Solar (after the application of all incentives).
- Construction of a 10 MW plant in the Nevada desert began in July 2008. First Solar is partnering with Sempra Generation, which will own and operate the PV power-plant, being built next to their natural gas plant.
- Stadtwerke Trier (SWT) in Trier, Germany is expected to produce over 9 GWh annually
- A 40 MW system is being installed by Juwi in Waldpolenz Solar Park, Germany. At the time of its announcement, it was both the largest planned and lowest cost PV system in the world. The price of 3.25 euros translated then (when the euro was equal to US$1.3) to $4.2 per installed watt.
- 4.8KW of thin film flexible solar panels manufactured by Uni-Solar Ovonic installed on a South Beach hurricane-prone residence in 2008.

Denver-based Conergy Americas and officials at California's South San Joaquin Irrigation District (SSJID) have installed what is believed to be the world's first single-axis solar tracking system featuring thin-film photovoltaic cells.

Chapter- 3

Thin-Film Optics and Amorphous Silicon

Thin-film optics

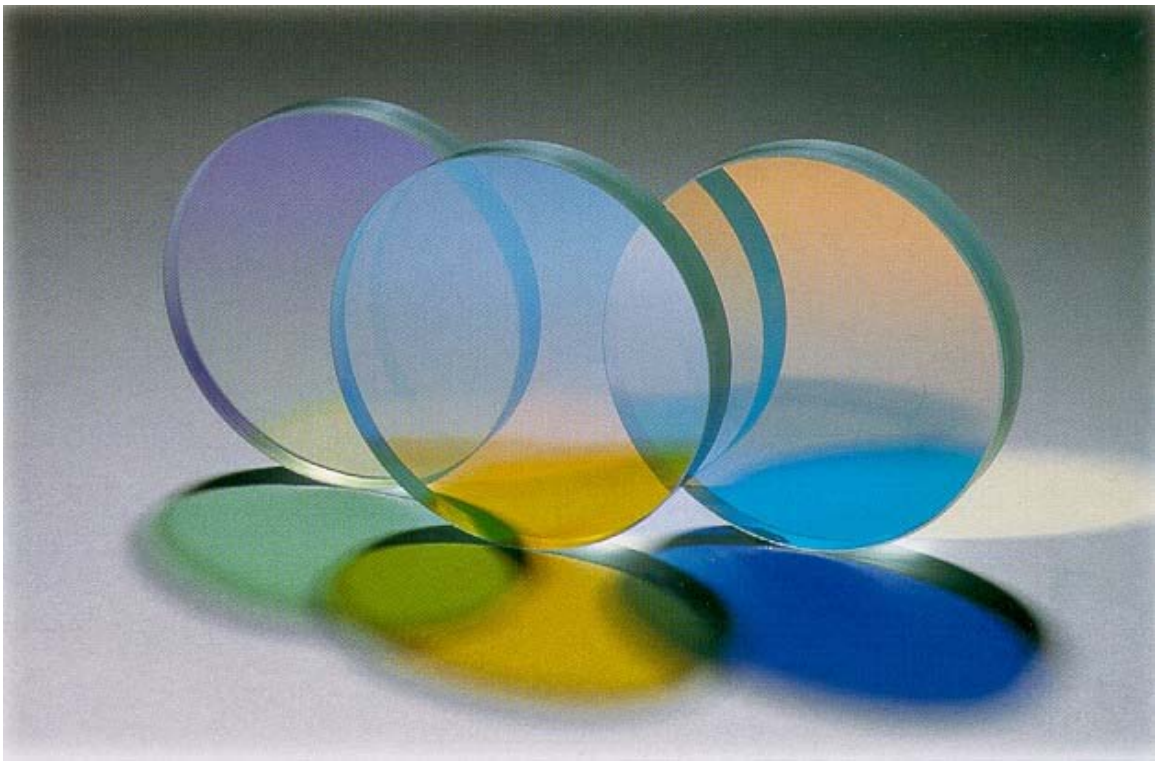

Dichroic filters are created using thin film optics.

A pattern of coloured light formed by interference between white light being reflected from the surface of a thin film of diesel fuel on the surface of water, and the diesel-water interface.

Thin-film optics is the branch of optics that deals with very thin structured layers of different materials. In order to exhibit thin-film optics, the thickness of the layers of material must be on the order of the wavelengths of visible light (about 500 nm). Layers at this scale can have remarkable reflective properties due to light wave interference and the difference in refractive index between the layers, the air, and the substrate. These effects alter the way the optic reflects and transmits light. This effect, known as thin-film interference, is observable in soap bubbles and oil slicks.

More general periodic structures, not limited to planar layers, are known as photonic crystals.

In manufacturing, thin film layers can be achieved through the deposition of one or more thin layers of material onto a substrate (usually glass). This is most often done using a

physical vapor deposition process, such as evaporation or sputter deposition, or a chemical process such as chemical vapor deposition.

Thin films are used to create optical coatings. Examples include low-emissivity panes of glass for houses and cars, anti-reflective coatings on glasses, reflective baffles on car headlights, and for high precision optical filters and mirrors. Another application of these coatings is spatial filtering.

Thin-film layers are common in the natural world. Their effects produce colors seen in soap bubbles and oil slicks, as well as in some animals. For example, the light collecting *tapetum lucidum* of many nocturnal species and the photophores of bioluminescent squid (e.g. the Bobtail squid). In many cases, iridescent colors that were once thought to result from planar layers, such as in opals, peacocks, and the Blue Morpho butterfly, turn out to result from more complex periodic photonic-crystal structures.

Amorphous silicon

Amorphous silicon (**a-Si** or **α-Si**) is the non-crystalline allotropic form of silicon. It can be deposited in thin films at low temperatures onto a variety of substrates, offering some unique capabilities for a variety of electronics.

Description

Silicon is a fourfold coordinated atom that is normally tetrahedrally bonded to four neighboring silicon atoms. In crystalline silicon this tetrahedral structure continues over a large range, thus forming a well-ordered crystal lattice.

In amorphous silicon this long range order is not present. Rather, the atoms form a continuous random network. Moreover, not all the atoms within amorphous silicon are fourfold coordinated. Due to the disordered nature of the material some atoms have a dangling bond. Physically, these dangling bonds represent defects in the continuous random network and may cause anomalous electrical behavior.

If desired, the material can be passivated by hydrogen, which bonds to the dangling bonds and can reduce the dangling bond density by several orders of magnitude. Hydrogenated amorphous silicon (a-Si:H) has a sufficiently low amount of defects to be used within devices. However, the hydrogen is unfortunately associated with light induced degradation of the material, termed the Staebler-Wronski Effect.

Amorphous silicon and carbon

Amorphous alloys of silicon and carbon (amorphous silicon carbide, also hydrogenated, a-$Si_{1-x}C_x$:H) are an interesting variant. Introduction of carbon atoms adds extra degrees of freedom for control of the properties of the material. The film could also be made transparent to visible light.

Increasing concentrations of carbon in the alloy widen the electronic gap between conduction and valence bands (also called "optical gap" and bandgap). This can potentially increase the light efficiency of solar cells made with amorphous silicon carbide layers. On the other hand, the electronic properties as a semiconductor (mainly electron mobility), are adversely affected by the increasing content of carbon in the alloy, due to the increased disorder in the atomic network.

Several studies are found in the scientific literature, mainly investigating the effects of deposition parameters on electronic quality, but practical applications of amorphous silicon carbide in commercial devices are still lacking.

Applications

While a-Si suffers from lower electronic performance compared to c-Si, it is much more flexible in its applications. For example, a-Si layers can be made thinner than c-Si, which may produce savings on silicon material cost.

One further advantage is that a-Si can be deposited at very low temperatures, e.g., as low as 75 degrees Celsius. This allows for deposition on not only glass, but plastic as well, making it a candidate for a roll-to-roll processing technique. Once deposited, a-Si can be doped in a fashion similar to c-Si, to form p-type or n-type layers and ultimately to form electronic devices.

Another advantage is that a-Si can be deposited over large areas by PECVD. The design of the PECVD system has great impact on the production cost of such panel, therefore most equipment suppliers put their focus on the design of PECVD for higher throughout, that leads to lower manufacturing cost.

Amorphous silicon has become the material of choice for the active layer in thin-film transistors (TFTs), which are most widely used in large-area electronics applications, mainly for liquid-crystal displays (LCDs).

Solar cells

a-Si has been used as a photovoltaic solar cell material for calculators for some time. Although they are lower performance than traditional c-Si solar cells, this is not important in calculators, which use very low power. a-Si's ability to be easily deposited during construction more than makes up for any downsides.

More recently, improvements in a-Si construction techniques have made them more attractive for large-area solar cell use as well. Here their lower inherent efficiency is made up, at least partially, by their thinness - higher efficiencies can be reached by stacking several thin-film cells on top of each other, each one tuned to work well at a specific frequency of light. This approach is not applicable to c-Si cells, which are thick as a result of their construction technique and are therefore largely opaque, blocking light from reaching other layers in a stack.

The main advantage of a-Si in large scale production is not efficiency, but cost. a-Si cells use approximately 1% of the silicon needed for typical c-Si cells, and the cost of the silicon is by far the largest factor in cell cost. However, the higher costs of manufacture due to the multi-layer construction have, to date, make a-Si unattractive except in roles where their thinness or flexibility are an advantage.

Typically, amorphous silicon thin-film cells use a p-i-n structure. Typical panel structure includes front side glass, TCO, thin film silicon, back contact, polyvinyl butyral (PVB) and back side glass. Uni-Solar produces a version of flexible backings, used in roll-on roofing products.

Microcrystalline and Micromorphous Silicon

Microcrystalline silicon (also called nanocrystalline silicon) is amorphous silicon, but also contains small crystals. It absorbs a broader spectrum of light and is flexible.

Micromorphous silicon module technology combines two different types of silicon, amorphous and microcrystalline silicon, in a top and a bottom photovoltaic cell. Sharp produces cells using this system in order to more efficiently capture blue light, increasing the efficiency of the cells during the time where there is no direct sunlight falling on them. Protocrystalline silicon is often used to optimize the open circuit voltage of a-Si photovoltaics.

Large-scale production

Xunlight Corporation, which has received over $40 million of institutional investments, has completed the installation of its first 25 MW wide-web, roll-to-roll photovoltaic manufacturing equipment for the production of thin-film silicon PV modules. Anwell Technologies has also completed the installation of its first 40 MW a-Si thin film solar panel manufacturing facility in Henan with its in-house designed multi-substrate-multi-chamber PECVD equipment.

Chapter- 4

Chemical Vapor Deposition

DC plasma (violet) enhances the growth of carbon nanotubes in this laboratory-scale PECVD apparatus.

Chemical vapor deposition (CVD) is a chemical process used to produce high-purity, high-performance solid materials. The process is often used in the semiconductor industry to produce thin films. In a typical CVD process, the wafer (substrate) is exposed to one or more volatile precursors, which react and/or decompose on the substrate surface to produce the desired deposit. Frequently, volatile by-products are also produced, which are removed by gas flow through the reaction chamber.

Microfabrication processes widely use CVD to deposit materials in various forms, including: monocrystalline, polycrystalline, amorphous, and epitaxial. These materials include: silicon, carbon fiber, carbon nanofibers, filaments, carbon nanotubes, SiO_2, silicon-germanium, tungsten, silicon carbide, silicon nitride, silicon oxynitride, titanium nitride, and various high-k dielectrics. The CVD process is also used to produce synthetic diamonds.

Types of chemical vapor deposition

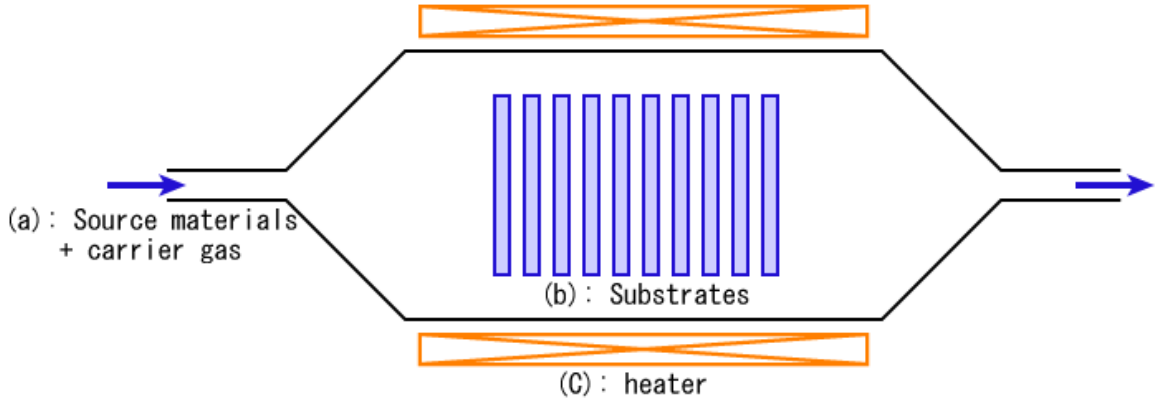

Hot-wall thermal CVD (batch operation type)

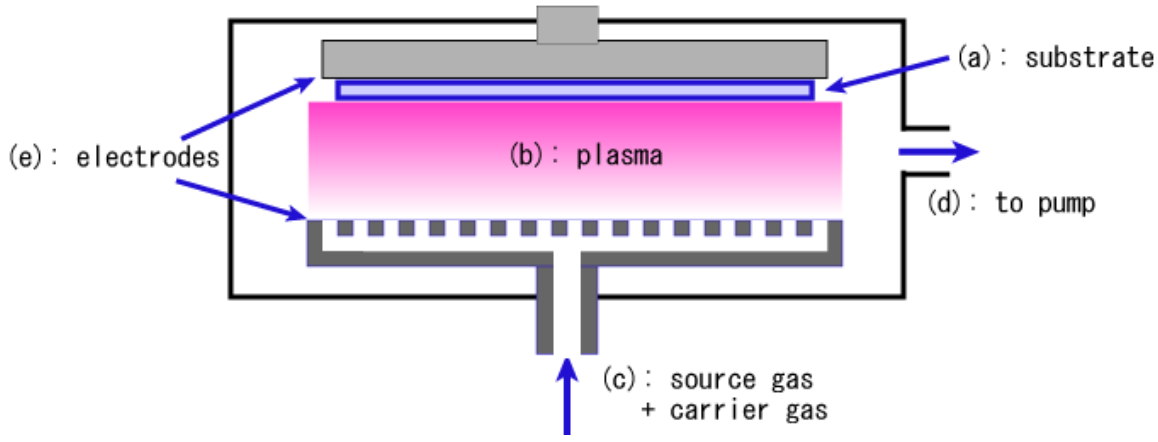

Plasma assisted CVD

A number of forms of CVD are in wide use and are frequently referenced in the literature. These processes differ in the means by which chemical reactions are initiated (e.g., activation process) and process conditions.

- Classified by operating pressure
  - *Atmospheric pressure CVD* (APCVD) - CVD processes at atmospheric pressure.
  - *Low-pressure CVD* (LPCVD) - CVD processes at subatmospheric pressures. Reduced pressures tend to reduce unwanted gas-phase reactions and improve film uniformity across the wafer. Most modern CVD processes are either LPCVD or UHVCVD.
  - *Ultrahigh vacuum CVD* (UHVCVD) - CVD processes at a very low pressure, typically below 10^{-6} Pa (~10^{-8} torr). Note that in other fields, a lower division between high and ultra-high vacuum is common, often 10^{-7} Pa.
- Classified by physical characteristics of vapor
  - *Aerosol assisted CVD* (AACVD) - A CVD process in which the precursors are transported to the substrate by means of a liquid/gas aerosol, which can be generated ultrasonically. This technique is suitable for use with non-volatile precursors.
  - *Direct liquid injection CVD* (DLICVD) - A CVD process in which the precursors are in liquid form (liquid or solid dissolved in a convenient solvent). Liquid solutions are injected in a vaporization chamber towards injectors (typically car injectors). Then the precursor vapors are transported to the substrate as in classical CVD process. This technique is suitable for use on liquid or solid precursors. High growth rates can be reached using this technique.
- Plasma methods
  - *Microwave plasma-assisted CVD* (MPCVD)
  - *Plasma-Enhanced CVD* (PECVD) - CVD processes that utilize plasma to enhance chemical reaction rates of the precursors. PECVD processing allows deposition at lower temperatures, which is often critical in the manufacture of semiconductors.
  - *Remote plasma-enhanced CVD* (RPECVD) - Similar to PECVD except that the wafer substrate is not directly in the plasma discharge region. Removing the wafer from the plasma region allows processing temperatures down to room temperature.
- *Atomic layer CVD* (ALCVD) – Deposits successive layers of different substances to produce layered, crystalline films.
- *Combustion Chemical Vapor Deposition* (CCVD) - nGimat's proprietary Combustion Chemical Vapor Deposition process is an open-atmosphere, flame-based technique for depositing high-quality thin films and nanomaterials.
- *Hot wire CVD* (HWCVD) - also known as catalytic CVD (Cat-CVD) or hot filament CVD (HFCVD). Uses a hot filament to chemically decompose the source gases.
- *Metalorganic chemical vapor deposition* (MOCVD) - CVD processes based on metalorganic precursors.
- *Hybrid Physical-Chemical Vapor Deposition* (HPCVD) - Vapor deposition processes that involve both chemical decomposition of precursor gas and vaporization of a solid source.

- *Rapid thermal CVD* (RTCVD) - CVD processes that use heating lamps or other methods to rapidly heat the wafer substrate. Heating only the substrate rather than the gas or chamber walls helps reduce unwanted gas phase reactions that can lead to particle formation.
- *Vapor phase epitaxy* (VPE)

Substances commonly deposited for ICs

Here we, discusses the CVD processes often used for integrated circuits (ICs). Particular materials are deposited best under particular conditions.

Polysilicon

Polycrystalline silicon is deposited from silane (SiH_4), using the following reaction:

$$SiH_4 \rightarrow Si + 2\ H_2$$

This reaction is usually performed in LPCVD systems, with either pure silane feedstock, or a solution of silane with 70-80% nitrogen. Temperatures between 600 and 650 °C and pressures between 25 and 150 Pa yield a growth rate between 10 and 20 nm per minute. An alternative process uses a hydrogen-based solution. The hydrogen reduces the growth rate, but the temperature is raised to 850 or even 1050 °C to compensate.

Polysilicon may be grown directly with doping, if gases such as phosphine, arsine or diborane are added to the CVD chamber. Diborane increases the growth rate, but arsine and phosphine decrease it.

Silicon dioxide

Silicon dioxide (usually called simply "oxide" in the semiconductor industry) may be deposited by several different processes. Common source gases include silane and oxygen, dichlorosilane ($SiCl_2H_2$) and nitrous oxide (N_2O), or tetraethylorthosilicate (TEOS; $Si(OC_2H_5)_4$). The reactions are as follows:

$$SiH_4 + O_2 \rightarrow SiO_2 + 2\ H_2$$
$$SiCl_2H_2 + 2\ N_2O \rightarrow SiO_2 + 2\ N_2 + 2\ HCl$$
$$Si(OC_2H_5)_4 \rightarrow SiO_2 + \text{byproducts}$$

The choice of source gas depends on the thermal stability of the substrate; for instance, aluminium is sensitive to high temperature. Silane deposits between 300 and 500 °C, dichlorosilane at around 900 °C, and TEOS between 650 and 750 °C, resulting in a layer of *low- temperature oxide* (LTO). However, silane produces a lower-quality oxide than the other methods (lower dielectric strength, for instance), and it deposits nonconformally. Any of these reactions may be used in LPCVD, but the silane reaction is also done in APCVD. CVD oxide invariably has lower quality than thermal oxide, but thermal oxidation can only be used in the earliest stages of IC manufacturing.

Oxide may also be grown with impurities (alloying or "doping"). This may have two purposes. During further process steps that occur at high temperature, the impurities may diffuse from the oxide into adjacent layers (most notably silicon) and dope them. Oxides containing 5–15% impurities by mass are often used for this purpose. In addition, silicon dioxide alloyed with phosphorus pentoxide ("P-glass") can be used to smooth out uneven surfaces. P-glass softens and reflows at temperatures above 1000 °C. This process requires a phosphorus concentration of at least 6%, but concentrations above 8% can corrode aluminium. Phosphorus is deposited from phosphine gas and oxygen:

$$4\ PH_3 + 5\ O_2 \rightarrow 2\ P_2O_5 + 6\ H_2$$

Glasses containing both boron and phosphorus (borophosphosilicate glass, BPSG) undergo viscous flow at lower temperatures; around 850 °C is achievable with glasses containing around 5 weight % of both constituents, but stability in air can be difficult to achieve. Phosphorus oxide in high concentrations interacts with ambient moisture to produce phosphoric acid. Crystals of BPO_4 can also precipitate from the flowing glass on cooling; these crystals are not readily etched in the standard reactive plasmas used to pattern oxides, and will result in circuit defects in integrated circuit manufacturing.

Besides these intentional impurities, CVD oxide may contain byproducts of the deposition process. TEOS produces a relatively pure oxide, whereas silane introduces hydrogen impurities, and dichlorosilane introduces chlorine.

Lower temperature deposition of silicon dioxide and doped glasses from TEOS using ozone rather than oxygen has also been explored (350 to 500 °C). Ozone glasses have excellent conformality but tend to be hygroscopic – that is, they absorb water from the air due to the incorporation of silanol (Si-OH) in the glass. Infrared spectroscopy and mechanical strain as a function of temperature are valuable diagnostic tools for diagnosing such problems.

Silicon nitride

Silicon nitride is often used as an insulator and chemical barrier in manufacturing ICs. The following two reactions deposit nitride from the gas phase:

$$3\ SiH_4 + 4\ NH_3 \rightarrow Si_3N_4 + 12\ H_2$$
$$3\ SiCl_2H_2 + 4\ NH_3 \rightarrow Si_3N_4 + 6\ HCl + 6\ H_2$$

Silicon nitride deposited by LPCVD contains up to 8% hydrogen. It also experiences strong tensile stress, which may crack films thicker than 200 nm. However, it has higher resistivity and dielectric strength than most insulators commonly available in microfabrication (10^{16} Ω·cm and 10 MV/cm, respectively).

Another two reactions may be used in plasma to deposit SiNH:

$$2\ SiH_4 + N_2 \rightarrow 2\ SiNH + 3\ H_2$$

$$SiH_4 + NH_3 \rightarrow SiNH + 3\ H_2$$

These films have much less tensile stress, but worse electrical properties (resistivity 10^6 to 10^{15} Ω·cm, and dielectric strength 1 to 5 MV/cm).

Metals

Some metals (notably aluminium and copper) are seldom or never deposited by CVD. As of 2010, a commercially, cost effective, viable CVD process for copper did not exist, though copper formate, copper(hfac)2, Cu(II) ethyl acetoacetate, and other precursors have been used. Copper deposition of the metal has been done mostly by electroplating, in order to reduce the cost. Aluminum can be deposited from tri-isobutyl aluminium (TIBAL), tri ethyl/methyl aluminum (TEA,TMA), or dimethylaluminum hydride (DMAH), but physical vapor deposition methods are usually preferred.

However, CVD processes for molybdenum, tantalum, titanium, nickel, and tungsten are widely used. These metals can form useful silicides when deposited onto silicon. Mo, Ta and Ti are deposited by LPCVD, from their pentachlorides. Nickel, molybdenum, and tungsten can be deposited at low temperatures from their carbonyl precursors. In general, for an arbitrary metal *M*, the reaction is as follows:

$$2\ MCl_5 + 5\ H_2 \rightarrow 2\ M + 10\ HCl$$

The usual source for tungsten is tungsten hexafluoride, which may be deposited in two ways:

$$WF_6 \rightarrow W + 3\ F_2$$
$$WF_6 + 3\ H_2 \rightarrow W + 6\ HF$$

Chapter- 5

Stranski–Krastanov Growth

Stranski-Krastanov growth (**SK growth**, also **Stransky-Krastanov** or **Stranski-Krastanow**) is one of the three primary modes by which thin films grow epitaxially at a crystal surface or interface. Also known as 'layer-plus-island growth', the SK mode follows a two step process: initially, complete films of adsorbates, up to several monolayers thick, grow in a layer-by-layer fashion on a crystal substrate. Beyond a critical layer thickness, which depends on strain and the chemical potential of the deposited film, growth continues through the nucleation and coalescence of adsorbate 'islands'. This growth mechanism was first noted by Ivan Stranski and Lyubomir Krastanov in 1939. It wasn't until 1958 however, in a seminal work by Ernst Bauer published in *Zeitschrift für Kristallographie*, that the SK, Volmer-Weber, and Frank-van der Merwe mechanisms were systematically classified as the primary thin film growth processes. Since then, SK growth has been the subject of intense investigation, not only to better understand the complex thermodynamics and kinetics at the core of thin film formation, but also as a route to fabricating novel nanostructures for application in the microelectronics industry.

Modes of thin film growth

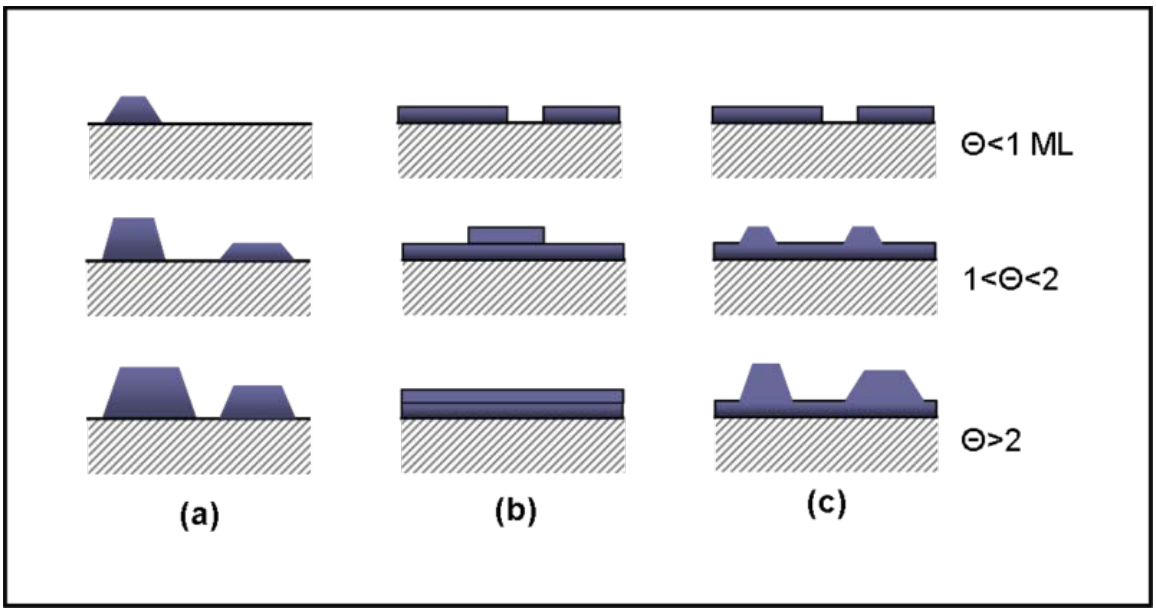

Figure 1. Cross-section views of the three primary modes of thin film growth including (a) Volmer-Weber (VW: island formation), (b) Frank-van der Merwe (FM: layer-by-layer), and (c) Stranski-Krastanov (SK: layer-plus-island). Each mode is shown for several different amounts of surface coverage, Θ.

The growth of epitaxial (homogenous or heterogeneous) thin films on a single crystal surface depends critically on the interaction strength between adatoms and the surface. While it is possible to grow epilayers from a liquid solution, most epitaxial growth occurs via a vapor phase technique such as molecular beam epitaxy (MBE). In **Volmer-Weber** (VW) growth, adatom-adatom interactions are stronger than those of the adatom with the surface, leading to the formation of three-dimensional adatom clusters or islands. Growth of these clusters, along with coarsening, will cause rough multi-layer films to grow on the substrate surface. Antithetically, during **Frank-van der Merwe** (FM) growth, adatoms attach preferentially to surface sites resulting in atomically smooth, fully formed layers. This layer-by-layer growth is two dimensional, indicating that complete films form prior to growth of subsequent layers. **Stranski-Krastanov** growth is an intermediary process characterized by both 2D layer and 3D island growth. Transition from the layer-by-layer to island-based growth occurs at a critical layer thickness which is highly dependent on the chemical and physical properties, such as surface energies and lattice parameters, of the substrate and film. Figure 1 is a schematic representation of the three main growth modes for various surface coverages.

Determining the mechanism by which a thin film grows requires consideration of the chemical potentials of the first few deposited layers. A model for the layer chemical potential per atom has been proposed by Markov as:

$$\mu(n) = \mu_\infty + [\varphi_a - \varphi_a'(n) + \varepsilon_d(n) + \varepsilon_e(n)]$$

where μ_∞ is the bulk chemical potential of the adsorbate material, φ_a is the desorption energy of an adsorbate atom from a wetting layer of the same material, $\varphi_a'(n)$ the desorption energy of an adsorbate atom from the substrate, $\varepsilon_d(n)$ is the per atom misfit dislocation energy, and $\varepsilon_e(n)$ the per atom homogeneous strain energy. In general, the values of φ_a, $\varphi_a'(n)$, $\varepsilon_d(n)$, and $\varepsilon_e(n)$ depend in a complex way on the thickness of the growing layers and lattice misfit between the substrate and adsorbate film. In the limit of small strains, $\varepsilon_{d,e}(n) \ll \mu_\infty$, the criterion for a film growth mode is dependent on $\frac{d\mu}{dn}$.

- VW growth: $\frac{d\mu}{dn} < 0$ (adatom cohesive force is stronger than surface adhesive force)
- FM growth: $\frac{d\mu}{dn} > 0$ (surface adhesive force is stronger than adatom cohesive force)

SK growth can be described by both of these inequalities. While initial film growth follows a FM mechanism, i.e. positive differential μ, non-trivial amounts of strain energy accumulate in the deposited layers. At a critical thickness, this strain induces a sign reversal in the chemical potential, i.e. negative differential μ, leading to a switch in the growth mode. At this point it is energetically favorable to nucleate islands and further growth occurs by a VW type mechanism. A thermodynamic criterion for layer growth similar to the one presented above can be obtained using a force balance of surface tensions and contact angle.

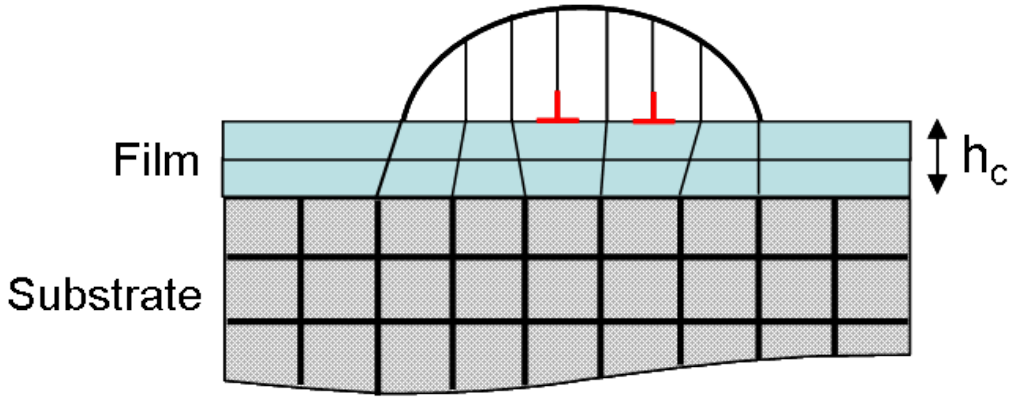

Figure 2. SK growth showing island formation after obtaining a critical thickness, h_C. Lines represent lattice planes with thicker lines for the substrate lattice and thinner lines for the growing film. Edge dislocations are highlighted in red at the film/island interface.

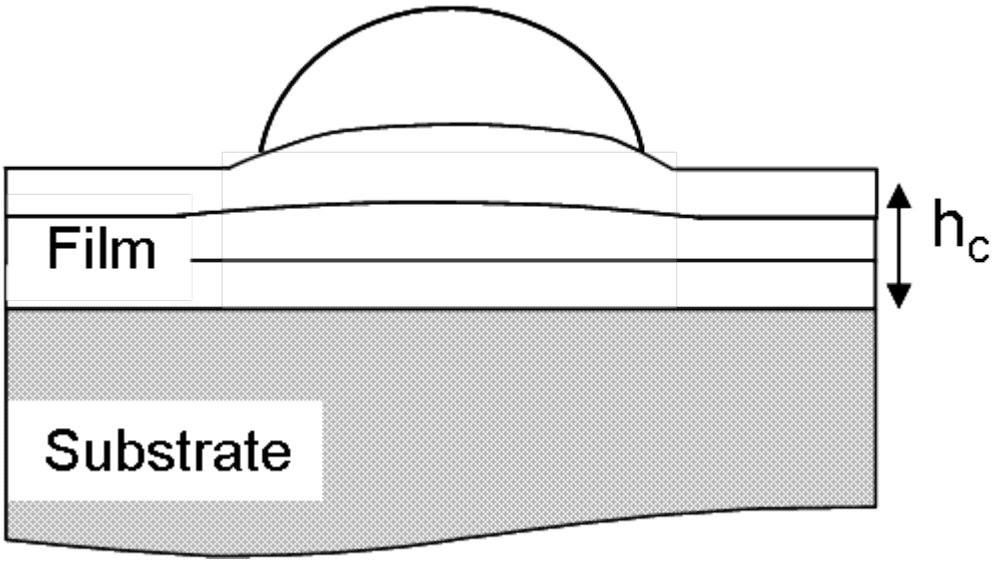

Figure 3. Coherent island formation under SK growth. Local curvature of the near surface region surrounding the island leads to elastic deformation of the island and wetting layer thereby reducing the accumulated strain. These islands are defect free.

Since the formation of wetting layers occurs in a commensurate fashion at a crystal surface, there is often an associated misfit between the film and the substrate due to the different lattice parameters of each material. Attachment of the thinner film to the thicker substrate induces a misfit strain at the interface given by $\frac{a_f - a_s}{a_s}$. Here a_f and a_s are the film and substrate lattice constants, respectively. As the wetting layer thickens, the associated strain energy increases rapidly. In order to relieve the strain, island formation can occur in either a dislocated or coherent fashion. In dislocated islands, strain relief arises by forming interfacial misfit dislocations. The reduction in strain energy accommodated by introducing a dislocation is generally greater than the concomitant cost of increased surface energy associated with creating the clusters. The thickness of the wetting layer at which island nucleation initiates, called the critical thickness h_C, is strongly dependent on the lattice mismatch between the film and substrate, with a greater mismatch leading to smaller critical thicknesses. Values of h_C can range from sub-monlayer coverage to up to several monolayers thick. Figure 2 illustrates a dislocated island during SK growth after reaching a critical layer height. A pure edge dislocation is shown at the island interface to illustrate the relieved structure of the cluster.

In some cases, most notably the Si/Ge system, nanoscale dislocation-free islands can be formed during SK growth by introducing undulations into the near surface layers of the substrate. These regions of local curvature serve to elastically deform both the substrate and island, relieving accumulated strain and bringing the wetting layer and island lattice constant closer to its bulk value. This elastic instability at h_C is known as the Grinfeld instability (formerly Asaro-Tiller-Grinfeld; ATG). The resulting islands are *coherent* and defect-free, garnering them significant interest for use in nanoscale electronic and opto-electronic devices. Such applications are discussed briefly later. A schematic of the

resulting epitaxial structure is shown in figure 3 which highlights the induced radius of curvature at the substrate surface and in the island. Finally, it should be noted that strain stabilization indicative of coherent SK growth decreases with decreasing inter-island separation. At large areal island densities (smaller spacing), curvature effects from neighboring clusters will cause dislocation loops to form leading to defected island creation.

Monitoring SK growth

Wide beam techniques

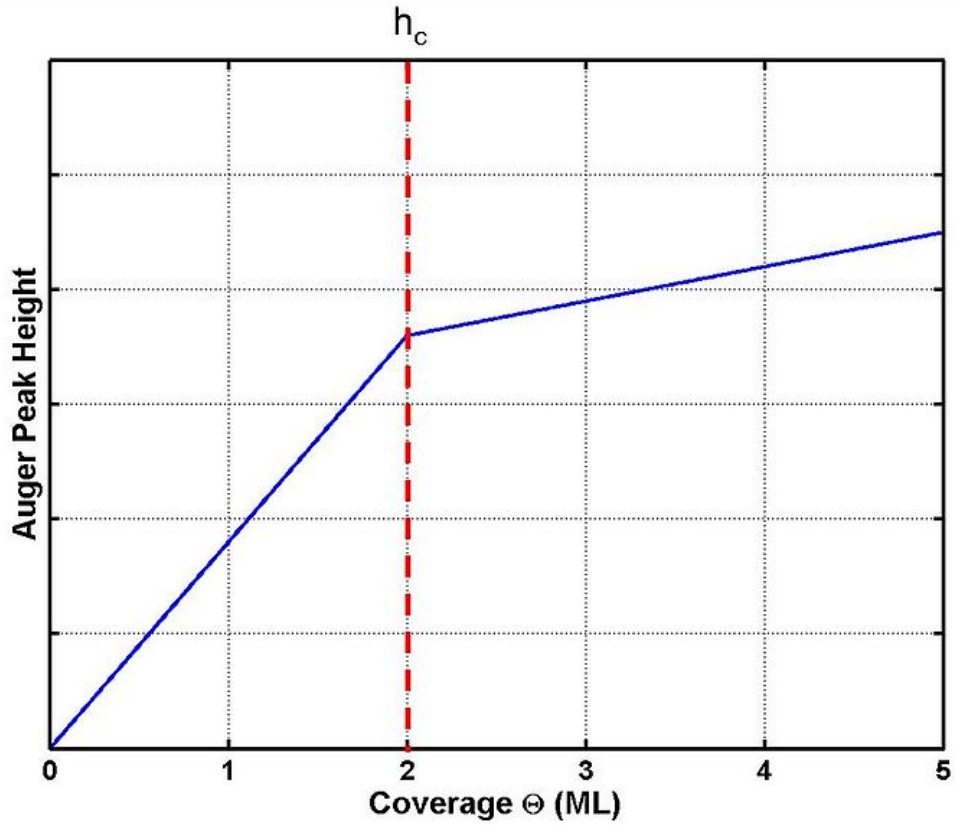

Figure 4. Evolution of Auger peak height as function of surface coverage during SK growth. The plot is a series of segmented linear curves with a clear break point indicating the critical thickness (clearly marked in the diagram) and the onset of island growth. Slope differences are due to the different modes of growth. The initial steep-sloped segment corresponds to the FM growth mode while the later, shallow-sloped region is representative of the VW mode. This schematic is characteristic of 'ideal' SK growth where nucleation onset begins at 2 monolayer coverage.

Analytical techniques such as Auger electron spectroscopy (AES), low-energy electron diffraction (LEED), and reflection high energy electron diffraction (RHEED), have been extensively used to monitor SK growth. AES data obtained *in situ* during film growth in a number model systems, such as Pd/W (100), Pb/Cu (110), Ag/W (110), and Ag/Fe (110),

show characteristic segmented curves like those presented in figure 4. Height of the film Auger peaks plotted as a function of surface coverage Θ, initially exhibits a straight line, which is indicative of AES data for FM growth. There is a clear break point at a critical adsorbate surface coverage followed by another linear segment at a reduced slope. The paired break point and shallow line slope is characteristic of island nucleation; a similar plot for FM growth would exhibit many such line and break pairs while a plot of the VW mode would be a single line of low slope. In some systems, reorganization of the 2D wetting layer results in decreasing AES peaks with increasing adsorbate coverage. Such situations arise when many adatoms are required to reach a critical nucleus size on the surface and at nucleation the resulting adsorbed layer constitutes a significant fraction of a monolayer. After nucleation, metastable adatoms on the surface are incorporated into the nuclei, causing the Auger signal to fall. This phenomenon is particularly evident for deposits on a molybdenum substrate.

Evolution of island formation during a SK transitions have also been successfully measured using LEED and RHEED techniques. Diffraction data obtained via various LEED experiments have been effectively used in conjunction with AES to measure the critical layer thickness at the onset of island formation. In addition, RHEED oscillations have proven very sensitive to the layer-to-island transition during SK growth, with the diffraction data providing detailed crystallographic information about the nucleated islands. Following the time dependence of LEED, RHEED, and AES signals, extensive information on surface kinetics and thermodynamics has been gathered for a number of technologically relevant systems.

Microscopies

Unlike the techniques presented in the last section in which probe size can be relatively large compared to island size, surface microscopies such scanning electron microscopy (SEM), transmission electron microscopy (TEM), scanning tunneling microscopy (STM), and Atomic force microscopy (AFM) offer the opportunity for direct viewing of deposit/substrate combination events. The extreme magnifications afforded by these techniques, often down to the nanometer length scale, make them particularly applicable for visualizing the strongly 3D islands. UHV-SEM and TEM are routinely used to image island formation during SK growth, enabling a wide range of information to be gathered, ranging from island densities to equilibrium shapes. AFM and STM have become increasingly utilized to correlate island geometry to the surface morphology of the surrounding substrate and wetting layer. These visualization tools are often used to complement quantitative information gathered during wide-beam analyses.

Application to nanotechnology

As mentioned previously, coherent island formation during SK growth has attracted increased interest as a means for fabricating epitaxial nanoscale structures, particularly quantum dots (QDs). Significant effort has been spent developing methods to control island organization, density, and size on a substrate. Techniques such as surface dimpling with a pulsed laser and control over growth rate have been successfully applied to alter

the onset of the SK transition or even suppress it altogether. The ability to control this transition either spatially or temporally enables manipulation of physical parameters of the nanostructures, like geometry and size, which, in turn, can alter their electronic or optoelectronic properties (i.e. band gap). For example, Schwarz-Selinger, *et al.* have used surface dimpling to create surface miscuts on Si that provide preferential Ge island nucleation sites surrounded by a denuded zone. In a similar fashion, lithographically patterned substrates have been used as nucleation templates for SiGe clusters. Several studies have also shown that island geometries can be altered during SK growth by controlling substrate relief and growth rate. Bimodal size distributions of Ge islands on Si are a striking example of this phenomenon in which pyramidal and dome-shaped islands coexist after Ge growth on a textured Si substrate. Such ability to control the size, location, and shape of these structures could provide invaluable techniques for 'bottom-up' fabrication schemes of next-generation devices in the microelectronics industry.

Chapter- 6

Thin Film Drug Delivery

Thin film drug delivery uses a **dissolving film** or **oral drug strip** to administer drugs via absorption in the mouth (buccally or sublingually) and/or via the small intestines (enterically). A film is prepared using hydrophilic polymers that rapidly dissolves on the tongue or buccal cavity, delivering the drug to the systemic circulation via dissolution when contact with liquid is made.

Zuplenz 8 mg (approved by FDA, July 7, 2010).

Thin film drug delivery has emerged as an advanced alternative to the traditional tablets, capsules and liquids often associated with prescription and OTC medications. Similar in size, shape and thickness to a postage stamp, thin film strips are typically designed for oral administration, with the user placing the strip on or under the tongue or along the inside of the cheek. As the strip dissolves, the drug can enter the blood stream enterically, buccally or sublingually. Evaluating the systemic transmucosal drug delivery, the buccal mucosa is the preferred region as compared to the sublingual mucosa.

Different buccal delivery products have been marketed or are proposed for certain diseases like trigeminal neuralgia, Meniere's disease, diabetes, and addiction. The first commercial non-drug product to use thin films was the Listerine PocketPaks breath freshening strips. Since then, thin film products for other breath fresheners, as well as a number of cold, cough, flu and anti-snoring medications, have entered the marketplace. There are currently several projects in development that will deliver prescription drugs using the thin film dosage form.

Formulation of oral drug strips involves the application of both aesthetic and performance characteristics such as strip-forming polymers, plasticizers, active pharmaceutical ingredient, sweetening agents, saliva stimulating agent, flavoring agents, coloring agents, stabilizing and thickening agents. From the regulatory perspectives, all excipients used in the formulation of oral drug strips should be approved for use in oral pharmaceutical dosage forms.

Undergraduate biomedical engineering students at Johns Hopkins University have created a new drug delivery system based on the thin film technology used by a breath freshener. Laced with a vaccine against rotavirus, the strips could be used to provide the vaccine to infants in impoverished areas.

Oral drug strip development

Strip forming polymers

The polymer employed should be non-toxic, non-irritant and devoid of leachable impurities. It should have good wetting and spreadability property. The polymer should exhibit sufficient peel, shear and tensile strengths. The polymer should be readily available and should not be very expensive. Film obtained should be tough enough so that there won't be any damage while handling or during transportation. Combination of microcrystalline cellulose and maltodextrin has been used to formulate Oral Strips of piroxicam made by hot melt extrusion technique. Pullulan has been the most widely used film former (used in Listerine PocketPak, Benadryl, etc)

Plasticizer

Plasticizer is a vital ingredient of the OS formulation. It helps to improve the flexibility of the strip and reduces the brittleness of the strip. Plasticizer significantly improves the strip properties by reducing the glass transition temperature of the polymer. Glycerol,

Propylene glycol, low molecular weight polyethylene glycols, phthalate derivatives like dimethyl, diethyl and dibutyl phthalate, Citrate derivatives such as tributyl, triethyl, acetyl citrate, triacetin and castor oil are some of the commonly used plasticizer excipients.

Active pharmaceutical ingredient

Since the size of the dosage form has limitation, high-dose molecules are difficult to be incorporated in OS. Generally 5%w/w to 30%w/w of active pharmaceutical ingredients can be incorporated in the OS.

Sweeting, flavoring and coloring agent

An important aspect of thin film drug technology is its taste and color. The sweet taste in formulation is more important in case of pediatric population. Natural sweeteners as well as artificial sweeteners are used to improve the flavor of the mouth dissolving formulations for the flavors changes from individual to individual. Pigments such as titaniumdioxide is incorporated for coloring.

Stabilizing and thickening agents

The stabilizing and thickening agents are employed to improve the viscosity and consistency of dispersion or solution of the strip preparation solution or suspension before casting. Drug content uniformity is a requirement for all dosage forms, particularly those containing low dose highly potent drugs. To uniquely meet this requirement, thin film formulations contain uniform dispersions of drug throughout the whole manufacturing process. Since this criteria is essential for the quality of the thin film and final pharmaceutical dosage form, the use of Laser Scanning Confocal Microscopy (LSCM) was recommended to follow the manufacturing process.

Commercial oral strip drugs

There are not yet many medications available in a thin film form on the market. Those that are include:

- Zuplenz: The first oral soluble film approved by the FDA as a prescription medication.
- Benadryl (diphenhydramine product, anti-cholinergic anti-histamine used for allergies and as a mild sedative)
- Gas-X (simethicone product for bloating, gas, and gastrointestinal complaint)
- Melatonin PM (hormonal product sold as a "dietary supplement" marketed for insomnia)
- Orajel Kids (benzocaine product for dental pain)
- Suboxone (buprenorphine and naloxone fixed dosage combination product for opioid addiction)
- Subutex (buprenorphine product for opioid addiction)

- Sudafed (phenylephrine or pseudoephedrine product for nasal congestion)
- Suppress
- TheraFlu (combination product of pain reliever, anti-pyretic and decongestant)
- Triaminic (children's anti-tussive product)

On July 2, 2010, Strativa Pharmaceuticals], the proprietary products division of Par Pharmaceutical, received approval from the US FDA for Zuplenz® (ondansetron) oral soluble film (OSF) for the prevention of postoperative, highly and moderately emetogenic cancer chemotherapy-induced, and radiotherapy-induced nausea and vomiting.

Advantages

The design of thin film, often referred to as PharmFilm, as an oral drug delivery technology offers several advantages over other modes of drug delivery, such as ingestible tablets, chewable tablets, orally dissolving tablets, softgels, liquids or inhalants:

- The sublingual and buccal delivery of a drug via thin film has the potential to improve the onset of action, lower the dosing, and enhance the efficacy and safety profile of the medicament.
    - All tablet dosage forms, softgels and liquid formulations primarily enter the blood stream via the gastrointestinal tract, which subjects the drug to degradation from stomach acid, bile, digestive enzymes and other first-pass effects. As a result, such formulations often require higher doses and generally have a delayed onset of action.
    - Conversely, buccal and sublingual thin-film drug delivery can avoid these issues and yield quicker onsets of action at lower doses.
- Thin film is more stable, durable and quicker dissolving than other conventional dosage forms.
- Thin film enables improved dosing accuracy relative to liquid formulations since every strip is manufactured to contain a precise amount of the drug.
- Thin film not only ensures more accurate administration of drugs but also can improve compliance due to the intuitive nature of the dosage form and its inherent ease of administration. These properties are especially beneficial for pediatric, geriatric and neurodegenerative disease patients where proper and complete dosing can be difficult.
- Thin film's ability to dissolve rapidly without the need for water provides an alternative to patients with swallowing disorders and to patients suffering from nausea, such as those patients receiving chemotherapy.
- Thin film drug delivery has the potential to allow the development of sensitive drug targets that may otherwise not be possible in tablet or liquid formulations.
- From a commercial perspective thin film drug delivery technology offers an opportunity to extend revenue lifecycles for pharmaceutical companies whose drug patent is expiring and will soon be vulnerable to generic competition.

- Sublingual film delivers a convenient, quick-dissolving therapeutic dose contained within an abuse-deterrent film matrix that cannot be crushed or injected by patients, and rapidly absorbs under the tongue to ensure compliance.

Chapter- 7

Thin Film Rechargeable Lithium Battery

Thin film lithium ion batteries are similar to lithium-ion batteries, but they are composed of thin materials, some only nanometers or micrometers thick, which allow for the finished battery to be just millimeters thick. They have been developed and advanced primarily within the last decade. These batteries consist of a substrate, electrolyte, current collector, anode, cathode, and a charge separator. There has been much research into the determination of the most effective components for this type of battery. It has been shown recently that even ordinary printer paper can be used as a charge separator and a substrate. These thin film batteries are an improvement on the common secondary, or rechargeable, lithium ion batteries in many ways. These batteries exhibit the same voltage and current as their bulky counterparts, but their thinner dimensions allow for greater applications such as making thinner electronic devices, like cell phones and laptops and even implantable medical devices and reducing the weight of common devices that are run on battery power because of the batteries' high energy density. These batteries can be formed into any shape and they can be stacked, to be used in parallel, thus even further reducing the space needed for a battery.

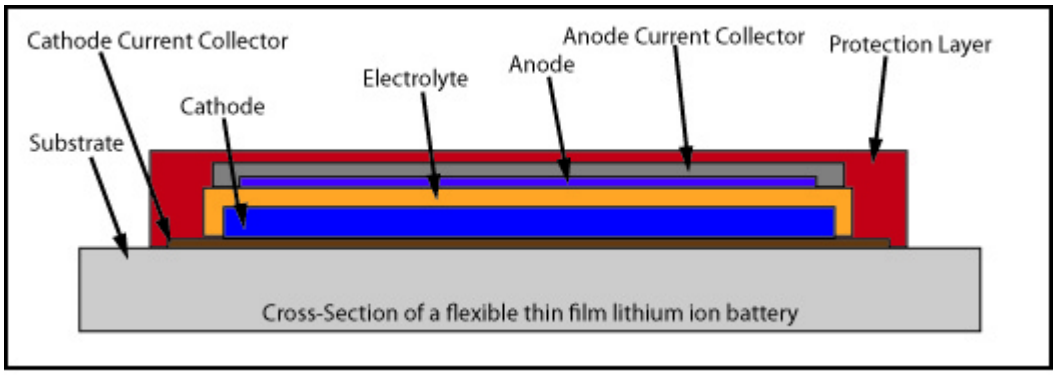

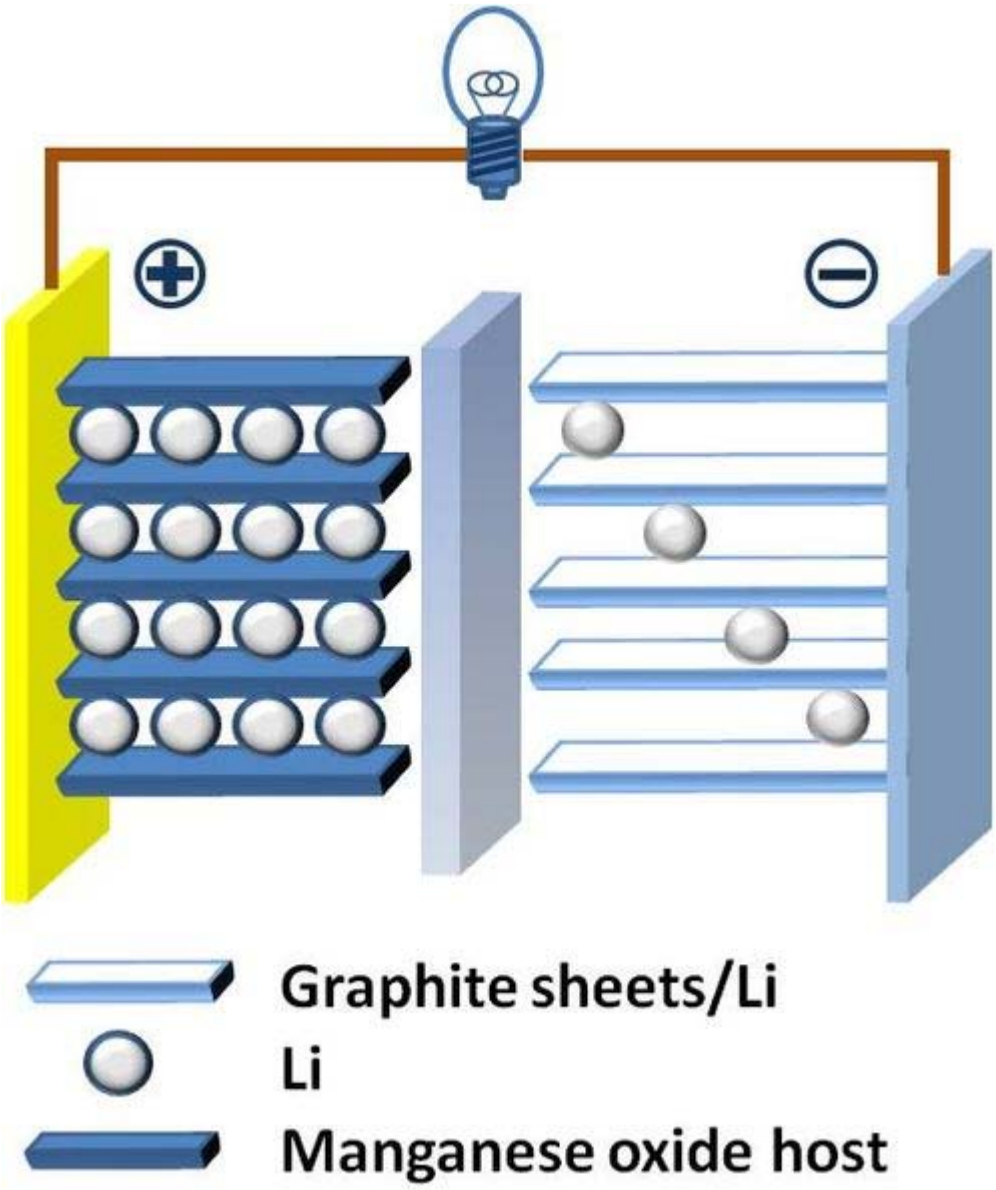

Lithium Ion Battery Cell

Background

Lithium-ion batteries are a newer battery technology that is preferable due to their ability to be recharged. Also they have high energy density and last longer than many similar battery technologies. In the battery cell lithium ions flow through the electrolyte from the anode to the cathode while the battery is being discharged. Upon recharging the battery the lithium ions move back to the anode. This Li-ion battery design is effective for large devises. However, as a more mobile, technology driven society we rely heavily on portable electronics, which require thin batteries for power. Research into thin film batteries has developed over the recent years to accommodate for this demand.

Components of Thin Film Battery

Cathode materials

Cathode materials in thin film lithium ion batteries are the same of what is seen in classical lithium ion batteries. They are normally metal oxides that are deposited as a film by various methods.

Metal oxide materials are shown below as well as their relative specific capacities (Λ), open circuit voltages (V_{OC}), and energy densities (D_E).

	Λ(Ah/kg)	V_{OC} (V)	D_E (Wh/kg)
$LiCoO_2$	145	4	580
$LiMn_2O_4$	148	4	592
$LiFePO_4$	170	3.4	578

Energy Density

$D_E = \Lambda V_{oc}$

Λ: capacity (mAh/g)

V_{oc}:Open circuit potential

Deposition methods for cathode materials

There are various methods being used in order to deposit a thin film cathode material onto the current collector.

Pulsed Laser Deposition (PLD)

In Pulsed Laser Deposition materials are fabricated with varying parameters such as laser energy and fluence, substrate temperature, background pressure, and target-substrate distance.

Magnetron Sputtering

In Magnetron Sputtering the substrate is cooled for deposition.

Chemical Vapor Deposition (CVD)

In Chemical Vapor Deposition volatile precursor materials is deposited onto a substrate material.

Sol-Gel Processing

Sol-gel processing allows for homogeneous mixing of precursor materials at the atomic level.

Electrolyte

The greatest difference between classical lithium ion batteries and thin, flexible, lithium ion batteries is in the electrolyte material used. Progress in lithium ion batteries relies as much on improvements in the electrolyte as it does in the electrode materials, as the electrolyte plays a major role in safe battery operation. The concept of thin film lithium ion batteries was increasingly motivated by manufacturing advantages presented by the polymer technology for their use as electrolytes. Lipon, lithium phosphorus oxynitride, is an amorphous polymer material used as an electrolyte material in thin film flexible batteries. Layers of Lipon are deposited over the cathode material at ambient temperatures by RF magnetron sputtering. This forms the solid electrolyte used for ion conduction between anode and cathode. Solid polymer electrolytes offer several advantages in comparison to a classical liquid lithium ion battery. Rather than having separate components of electrolyte, binder, and separator, these solid electrolytes can act as all three. This increases the overall energy density of the assembled battery because the constituents of the entire cell are more tightly packed.

Separator Material

Separator materials in lithium ion batteries must have the ability to transport ions through their porous membranes while maintaining a physical separation between the anode and cathode materials in order to prevent short-circuiting. In a thin film based system, the electrolyte is normally a solid electrolyte, capable of conforming to the shape of the battery. Typically this material is a polymer based material and as mentioned above, this polymer commonly acts as both the separator and electrolyte. Since thin film batteries are made of all solid materials, this affords to use of simpler separator materials in these systems such as Xerox paper rather than in liquid based Li-ion batteries.

Current Collector

Current collectors in thin film batteries must be flexible, have high surface area, and cost-effective. Silver nanowires with improved surface area and loading weight have been

shown to work as a current collector in these battery systems, but still are not as cost-effective as desired. Extending graphite technology to lithium ion batteries, solution processed carbon nanotubes (CNT) films are being looked into for use as both the current collector and anode material. CNTs have the ability to intercalate lithium and maintain high operating voltages, all with low mass loading and flexibility.

Advantages and Challenges

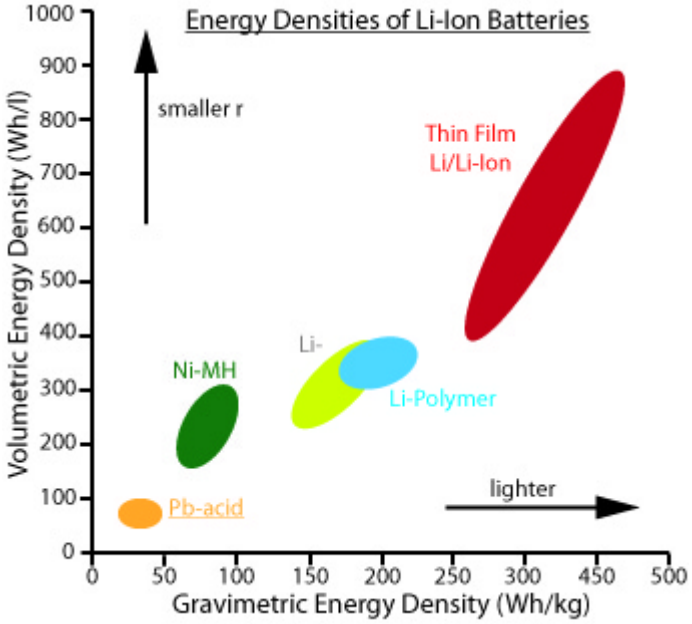

Thin film lithium ion batteries offer improved performance by having a higher average output voltage, lighter weights thus higher energy density, and longer cycling life than typical rechargeable batteries. In the thin film lithium ion battery, both electrodes are capable of reversible lithium insertion, thus forming a Li-ion transfer cell. Li-ion transfer cells are the most promising systems for satisfying the demand of high specific energy and high power. In order to construct a thin film battery it is necessary to fabricate all the battery components, as an anode, a solid electrolyte, a cathode and current leads into multi-layered thin films by suitable technologies.

In a thin film based system, the electrolyte is normally a solid electrolyte, capable of conforming to the shape of the battery. This is in contrast to classical lithium ion batteries, which normally have liquid electrolyte material. Liquid electrolytes can be challenging to utilized if they are not compatible with the separator. Also liquid electrolytes in general call for an increase in the overall volume of the battery, which is not ideal for designing a system that has high energy density. Additionally, in a thin film flexible Li-ion battery, the electrolyte, which is normally polymer-based, can act as the electrolyte, separator, and binder material. This provides the ability to have flexible systems since the issue of electrolyte leakage is circumvented. Finally, solid systems can be packed together tightly which affords an increase in energy density when compared to classical lithium ion batteries.

Separator materials in lithium ion batteries must have the ability to transport ions through their porous membranes while maintaining a physical separation between the anode and cathode materials in order to prevent short-circuiting. Furthermore, the separator must be resistant to degradation during the battery's operation. In a thin film Li-ion battery, the separator must be a thin and flexible solid. Typically today, this material is a polymer-based material. Since thin film batteries are made of all solid materials, allows one to use simpler separator materials in these systems such as Xerox paper rather than in liquid based Li-ion batteries.

Scientific Development

Development of thin solid state batteries allows for roll to roll type production of batteries which would decrease production costs. Solid-state batteries can also afford increased energy density due to decrease in overall device weight. Where as the flexible nature allows for novel battery design and incorporation into electronics. Development is still required in cathode materials which will resist decreased capacity due to cycling.

Prior Technology	Replacement Technology	Result
Solution based electrolyte	Solid state electrolyte	Increased safety and cycle life
Polymer separators	Paper separator	Decreased cost increased rate of ion conduction
Metallic current collectors	Carbon nanotube current collectors	Decreased device weight, increased energy density
Graphite anode	Carbon nanotube anode	Decreased device complexity

Applications

The advancements made to the thin film lithium ion battery have allowed for many potential applications. The majority of these applications are aimed at improving the currently available consumer and medical products. Thin film lithium ion batteries can be used to make thinner portable electronics, because the thickness of the battery required to operate the device can be reduced greatly. These batteries have the ability to be an integral part of implantable medical devices, such as defibrillators and neural stimulators, "smart" cards, radio frequency identification, or RFID, tags and wireless sensors. They can also serve as a way to store energy collected from solar cells or other harvesting devices. Each of these applications is possible because of the flexibility in the size and shape of the batteries. The size of these devices does not have to revolve around the size of the space needed for the battery anymore. The thin film batteries can be attached to the inside of the casing or in some other convenient way. The opportunities in which to use this type of batteries are endless.

Solar Cell Storage Devices

The thin film lithium ion battery can serve as a storage device for the energy collected from a solar cell. These batteries can be made to have a low self discharge rate, which means that these batteries can be stored for long periods of time without a major loss of the energy that was used to charge it. These fully charged batteries could then be used to power some or all of the other potential applications listed below.

Smart Cards

Smart cards are basically the same size as a credit card, but they contain a microchip that can be used to access information, give authorization, or process an application. These cards can go through harsh production conditions, with temperatures in the range of 130 to 150°C, in order to complete the high temperature, high pressure lamination processes. These conditions can cause other batteries to fail because of degassing or degradation of organic components within the battery. Thin film lithium ion batteries have been shown to withstand temperatures of -40 to 150°C. This use of thin film lithium ion batteries is hopeful for other extreme temperature applications.

RFID tags

Radio Frequency Identification (RFID) tags can be used in many different applications. These tags can be used in packaging, inventory control, used to verify authenticity and even allow or deny access to something. These ID tags can even have other integrated sensors to allow for the physical environment to be monitored, such as temperature or shock during travel or shipping. Also, the distance required to read the information in the tag depends on the strength of the battery. The farther away you want to be able to read the information, the stronger the output will have to be and thus the greater the power supply to accomplish this output. As these tags get more and more complex, the battery requirements will need to keep up. Thin film lithium ion batteries have shown that they can fit into the designs of the tags because of the flexibility of the battery in size and shape and are sufficiently powerful enough to accomplish the goals of the tag. Low cost production methods, like roll to roll lamination, of these batteries may even allow for this kind of RFID technology to be implemented in disposable applications.

Implantable Medical Devices

Thin films of $LiCoO_2$ have been synthesized in which the strongest x ray reflection is either weak or missing, indicating a high degree of preferred orientation. Thin film solid state batteries with these textured cathode films can deliver practical capacities at high current densities. For example, for one of the cells 70% of the maximum capacity between 4.2 V and 3 V (approximately 0.2 mAh/cm^2) was delivered at a current of 2 mA/cm^2. When cycled at rates of 0.1 mA/cm^2, the capacity loss was 0.001%/cycle or less. The reliability and performance of Li $LiCoO_2$ thin-film batteries make them attractive for application in implantable devices such as neural stimulators, pacemakers, and defibrillators.

Implantable medical devices require batteries that can deliver a steady, reliable power source for as long as possible. These applications call for a battery that has a low self-discharge rate, for when it's not in use, and a high power rate, for when it needs to be used, especially in the case of an implantable defibrillator. Also, users of the product will want a battery that can go through many cycles, so these devices will not have to be replaced or serviced often. Thin film lithium ion batteries have the ability to meet these requirements. The advancement from a liquid to a solid electrolyte has allowed these batteries to take almost any shape without the worry of leaking, and it has been shown that certain types of thin film rechargeable lithium batteries can last for around 50,000 cycles. Another advantage to these thin film batteries is that they can be arranged in series to give a larger voltage equal to the sum of the individual battery voltages. This fact can be used in reducing the "footprint" of the battery, or the size of the space needed for the battery, in the design of a device.

Wireless Sensors

Wireless sensors need to be in use for the duration of their application, whether that may be in package shipping or in the detection of some unwanted compound, or controlling inventory in a warehouse. If the wireless sensor cannot transmit its data due to low or no battery power, the consequences could potentially be severe based on the application. Also, the wireless sensor must be adaptable to each application. Therefore the battery must be able to fit within the designed sensor. This means that the desired battery for these devices must be long-lasting, size specific, low cost, if they are going to be used in disposable technologies, and must meet the requirements of the data collection and transmission processes. Once again, thin film lithium ion batteries have shown the ability to meet all of these requirements.

Chapter- 8

Self-Assembled Monolayer

A **self assembled monolayer** (**SAM**) is an organized layer of amphiphilic molecules in which one end of the molecule, the "head group" shows a special affinity for a substrate. SAMs also consist of a tail with a functional group at the terminal end as seen in Figure 1.

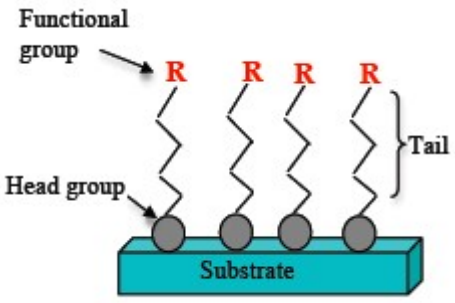

Figure 1. Representation of a SAM structure

SAMs are created by the chemisorption of hydrophilic "head groups" onto a substrate from either the vapor or liquid phase followed by a slow two-dimensional organization of hydrophobic "tail groups". Initially, adsorbate molecules form either a disordered mass of molecules or form a "lying down phase", and over a period of hours, begin to form crystalline or semicrystalline structures on the substrate surface. The hydrophilic "head groups" assemble together on the substrate, while the hydrophobic tail groups assemble far from the substrate. Areas of close-packed molecules nucleate and grow until the surface of the substrate is covered in a single monolayer.

Adsorbate molecules adsorb readily because they lower the surface energy of the substrate and are stable due to the strong chemisorption of the "head groups." These bonds create monolayers that are more stable than the physisorbed bonds of Langmuir–Blodgett films. Thiol-metal bonds, for example, are on the order of 100 kJ/mol, making the bond stable in a wide variety of temperature, solvents, and potentials. The monolayer

packs tightly due to van der Waals interactions, thereby reducing its own free energy. The adsorption can be described by the Langmuir adsorption isotherm if lateral interactions are neglected. If they cannot be neglected, the adsorption is better described by the Frumkin isotherm.

Types of SAMs

Selecting the type of head group depends on the application of the SAM. Typically, head groups are connected to an alkyl chain in which the terminal end can be functionalized (i.e. adding –OH, –NH3, or –COOH groups) to vary the wetting and interfacial properties. An appropriate substrate is chosen to react with the head group. Substrates can be planar surfaces, such as silicon and metals, or curved surfaces, such as nanoparticles. Alkanethiols are the most commonly used molecules for SAMs. Alkanethiols are molecules with an alkyl chain, $(C\text{-}C)^n$ chain, as the back bone, a tail group, and a S-H head group. They are used on noble metal substrates because of the strong affinity of sulfur for these metals. The sulfur gold interaction is semi-covalent @45kcal/mol. In addition, gold is an inert and biocompatible material that is easy to acquire. It is also easy to pattern via lithography, a useful feature for applications in nanoelectromechanical systems (NEMS). Additionally, it can withstand harsh chemical cleaning treatments. Silanes are generally used on nonmetallic oxide surfaces.

Preparation of SAMs

Metal substrates for use in SAMs can be produced through physical vapor deposition techniques, electrodeposition or electroless deposition. Alkanethiol SAMs produced by adsorption from solution are made by immersing a substrate into a dilute solution of alkane thiol in ethanol for 12 to 72 hours at room temperature and dried with nitrogen. SAMs can also be adsorbed from the vapor phase. For example, chlorosilane SAMs (which can also be adsorbed from the liquid phase), are often created in a reaction chamber by silanization in which silane vapor flows over the substrate to form the monolayer.

Characterization of SAMs

The structures of SAMs are most commonly determined using scanning probe microscopy techniques such as atomic force microscopy (AFM) and scanning tunneling microscopy (STM). STM has been able to help understand the mechanisms of SAM formation as well as determine the important structural features that lend SAMs their integrity as surface-stable entities. In particular STM can image the shape, spatial distribution, terminal groups and their packing structure. AFM offers an equally powerful tool without the requirement of the SAM being conducting or semi-conducting. The AFM has been used to determine chemical functionality, conductance, magnetic properties, surface charge, and frictional forces of SAMs. More recently, however, diffractive methods have also been used. The structure can be used to characterize the kinetics and defects found on the monolayer surface. These techniques have also shown physical differences between SAMs with planar substrates and nanoparticle substrates.

An alternative characterisation instrument for measuring the self assembly in real time is dual polarisation interferometry where the refractive index, thickness, mass and birefringence of the self assembled layer are quantified at high resolution.

Defects

Defects due to both external and intrinsic factors may appear. External factors include the cleanliness of the substrate, method of preparation, and purity of the adsorbates. SAMs intrinsically form defects due to the thermodynamics of formation, e.g. thiol SAMs on gold typically exhibit etch pits (monoatomic vacancy islands) likely due to extraction of adatoms from the substrate and formation of adatom-adsorbate moieties.

Nanoparticle properties

The structure of SAMs is also dependent on the curvature of the substrate. SAMs on nanoparticles including colloids and nanocrystals, “stabilize the reactive surface of the particle and present organic functional groups at the particle-solvent interface”. These organic functional groups are useful for applications, such as immunoassays, that are dependent on chemical composition of the surface.

Kinetics

There is evidence that SAM formation occurs in two steps, an initial fast step of adsorption and a second slower step of monolayer organization. Adsorption occurs at the liquid-liquid, liquid-vapor, and liquid-solid interfaces. The transport of molecules to the surface occurs due to a combination of diffusion and convective transport. According to the Langmuir or Avrami kinetic model the rate of deposition onto the surface is proportional to the free space of the surface.

$$\mathbf{k}(\mathbf{1}-\theta)=\frac{d\theta}{dt}.$$

Where **θ** is the proportional amount of area deposited and **k** is the rate constant. Although this model is robust it is only used for approximations because it fails to take into account intermediate processes. Dual polarisation interferometry being a real time technique with ~10Hz resolution can measure the kinetics of monolayer self assembly directly.

Once the molecules are at the surface the self organization occurs in three phases:

1. A low density phase with random dispersion of molecules on the surface.
2. An intermediate density phase with conformational disordered molecules or molecules lying flat on the surface.
3. A high density phase with close packed order and molecules standing normal to the substrate's surface.

The phase transitions in which a SAM forms depends on the temperature of the environment relative to the triple point temperature, the temperature in which the tip of the low density phase intersects with the intermediate phase region. At temperatures below the triple point the growth goes from phase 1 to phase 2 where many islands form with the final SAM structure, but are surrounded by random molecules. Similar to nucleation in metals, as these islands grow larger they intersect forming boundaries until they end up in phase 3, as seen below.

At temperatures above the triple point the growth is more complex and can take two paths. In the first path the heads of the SAM organize to their near final locations with the tail groups loosely formed on top. Then as they transit to phase 3, the tail groups become ordered and straighten out. In the second path the molecules start in a laying down position along the surface. These then form into islands of ordered SAMs, where they grow into phase 3, as seen below.

The nature in which the tail groups organize themselves into a straight ordered monolayer is dependent on the inter-molecular attraction, or Van der Waals forces, between the alkyl and tail groups. To minimize the free energy of the organic layer the molecules adopt conformations that allow high degree of Van der Waals forces with some hydrogen bonding. The small size of the SAM molecules are important here because Van der Waals forces arise from the dipoles of molecules and are thus much weaker than the surrounding surface forces at larger scales. The assembly process begins with a small group of molecules, usually two, getting close enough that the Van der Waals forces overcome the surrounding force. The forces between the molecules orientate themselves so they are in their straight, optimal, configuration. Then as other molecules come close by they interact with these already organized molecules in the same fashion and become a part of the conformed group. When this occurs across a large area the molecules support each other into forming their SAM shape seen in Figure 1. The orientation of the molecules can be described with 2 parameters, α and β. α is the angle of tilt of the backbone from the surface normal. In typical applications α varies from 0 to 60 degrees depending on the substrate and type of SAM molecule. β is the angel of rotation along the long axis of tee molecule. β is usually between 30 and 40 degrees.

Many of the SAM properties, such as thickness, are determined in the first few minutes. However, it may take hours for defects to be eliminated via annealing and for final SAM properties to be determined. The exact kinetics of SAM formation depends on the adsorbate, solvent and substrate properties. In general, however, the kinetics are dependent on both preparations conditions and material properties of the solvent, adsorbate and substrate. Specifically, kinetics for adsorption from a liquid solution are dependent on:

- Temperature – room temperature preparation improves kinetics and reduces defects.
- Concentration of adsorbate in the solution – low concentrations require longer immersion times and often create highly crystalline domains.

- Purity of the adsorbate – impurities can affect the final physical properties of the SAM
- Dirt or contamination on the substrate – imperfections can cause defects in the SAM

The final structure of the SAM is also dependent on the chain length and the structure of both the adsorbate and the substrate. Steric hindrance and metal substrate properties, for example, can affect the packing density of the film, while chain length affects SAM thickness. Longer chain length also increases the thermodynamic stability.

Patterning of SAMs

1. Locally attract

This first strategy involves locally depositing self-assembled monolayers on the surface only where the nanostructure will later be located. This strategy is advantageous because it involves high throughput methods that generally involve less steps than the other two strategies. The major techniques that use this strategy are:

- Micro-contact printing

  Micro-contact printing or soft lithography is analogous to printing ink with a rubber stamp. The SAM molecules are inked onto an pre-shaped elastomeric stamp with a solvent and transferred to the substrate surface by stamping. The SAM solution is applied to the entire stamp but only areas that make contact with the surface allow transfer of the SAMs. The transfer of the SAMs is a complex diffusion process that depends on the type of molecule, concentration, duration of contact, and pressure applied. Typical stamps use PDMS because its elastomeric properties, $E = 1.8$ MPa, allow it to fit the countour of micro surfaces and its low surface energy, $\gamma = 21.6$ dyn/cm^2. This is a parallel process and can thus place nanoscale objects over a large area in a short time.

- Dip-pen nanolithography

  Dip-pen nanolithography is a process that uses an atomic force microscope to transfer molecules on the tip to a substrate. Initially the tip is dipped into a reservoir with an ink. The ink on the tip evaporates and leaves the desired molecules attached to the tip. When the tip is brought into contact with the surface a water meniscus forms between the tip and the surface resulting in the diffusion of molecules from the tip to the surface. These tips can have radii in the tens of nanometers, and thus SAM molecules can be very precisely deposited onto a specific location of the surface. This process was discovered by Chad Mirkin and co-workers at Northwestern University.

2. Locally remove

The locally remove strategy begins with covering the entire surface with a SAM. Then individual SAM molecules are removed from locations where the deposition of nanostructures is not desired. The end result is the same as in the locally attract strategy, the difference being in the way this is achieved. The major techniques that use this strategy are:

- Scanning tunneling microscope

  The scanning tunneling microscope can remove SAM molecules in many different ways. The first is to remove them mechanically by dragging the tip across the substrate surface. This is not the most desired technique as these tips are expensive and dragging them causes a lot of wear and reduction of the tip quality. The second way is to degrade or desorb the SAM molecules by shooting them with an electron beam. The scanning tunneling microscope can also remove SAMs by field desorption and field enhanced surface diffusion.

- Atomic force microscope

  The most common use of this technique is to remove the SAM molecules in a process called shaving, where the atomic force microscope tip is dragged along the surface mechanically removing the molecules. An atomic force microscope can also remove SAM molecules by local oxidation nanolithography.

- Ultraviolet irradiation

  In this process, UV light is projected onto the surface with a SAM through a pattern of apperatures in a chromium film. This leads to photo oxidation of the SAM molecules. These can then be washed away in a polar solvent. This process has 100nm resolutions and requires exposure time of 15-20 minutes.

3. Modify tail groups

The final strategy focuses not on the deposition or removal of SAMS, but the modification of terminal groups. In the first case the terminal group can be modified to remove functionality so that SAM molecule will be inert. In the same regards the terminal group can be modified to add functionality so it can accept different materials or have different properties than the original SAM terminal group. The major techniques that use this strategy are:

- Focused electron beam and ultraviolet irradiation

  Exposure to electron beams and UV light changes the terminal group chemistry. Some of the changes that can occur include the cleavage of bonds, the forming of

double carbon bonds, cross-linking of adjacent molecules, fragmentation of molecules, and confromational disorder.

- Atomic force microscope

  A conductive AFM tip can create an electrochemical reaction that can change the terminal group.

Applications of SAMs

Thin Film SAMs

SAMs are an inexpensive and versatile surface coating for applications including control of wetting and adhesion, chemical resistance, bio compatibility, sensitization, and molecular recognition for sensors and nano fabrication. Areas of application for SAMs include biology, electrochemistry and electronics, nanoelectromechanical systems (NEMS) and microelectromechanical systems (MEMS), and everyday household goods. SAMs can serve as models for studying membrane properties of cells and organelles and cell attachment on surfaces. SAMs can also be used to modify the surface properties of electrodes for electrochemistry, general electronics, and various NEMS and MEMS. For example, the properties of SAMs can be used to control electron transfer in electrochemistry. They can serve to protect metals from harsh chemicals and etchants. SAMs can also reduce sticking of NEMS and MEMS components in humid environments. In the same way, SAMs can alter the properties of glass. A common household product, Rain-X, utilizes SAMs to create a hydrophobic monolayer on car windshields to keep them clear of rain.

Thin film SAMs can also be placed on nanostructures. In this way they functionalize the nanostructure. This is advantageous because the nanostructure can now selectively attach itself to other molecules or SAMs. This technique is useful in biosensors or other MEMS devices that need to separate one type of molecule from its environment. One example is the use of magnetic nanoparticles to remove a fungus from a blood stream. The nanoparticle is coated with a SAM that binds to the fungus. As the contaminated blood is filtered through a MEMS device the magnetic nanoparticles are inserted into the blood where they bind to the fungus and are then magnetically driven out of the blood stream into a nearby laminar waste stream.

Patterned SAMs

SAMs are also useful in depositing nanostructures, because each adsorbate molecule can be tailored to attract two different materials. Current techniques utilize the head to attract to a surface, like a plate of gold. The terminal group is then modified to attract a specific material like a particular nanoparticle, wire, ribbon, or other nanostructure. In this way, wherever the a SAM is patterned to a surface there will be nanostructures attached to the tail groups. One example is the use of two types of SAMs to align single wall carbon nanotubes, SWNTs. Dip pen nanolithography was used to pattern a 16-

mercaptohexadecanoic acid (MHA)SAM and the rest of the surface was passivated with 1-octadecanethiol (ODT) SAM. As the solvent that was carrying the SWNTs evaporated, the SWNTs became attracted to the MHA SAM because of its hydrophilic nature. Once the SWNTs became close enough to the MHA SAM they attached to it due to Van der Waals forces. Using this technique Chad Mirkin, Schatz and their co-workers were able to make complex two dimensional shapes, a representation of a shape created is shown to the right.

Another application of patterned SAMs is the functionalization of biosensors. The tail groups can be modified so they have an affinity for cells, proteins, or molecules. The SAM can then be placed onto a biosensor so that binding of these molecules can be detected. The ability to pattern these SAMs allows them to be placed in configurations that increase sensitivity and do not damage or interfere with other components of the biosensor.

Chapter- 9

Sputtering

Sputtering is a process whereby atoms are ejected from a solid target material due to bombardment of the target by energetic particles. It is commonly used for thin-film deposition, etching and analytical techniques.

A commercial sputtering system

Physics of sputtering

Physical sputtering is driven by momentum exchange between the ions and atoms in the materials, due to collisions.

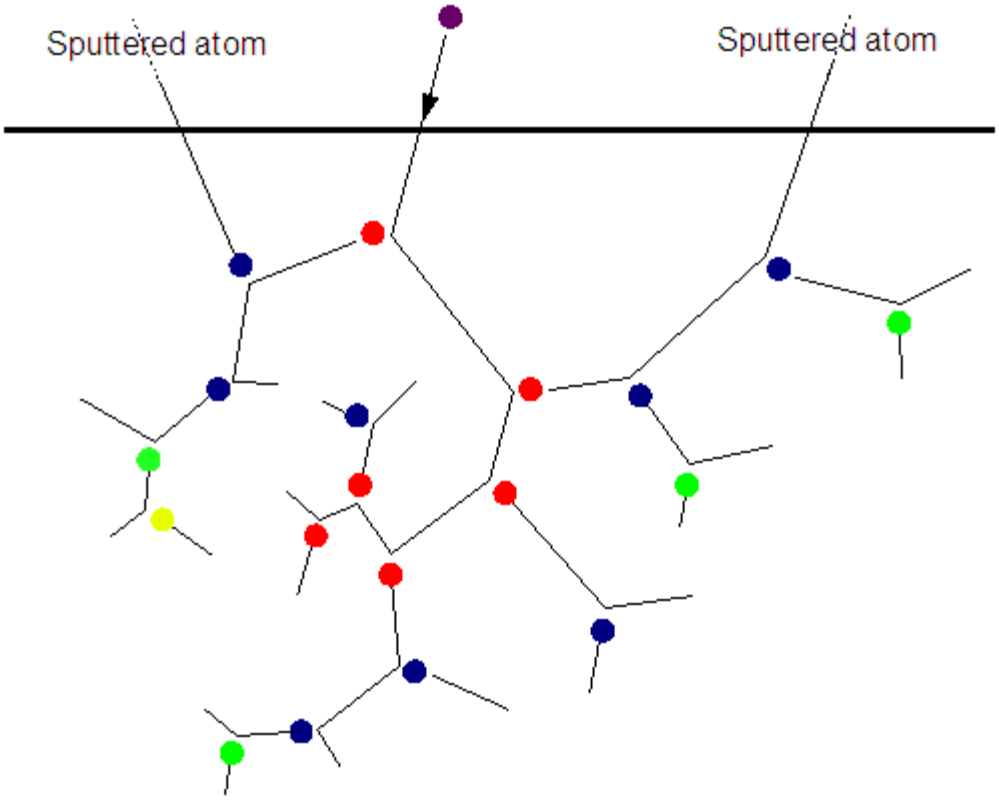

Sputtering from a linear collision cascade. The thick line illustrates the position of the surface, and the thinner lines the ballistic movement paths of the atoms from beginning until they stop in the material. The purple circle is the incoming ion. Red, blue, green and yellow circles illustrate primary, secondary, tertiary and quaternary recoils, respectively. Two of the atoms happen to move out from the sample, i.e. be sputtered.

The incident ions set off collision cascades in the target. When such cascades recoil and reach the target surface with an energy above the surface binding energy, an atom can be ejected. If the target is thin on an atomic scale the collision cascade can reach the back side of the target and atoms can escape the surface binding energy `in transmission'. The average number of atoms ejected from the target per incident ion is called the sputter yield and depends on the ion incident angle, the energy of the ion, the masses of the ion and target atoms, and the surface binding energy of atoms in the target. For a crystalline target the orientation of the crystal axes with respect to the target surface is relevant.

The primary particles for the sputtering process can be supplied in a number of ways, for example by a plasma, an ion source, an accelerator or by a radioactive material emitting alpha particles.

A model for describing sputtering in the cascade regime for amorphous flat targets is Thompson's analytical model. An algorithm that simulates sputtering based on a quantum mechanical treatment including electrons stripping at high energy is implemented in the program TRIM.

A different mechanism of physical sputtering is **heat spike sputtering**. This may occur when the solid is dense enough, and the incoming ion heavy enough, that the collisions occur very close to each other. Then the binary collision approximation is no longer valid, but rather the collisional process should be understood as a many-body process. The dense collisions induce a heat spike (also called thermal spike), which essentially melts the crystal locally. If the molten zone is close enough to a surface, large amounts of atoms may sputter due to flow of liquid to the surface and/or microexplosions. Heat spike sputtering is most important for heavy ions (say Xe or Au or cluster ions) with energies in the keV–MeV range bombarding dense but soft metals with a low melting point (Ag, Au, Pb, ..). The heat spike sputtering often increases nonlinearly with energy, and can for small cluster ions lead to dramatic sputtering yields per cluster of the order of 10000.

Physical sputtering has a well-defined minimum energy threshold which is equal to or larger than the ion energy at which the maximum energy transfer of the ion to a sample atom equals the binding energy of a surface atom. This threshold typically is somewhere in the range 10–100 eV.

Preferential sputtering can occur at the start when a multicomponent solid target is bombarded and there is no solid state diffusion. If the energy transfer is more efficient to one of the target components, and/or it is less strongly bound to the solid, it will sputter more efficiently than the other. If in an AB alloy the component A is sputtered preferentially, the surface of the solid will, during prolonged bombardment, become enriched in the B component thereby increasing the probability that B is sputtered such that the composition of the sputtered material will be AB.

Electronic sputtering

The term **electronic sputtering** can mean either sputtering induced by energetic electrons (for example in a transmission electron microscope), or sputtering due to very high-energy or highly charged heavy ions which lose energy to the solid mostly by electronic stopping power, where the electronic excitations cause sputtering. Electronic sputtering produces high sputtering yields from insulators, as the electronic excitations that cause sputtering are not immediately quenched, as they would be in a conductor. One example of this is Jupiter's ice-covered moon Europa, where an MeV sulfur ion from Jupiter's magnetosphere can eject up to 10,000 H_2O molecules.

Potential sputtering

In the case of multiply charged projectile ions a particular form of electronic sputtering can take place which has been termed **potential sputtering**. In these cases the potential energy stored in multiply charged ions (i.e., the energy necessary to produce an ion of this charge state from its neutral atom) is liberated when the ions recombine during impact on a solid surface (formation of hollow atoms). This sputtering process is characterized by a strong dependence of the observed sputtering yields on the charge state of the impinging ion and can already take place at ion impact energies well below the physical sputtering threshold. Potential sputtering has only been observed for certain target species and requires a minimum potential energy.

Etching and chemical sputtering

Removing atoms by sputtering with an inert gas is called `ion milling' or 'ion etching'.

Sputtering can also play a role in reactive ion etching (RIE), a plasma process carried out with chemically active ions and radicals, for which the sputtering yield may be enhanced significantly compared to pure physical sputtering. Reactive ions are frequently used in Secondary Ion Mass Spectrometry (SIMS) equipment to enhance the sputter rates. The mechanisms causing the sputtering enhancement are not always well understood, but for instance the case of fluorine etching of Si has been modeled well theoretically.

Sputtering which is observed to occur below the threshold energy of physical sputtering, is also often called chemical sputtering. The mechanisms behind such sputtering are not always well understood, and may be hard to distinguish from chemical etching. At elevated temperatures, chemical sputtering of carbon can be understood to be due to the incoming ions weakening bonds in the sample, which then desorb by thermal activation. The hydrogen-induced sputtering of carbon-based materials observed at low temperatures has been explained by H ions entering between C-C bonds and thus breaking them, a mechanism dubbed **swift chemical sputtering**.

Applications and phenomena

Film deposition

Sputter deposition is a method of depositing thin films by sputtering, i.e. eroding, material from a "target," e.g., SiO_2, which then deposits onto a "substrate," e.g., a silicon wafer. Resputtering, in contrast, involves re-emission of the deposited material, e.g., SiO_2, during the deposition also by ion bombardment.

Sputtered atoms ejected into the gas phase are not in their thermodynamic equilibrium state, and tend to deposit on all surfaces in the vacuum chamber. A substrate (such as a wafer) placed in the chamber will be coated with a thin film. Sputtering usually uses an argon plasma.

Etching

In semiconductor industry sputtering is used to etch the target. Sputter etching is chosen in cases where a high degree of etching anisotropy is needed and selectivity is not a concern. One major drawback of this technique is wafer damage.

For analysis

Another application of sputtering is to etch away the target material. One such example occurs in Secondary Ion Mass Spectrometry (SIMS), where the target sample is sputtered at a constant rate. As the target is sputtered, the concentration and identity of sputtered atoms are measured using Mass Spectrometry. In this way the composition of the target material can be determined and even extremely low concentrations (20 μg/kg) of impurities detected. Furthermore, because the sputtering continually etches deeper into the sample, concentration profiles as a function of depth can be measured.

In space

Sputtering is one of the forms of space weathering, a process that changes the physical and chemical properties of airless bodies, such as asteroids and our moon. It is also one of the possible ways that Mars has lost most of its atmosphere and that Mercury continually replenishes its tenuous surface-bounded exosphere.

Chapter- 10

Pulsed Laser Deposition

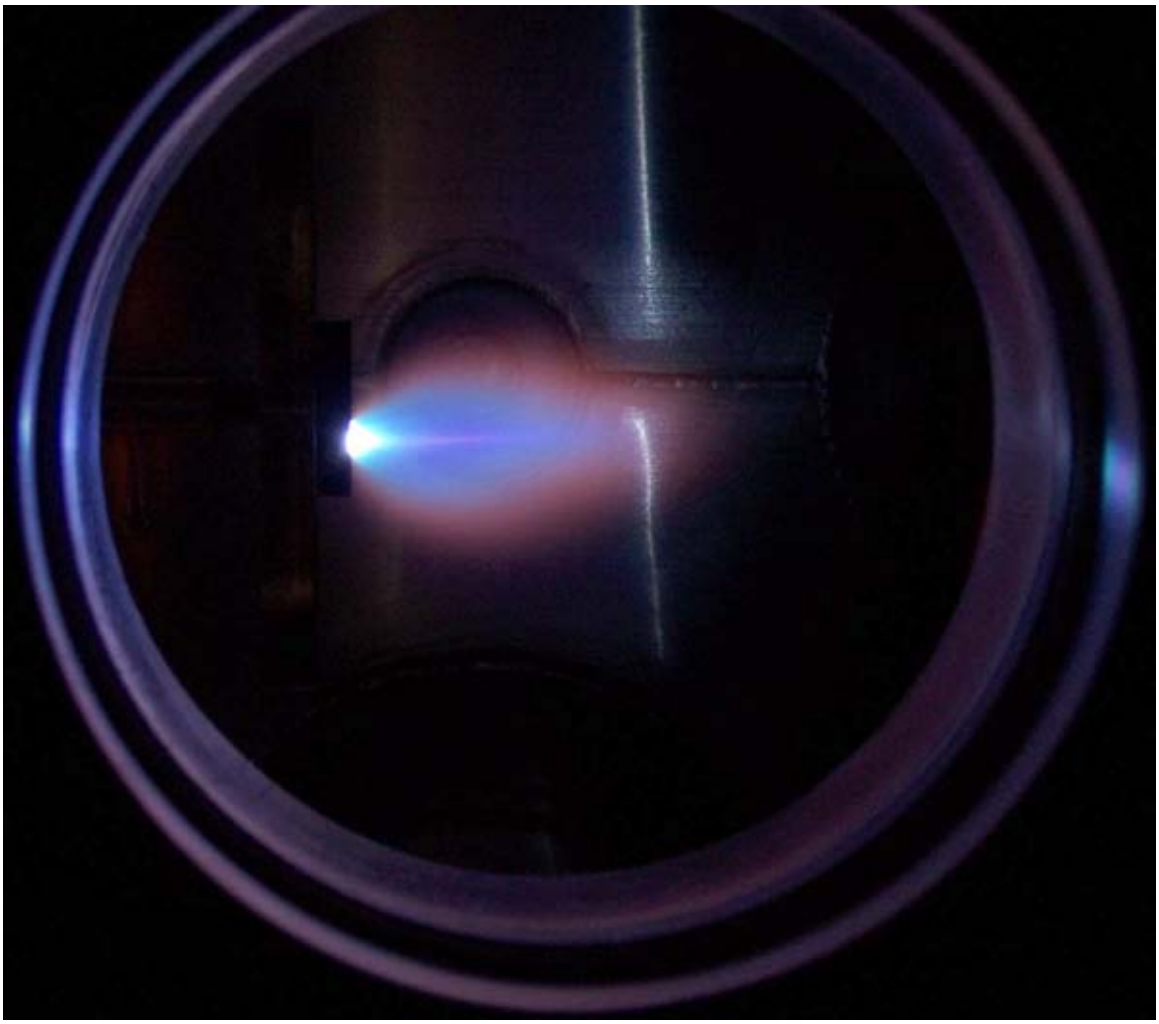

A plume ejected from a $SrRuO_3$ target during pulsed laser deposition.

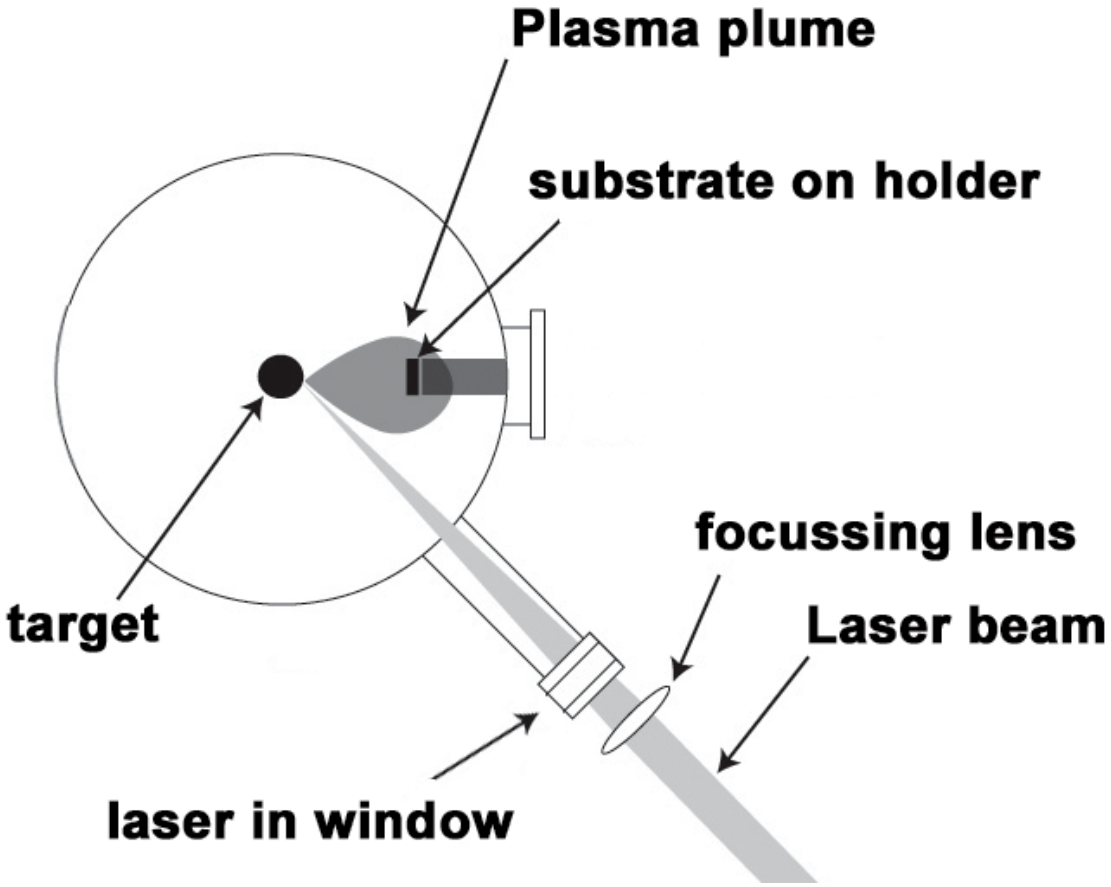

One possible configuration of a PLD deposition chamber.

Pulsed laser deposition (PLD) is a thin film deposition (specifically a physical vapor deposition, PVD) technique where a high power pulsed laser beam is focused inside a vacuum chamber to strike a target of the material that is to be deposited. This material is vaporized from the target (in a plasma plume) which deposits it as a thin film on a substrate (such as a silicon wafer facing the target). This process can occur in ultra high vacuum or in the presence of a background gas, such as oxygen which is commonly used when depositing oxides to fully oxygenate the deposited films.

While the basic-setup is simple relative to many other deposition techniques, the physical phenomena of laser-target interaction and film growth are quite complex. When the laser pulse is absorbed by the target, energy is first converted to electronic excitation and then into thermal, chemical and mechanical energy resulting in evaporation, ablation, plasma formation and even exfoliation. The ejected species expand into the surrounding vacuum in the form of a plume containing many energetic species including atoms, molecules, electrons, ions, clusters, particulates and molten globules, before depositing on the typically hot substrate.

Process

The detailed mechanisms of PLD are very complex including the ablation process of the target material by the laser irradiation, the development of a plasma plume with high energetic ions, electrons as well as neutrals and the crystalline growth of the film itself on the heated substrate. The process of PLD can generally be divided into four stages:

- Laser ablation of the target material and creation of a plasma
- Dynamic of the plasma
- Deposition of the ablation material on the substrate
- Nucleation and growth of the film on the substrate surface

Each of these steps is crucial for the crystallinity, uniformity and stoichiometry of the resulting film.

Laser ablation of the target material and creation of a plasma

The ablation of the target material upon laser irradiation and the creation of plasma are very complex processes. The removal of atoms from the bulk material is done by vaporization of the bulk at the surface region in a state of non-equilibrium and is caused by a Coulomb explosion. In this the incident laser pulse penetrates into the surface of the material within the penetration depth. This dimension is dependent on the laser wavelength and the index of refraction of the target material at the applied laser wavelength and is typically in the region of 10 nm for most materials. The strong electrical field generated by the laser light is sufficiently strong to remove the electrons from the bulk material of the penetrated volume. This process occurs within 10 ps of a ns laser pulse and is caused by non-linear processes such as multiphoton ionization which are enhanced by microscopic cracks at the surface, voids, and nodules, which increase the electric field. The free electrons oscillate within the electromagnetic field of the laser light and can collide with the atoms of the bulk material thus transferring some of their energy to the lattice of the target material with in the surface region. The surface of the target is then heated up and the material is vaporized.

Dynamic of the plasma

In the second stage the material expands in a plasma parallel to the normal vector of the target surface towards the substrate due to Coulomb repulsion and recoil from the target surface. The spatial distribution of the plume is dependent on the background pressure inside the PLD chamber. The density of the plume can be described by a $\cos^n(x)$ law with a shape similar to a Gaussian curve. The dependency of the plume shape on the pressure can be described in three stages:

- The vacuum stage, where the plume is very narrow and forward directed; almost no scattering occurs with the background gases.

- The intermediate region where a splitting of the high energetic ions from the less energetic species can be observed. The time-of-flight (TOF) data can be fitted to a shock wave model; however, other models could also be possible.
- High pressure region where we find a more diffusion-like expansion of the ablated material. Naturally this scattering is also dependent on the mass of the background gas and can influence the stoichiometry of the deposited film.

The most important consequence of increasing the background pressure is the slowing down of the high energetic species in the expanding plasma plume. It has been shown that particles with kinetic energies around 50 eV can resputter the film already deposited on the substrate. This results in a lower deposition rate and can furthermore result in a change in the stoichiometry of the film.

Deposition of the ablation material on the substrate

The third stage is important to determine the quality of the deposited films. The high energetic species ablated from the target are bombarding the substrate surface and may cause damage to the surface by sputtering off atoms from the surface but also by causing defect formation in the deposited film. The sputtered species from the substrate and the particles emitted from the target form a collision region, which serves as a source for condensation of particles. When the condensation rate is high enough, a thermal equilibrium can be reached and the film grows on the substrate surface at the expense of the direct flow of ablation particles and the thermal equilibrium obtained..

Nucleation and growth of the film on the substrate surface

The nucleation process and growth kinetics of the film depend on several growth parameters including:

- *Laser parameters* – several factors such as the laser fluence [Joule/cm^2], laser energy, and ionization degree of the ablated material will affect the film quality, the stoichiometry, and the deposition flux. Generally, the nucleation density increases when the deposition flux is increased.
- *Surface temperature* – The surface temperature has a large affect on the nucleation density. Generally, the nucleation density decreases as the temperature is increased.
- *Substrate surface* – The nucleation and growth can be affected by the surface preparation (such as chemical etching), the miscut of the substrate, as well as the roughness of the substrate.
- *Background pressure* – Common in oxide deposition, an oxygen background is needed to ensure stoichiometric transfer from the target to the film. If, for example, the oxygen background is too low, the film will grow off stoichiometry which will affect the nucleation density and film quality.

In PLD, a large supersaturation occurs on the substrate during the pulse duration. The pulse lasts around 10–40 microseconds depending on the laser parameters. This high

supersaturation causes a very large nucleation density on the surface as compared to Molecular Beam Epitaxy or Sputtering Deposition. This nucleation density increases the smoothness of the deposited film.

In PLD, [depending on the deposition parameters above] three growth modes are possible:

- *Step-flow growth* – All substrates have a miscut associated with the crystal. These miscuts give rise to atomic steps on the surface. In step-flow growth, atoms land on the surface and diffuse to a step edge before they have a chance to nucleated a surface island. The growing surface is viewed as steps traveling across the surface. This growth mode is obtained by deposition on a high miscut substrate, or depositing at elevated temperatures
- *Layer-by-layer growth* – In this growth mode, islands nucleate on the surface until a critical island density is reached. As more material is added, the islands continue to grow until the islands begin to run into each other. This is know a coalescence. Once coalescence is reached, the surface has a large density of pits. When additional material is added to the surface the atoms diffuse into these pits to complete the layer. This process is repeated for each subsequent layer.
- *3D growth* – This mode is similar to the layer-by-layer growth, except that once an island is formed an additional island will nucleate on top of the 1st island. Therefore the growth does not persist in a layer by layer fashion, and the surface roughens each time material is added.

History

Pulsed laser deposition is only one of many thin film deposition techniques. Other methods include molecular beam epitaxy (MBE), chemical vapor deposition (CVD), sputter deposition (RF, Magnetron, and ion beam). The history of laser-assisted film growth started soon after the technical realization of the first laser in 1960 by Maiman. Smith and Turner utilized a ruby laser to deposit the first thin films in 1965, three years after Breech and Cross studied the laser-vaporization and excitation of atoms from solid surfaces. However, the deposited films were still inferior to those obtained by other techniques such as chemical vapor deposition and molecular beam epitaxy. In the early 1980s, a few research groups (mainly in the former USSR) achieved remarkable results on manufacturing of thin film structures utilizing laser technology. The breakthrough came in 1987 when Dijkkamp and Venkatesan were able to laser deposit a thin film of $YBa_2Cu_3O_7$, a high temperature superconductive material, which was of more superior quality than films deposited with alternative techniques. Since then, the technique of Pulsed Laser Deposition has been utilized to fabricate high quality crystalline films. The deposition of ceramic oxides, nitride films, metallic multilayers and various superlattices has been demonstrated. In the 1990s the development of new laser technology, such as lasers with high repetition rate and short pulse durations, made PLD a very competitive tool for the growth of thin, well defined films with complex stoichiometry.

Technical aspects

There are many different arrangements to build a deposition chamber for PLD. The target material which is evaporated by the laser is normally found as a rotating disc attached to a support. However, it can also be sintered into a cylindrical rod with rotational motion and a translational up and down movement along its axis. This special configuration allows not only the utilization of a synchronized reactive gas pulse but also of a multicomponent target rod with which films of different multilayers can be created.

Some factors that influence deposition thickness:

- Target material
- Pulse energy of laser
- Distance from target to substrate
- Type of gas and pressure in chamber (oxygen, argon, etc.)

Chapter- 11

Dye-Sensitized Solar Cell

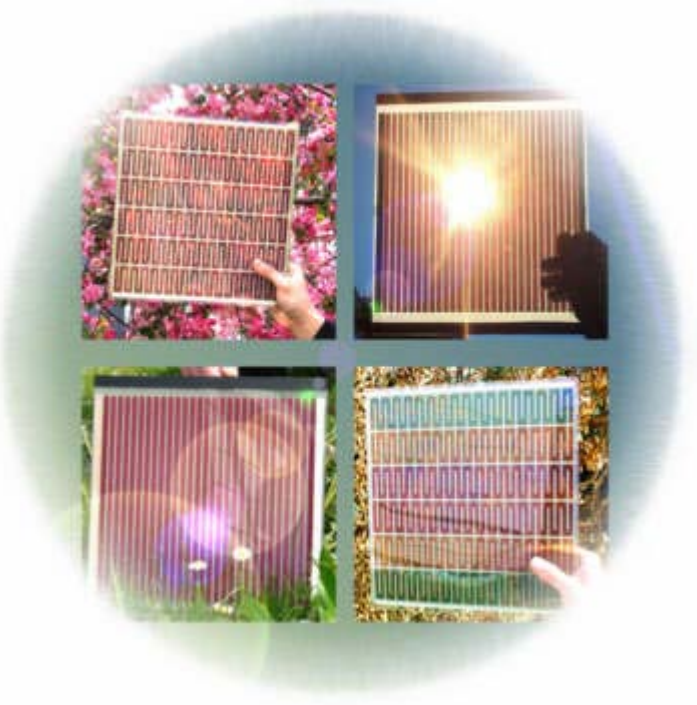

A selection of dye-sensitized solar cells

A **dye-sensitized solar cell** (**DSSC**, **DSC** or **DYSC**) is a class of low-cost solar cell belonging to the group of thin film solar cells. It is based on a semiconductor formed between a photo-sensitized anode and an electrolyte; a *photoelectrochemical* system. This cell was invented by Michael Grätzel and Brian O'Regan at the École Polytechnique Fédérale de Lausanne in 1991 and are also known as **Grätzel cells**. Michael Grätzel won the 2010 Millennium Technology Prize for the invention of the Grätzel cell.

Because it is made of low-cost materials and does not require elaborate apparatus to manufacture, this cell is technically attractive. Likewise, manufacture can be significantly less expensive than older solid-state cell designs. It can also be engineered into flexible

sheets and is mechanically robust, requiring no protection from minor events like hail or tree strikes. Although its conversion efficiency is less than the best thin-film cells, in theory its price/performance ratio (kWh/(m^2·annum·dollar)) should be high enough to allow them to compete with fossil fuel electrical generation by achieving grid parity. Commercial applications, which were held up due to chemical stability problems, are now forecast in the European Union Photovoltaic Roadmap to significantly contribute to renewable electricity generation by 2020.

Current technology: semiconductor solar cells

In a traditional solid-state semiconductor, a solar cell is made from two doped crystals, one doped with n-type impurities (n-type semiconductor), which has "extra free" electrons, and the other doped with p type impurities (p-type semiconductor), which is lacking free electrons. When placed in contact, some of the electrons in the n-type portion flow into the p-type to "fill in" the missing electrons, also known as electron holes. Eventually enough electrons will flow across the boundary to equalize the Fermi levels of the two materials. The result is a region at the interface, the p-n junction, where charge carriers are depleted and/or accumulated on each side of the interface. In silicon, this transfer of electrons produces a potential barrier of about 0.6 to 0.7 V.

When placed in the sun, photons of the sunlight can excite electrons on the n-type side of the semiconductor, a process known as photoexcitation. In silicon, sunlight can provide enough energy to push an electron out of the lower-energy valence band into the higher-energy conduction band. As the name implies, electrons in the conduction band are free to move about the silicon. When a load is placed across the cell as a whole, these electrons will flow out of the n-type side into the p-type side, lose energy while moving through the external circuit, and then back into the n-type material where they can once again re-combine with the valence-band hole they left behind. In this way, sunlight creates an electrical current.

In any semiconductor, the band gap means that only photons with that amount of energy, or more, will contribute to producing a current. In the case of silicon, the majority of visible light from red to violet has sufficient energy to make this happen. Unfortunately higher energy photons, those at the blue and violet end of the spectrum, have more than enough energy to cross the band gap; although some of this extra energy is transferred into the electrons, the majority of it is wasted as heat. Another issue is that in order to have a reasonable chance of capturing a photon, the n-type layer has to be fairly thick. This also increases the chance that a freshly ejected electron will meet up with a previously created hole in the material before reaching the p-n junction. These effects produce an upper limit on the efficiency of silicon solar cells, currently around 12 to 15% for common modules and up to 25% for the best laboratory cells (about 30% is the theoretical maximum efficiency for single band gap solar cells).

By far the biggest problem with the conventional approach is cost; solar cells require a relatively thick layer of doped silicon in order to have reasonable photon capture rates, and silicon processing is expensive. There have been a number of different approaches to

reduce this cost over the last decade, notably the thin-film approaches, but to date they have seen limited application due to a variety of practical problems. Another line of research has been to dramatically improve efficiency through the multi-junction approach, although these cells are very high cost and suitable only for large commercial deployments. In general terms the types of cells suitable for rooftop deployment have not changed significantly in efficiency, although costs have dropped somewhat due to increased supply.

Dye-sensitized solar cells

A DSSC is composed of a porous layer of titanium dioxide nanoparticles, covered with a molecular dye that absorbs sunlight, like the chlorophyll in green leaves. The titanium dioxide is immersed under an electrolyte solution, above which is a platinum-based catalyst. As in a conventional alkaline battery, an anode (the titanium dioxide) and a cathode (the platinum) are placed on either side of a liquid conductor (the electrolyte).

Sunlight passes through the transparent electrode into the dye layer where it can excite electrons that then flow into the titanium dioxide. The electrons flow toward the transparent electrode where they are collected for powering a load. After flowing through the external circuit, they are re-introduced into the cell on a metal electrode on the back, flowing into the electrolyte. The electrolyte then transports the electrons back to the dye molecules.

Dye-sensitized solar cells separate the two functions provided by silicon in a traditional cell design. Normally the silicon acts as both the source of photoelectrons, as well as providing the electric field to separate the charges and create a current. In the dye-sensitized solar cell, the bulk of the semiconductor is used solely for charge transport, the photoelectrons are provided from a separate photosensitive dye. Charge separation occurs at the surfaces between the dye, semiconductor and electrolyte.

The dye molecules are quite small (nanometer sized), so in order to capture a reasonable amount of the incoming light the layer of dye molecules needs to be made fairly thick, much thicker than the molecules themselves. To address this problem, a nanomaterial is used as a scaffold to hold large numbers of the dye molecules in a 3-D matrix, increasing the number of molecules for any given surface area of cell. In existing designs, this scaffolding is provided by the semiconductor material, which serves double-duty.

Construction

In the case of the original Grätzel and O'Regan design, the cell has 3 primary parts. On top is a transparent anode made of fluoride-doped tin dioxide (SnO_2:F) deposited on the back of a (typically glass) plate. On the back of this conductive plate is a thin layer of titanium dioxide (TiO_2), which forms into a highly porous structure with an extremely high surface area. TiO_2 only absorbs a small fraction of the solar photons (those in the UV). The plate is then immersed in a mixture of a photosensitive ruthenium-polypyridine

dye (also called molecular sensitizers) and a solvent. After soaking the film in the dye solution, a thin layer of the dye is left covalently bonded to the surface of the TiO_2.

A separate plate is then made with a thin layer of the iodide electrolyte spread over a conductive sheet, typically platinum metal. The two plates are then joined and sealed together to prevent the electrolyte from leaking. The construction is simple enough that there are hobby kits available to hand-construct them. Although they use a number of "advanced" materials, these are inexpensive compared to the silicon needed for normal cells because they require no expensive manufacturing steps. TiO_2, for instance, is already widely used as a paint base.

Operation

Sunlight enters the cell through the transparent SnO_2:F top contact, striking the dye on the surface of the TiO_2. Photons striking the dye with enough energy to be absorbed create an excited state of the dye, from which an electron can be "injected" directly into the conduction band of the TiO_2. From there it moves by diffusion (as a result of an electron concentration gradient) to the clear anode on top.

Meanwhile, the dye molecule has lost an electron and the molecule will decompose if another electron is not provided. The dye strips one from iodide in electrolyte below the TiO_2, oxidizing it into triiodide. This reaction occurs quite quickly compared to the time that it takes for the injected electron to recombine with the oxidized dye molecule, preventing this recombination reaction that would effectively short-circuit the solar cell.

The triiodide then recovers its missing electron by mechanically diffusing to the bottom of the cell, where the counter electrode re-introduces the electrons after flowing through the external circuit.

Efficiency

Several important measures are used to characterize solar cells. The most obvious is the total amount of electrical power produced for a given amount of solar power shining on the cell. Expressed as a percentage, this is known as the *solar conversion efficiency*. Electrical power is the product of current and voltage, so the maximum values for these measurements are important as well, J_{sc} and V_{oc} respectively. Finally, in order to understand the underlying physics, the "quantum efficiency" is used to compare the chance that one photon (of a particular energy) will create one electron.

In quantum efficiency terms, DSSCs are extremely efficient. Due to their "depth" in the nanostructure there is a very high chance that a photon will be absorbed, and the dyes are very effective at converting them to electrons. Most of the small losses that do exist in DSSC's are due to conduction losses in the TiO_2 and the clear electrode, or optical losses in the front electrode. The overall quantum efficiency for green light is about 90%, with the "lost" 10% being largely accounted for by the optical losses in top electrode. The

quantum efficiency of traditional designs vary, depending on their thickness, but are about the same as the DSSC.

In theory, the maximum voltage generated by such a cell is simply the difference between the (*quasi*-)Fermi level of the TiO_2 and the redox potential of the electrolyte, about 0.7 V under solar illumination conditions (V_{oc}). That is, if an illuminated DSSC is connected to a voltmeter in an "open circuit", it would read about 0.7 V. In terms of voltage, DSSCs offer slightly higher V_{oc} than silicon, about 0.7 V compared to 0.6 V. This is a fairly small difference, so real-world differences are dominated by current production, J_{sc}.

Although the dye is highly efficient at converting absorbed photons into free electrons in the TiO_2, only photons absorbed by the dye ultimately produce current. The rate of photon absorption depends upon the absorption spectrum of the sensitized TiO_2 layer and upon the solar flux spectrum. The overlap between these two spectra determines the maximum possible photocurrent. Typically used dye molecules generally have poorer absorption in the red part of the spectrum compared to silicon, which means that fewer of the photons in sunlight are usable for current generation. These factors limit the current generated by a DSSC, for comparison, a traditional silicon-based solar cell offers about 35 mA/cm^2, whereas current DSSCs offer about 20 mA/cm^2.

Combined with a fill factor of about 45%, overall peak power production efficiency for current DSSCs is about 11%.

Degradation

DSSCs degrade when exposed to ultraviolet radiation. The barrier layer may include UV stabilizers and/or UV absorbing luminescent chromophores (which emit at longer wavelengths) and antioxidants to protect and improve the efficiency of the cell.

Advantages and drawbacks

DSSCs are currently the most efficient third-generation (2005 Basic Research Solar Energy Utilization 16) solar technology available. Other thin-film technologies are typically between 5% and 13%, and traditional low-cost commercial silicon panels operate between 12% and 15%. This makes DSSCs attractive as a replacement for existing technologies in "low density" applications like rooftop solar collectors, where the mechanical robustness and light weight of the glass-less collector is a major advantage. They may not be as attractive for large-scale deployments where higher-cost higher-efficiency cells are more viable, but even small increases in the DSSC conversion efficiency might make them suitable for some of these roles as well.

There is another area where DSSCs are particularly attractive. The process of injecting an electron directly into the TiO_2 is qualitatively different to that occurring in a traditional cell, where the electron is "promoted" within the original crystal. In theory, given low rates of production, the high-energy electron in the silicon could re-combine with its own hole, giving off a photon (or other form of energy) and resulting in no current being

generated. Although this particular case may not be common, it is fairly easy for an electron generated in another molecule to hit a hole left behind in a previous photoexcitation.

In comparison, the injection process used in the DSSC does not introduce a hole in the TiO_2, only an extra electron. Although it is energetically possible for the electron to recombine back into the dye, the rate at which this occurs is quite slow compared to the rate that the dye regains an electron from the surrounding electrolyte. Recombination directly from the TiO_2 to species in the electrolyte is also possible although, again, for optimized devices this reaction is rather slow. On the contrary, electron transfer from the platinum coated electrode to species in the electrolyte is necessarily very fast.

As a result of these favorable "differential kinetics", DSSCs work even in low-light conditions. DSSCs are therefore able to work under cloudy skies and non-direct sunlight, whereas traditional designs would suffer a "cutout" at some lower limit of illumination, when charge carrier mobility is low and recombination becomes a major issue. The cutoff is so low they are even being proposed for indoor use, collecting energy for small devices from the lights in the house.

A practical advantage, one DSSCs share with most thin-film technologies, is that the cell's mechanical robustness indirectly leads to higher efficiencies in higher temperatures. In any semiconductor, increasing temperature will promote some electrons into the conduction band "mechanically". The fragility of traditional silicon cells requires them to be protected from the elements, typically by encasing them in a glass box similar to a greenhouse, with a metal backing for strength. Such systems suffer noticeable decreases in efficiency as the cells heat up internally. DSSCs are normally built with only a thin layer of conductive plastic on the front layer, allowing them to radiate away heat much easier, and therefore operate at lower internal temperatures.

The major disadvantage to the DSSC design is the use of the liquid electrolyte, which has temperature stability problems. At low temperatures the electrolyte can freeze, ending power production and potentially leading to physical damage. Higher temperatures cause the liquid to expand, making sealing the panels a serious problem. Another major drawback is the electrolyte solution, which contains volatile organic solvents and must be carefully sealed. This, along with the fact that the solvents permeate plastics, has precluded large-scale outdoor application and integration into flexible structure.

Replacing the liquid electrolyte with a solid has been a major ongoing field of research. Recent experiments using solidified melted salts have shown some promise, but currently suffer from higher degradation during continued operation, and are not flexible.

Photocathodes and tandem cells

Grätzel’s cell operates as a photoanode (n-DSC), where photocurrent result from electron injection by the sensitized dye. Photocathodes (p-DSCs)operate in an inverse mode compared to the conventional n-DSC, where dye-excitation is followed by rapid electron

transfer from a p-type semiconductor to the dye (dye-sensitized hole injection, instead of electron injection). Such p-DSCs and n-DSCs can be combined to construct tandem solar cells (pn-DSCs) and the theoretical efficiency of tandem DSCs is well beyond that of single-junction DSCs.

A standard tandem cell consists of one n-DSC and one p-DSC in a simple sandwich configuration with an intermediate electrolyte layer. n-DSC and p-DSC are connected in series, which implies that the resulting photocurrent will be controlled by the weakest photoelectrode, whereas photovoltages are additive. Thus, Photocurrent matching is very important for the construction of highly efficient tandem pn-DSCs. However, unlike n-DSCs, fast charge recombination following dye-sensitized hole injection usually resulted in low photocurrents in p-DSC and thus hampered the efficiency of the overall device.

Researchers have found that using dyes comprising a perylenemonoimid (PMI) as the acceptor and an oligothiophene coupled to triphenylamine as the donor greatly improve the performance of p-DSC by reducing charge recombination rate following dye-sensitized hole injection. The researchers constructed a tandem DSC device with NiO on the p-DSC side and TiO_2 on the n-DSC side. Photocurrent matching was achieved through adjustment of NiO and TiO_2 film thicknesses to control the optical absorptions and therefore match the photocurrents of both electrodes. The energy conversion efficiency of the device is 1.91%, which exceeds the efficiency of its individual components, but is still much lower than that of high performance n-DSC devices (6%–11%). The results are still promising since the tandem DSC was in itself rudimentary. The dramatic improvement in performance in p-DSC can eventually lead to tandem devices with much greater efficiency than lone n-DSCs.

Development

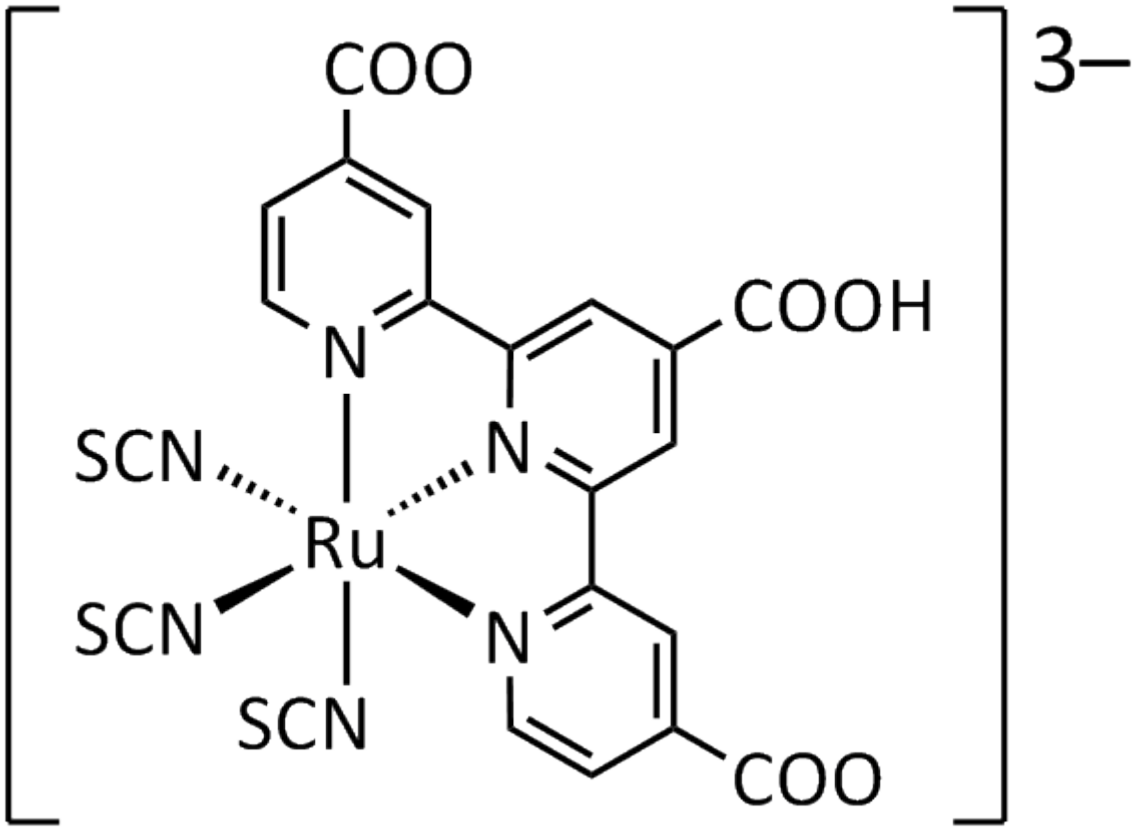

"Black Dye", an anionic Ru-terpyridine complex

The dyes used in early experimental cells (circa 1995) were sensitive only in the high-frequency end of the solar spectrum, in the UV and blue. Newer versions were quickly introduced (circa 1999) that had much wider frequency response, notably "triscarboxy-ruthenium terpyridine" [Ru(4,4',4"-$(COOH)_3$-terpy)$(NCS)_3$], which is efficient right into the low-frequency range of red and IR light. The wide spectral response results in the dye having a deep brown-black color, and is referred to simply as "black dye". The dyes have an excellent chance of converting a photon into an electron, originally around 80% but improving to almost perfect conversion in more recent dyes, the overall efficiency is about 90%, with the "lost" 10% being largely accounted for by the optical losses in top electrode.

A solar cell must be capable of producing electricity for at least twenty years, without a significant decrease in efficiency (life span). The "black dye" system was subjected to 50 million cycles, the equivalent of ten years' exposure to the sun in Switzerland. No discernible performance decrease was observed. However the dye is subject to breakdown in high-light situations. Over the last decade an extensive research program has been carried out to address these concerns. The newer dyes included 1-ethyl-3 methylimidazolium tetrocyanoborate [$EMIB(CN)_4$] which is extremely light- and

temperature-stable, copper-diselenium [Cu(In,GA)Se_2] which offers higher conversion efficiencies, and others with varying special-purpose properties.

DSSCs are still at the start of their development cycle. Efficiency gains are possible and have recently started more widespread study. These include the use of quantum dots for conversion of higher-energy (higher frequency) light into multiple electrons, using solid-state electrolytes for better temperature response, and changing the doping of the TiO_2 to better match it with the electrolyte being used.

New developments

2003

A group of researchers at the Swiss Federal Institute of Technology has reportedly increased the thermostability of DSC by using amphiphilic ruthenium sensitizer in conjunction with quasi-solid-state gel electrolyte. The stability of the device matches that of a conventional inorganic silicon based solar cells. The cell sustained heating for 1,000 h at 80 °C.

The group has previously prepared an ruthenium amphiphilic dye Z-907 (cis-Ru(H_2dcbpy)(dnbpy)$(NCS)_2$,where the ligand H_2dcbpy is 4,4′-dicarboxylic acid-2,2′-bipyridine and dnbpy is 4,4′-dinonyl-2,2′-bipyridine) to increase dye tolerance to water in the electrolytes. In addition, the group also prepared a quasi-solid-state gel electrolye with a 3-methoxypropionitrile (MPN)-based liquid electrolyte that was solidified by a photochemically stable fluorine polymer, poly(vinylidenefluoride-co-hexafluoropropylene (PVDF-HFP).

The use of the amphiphilic Z-907 dye in conjunction with the polymer gel electrolyte in DSC achieved an energy conversion efficiency of 6.1%. More importantly, the device was stable under thermal stress and soaking with light. The high conversion efficiency of the cell was sustained after heating for 1,000 h at 80 °C, maintaining 94% of its initial value. After accelerated testing in a solar simulator for 1,000 h of light-soaking at 55 °C (100 mW cm^{-2}) the efficiency had decreased by less than 5% for cells covered with an ultraviolet absorbing polymer film. These results are well within the limit for that of traditional inorganic silicon solar cells.

The enhanced performance may arise from a decrease in solvent permeation across the sealant due to the application of the polymer gel electrolyte. The polymer gel electrolyte is quasi-solid at room temperature, and becomes a viscous liquid (viscosity: 4.34 mPa·s) at 80 °C compared with the traditional liquid electrolyte (viscosity: 0.91 mPa·s). The much improved stabilities of the device under both thermal stress and soaking with light has never before been seen in DSCs, and they match the durability criteria applied to solar cells for outdoor use, which makes these devices viable for practical application.

2006

The first successful solid-hybrid dye-sensitized solar cells were reported.

To improve electron transport in these solar cells, while maintaining the high surface area needed for dye adsorption, two researchers have designed alternate semiconductor morphologies, such as arrays of nanowires and a combination of nanowires and nanoparticles, to provide a direct path to the electrode via the semiconductor conduction band. Such structures may provide a means to improve the quantum efficiency of DSSCs in the red region of the spectrum, where their performance is currently limited.

On August 2006, to prove the chemical and thermal robustness of the 1-ethyl-3 methylimidazolium tetracyanoborate solar cell, the researchers subjected the devices to heating at 80 °C in the dark for 1000 hours, followed by light soaking at 60 °C for 1000 hours. After dark heating and light soaking, 90% of the initial photovoltaic efficiency was maintained – the first time such excellent thermal stability has been observed for a liquid electrolyte that exhibits such a high conversion efficiency. Contrary to silicon solar cells, whose performance declines with increasing temperature, the dye-sensitized solar-cell devices were only negligibly influenced when increasing the operating temperature from ambient to 60 °C.

April 2007

Wayne Campbell at Massey University, New Zealand, has experimented with a wide variety of organic dyes based on porphyrin. In nature, porphyrin is the basic building block of the hemoproteins, which include chlorophyll in plants and hemoglobin in animals. He reports efficiency on the order of 5.6% using these low-cost dyes.

June 2008

An article published in *Nature Materials* demonstrated cell efficiencies of 8.2% using a new solvent-free liquid redox electrolyte consisting of a melt of three salts, as an alternative to using organic solvents as an electrolyte solution. Although the efficiency with this electrolyte is less than the 11% being delivered using the existing iodine-based solutions, the team is confident the efficiency can be improved.

2009

A group of researchers at Georgia Tech made dye-sensitized solar cells with a higher effective surface area by wrapping the cells around a quartz optical fiber. The researchers removed the cladding from optical fibers, grew zinc oxide nanowires along the surface, treated them with dye molecules, surrounded the fibers by an electrolyte and a metal film that carries electrons off the fiber. The cells are six times more efficient than a zinc oxide cell with the same surface area. Photons bounce inside the fiber as they travel, so there are more chances to interact with the solar cell and produce more current. These devices only collect light at the tips, but future fiber cells could be made to absorb light along the

entire length of the fiber, which would require a coating that is conductive as well as transparent. Max Shtein of the University of Michigan said a sun-tracking system would not be necessary for such cells, and would work on cloudy days when light is diffuse.

2010

Researchers at the École Polytechnique Fédérale de Lausanne and at the Université du Québec à Montréal claim to have overcome two of the DSC's major issues:

- "new molecules" have been created for the electrolyte, resulting in a liquid or gel that is transparent and non-corrosive, which can increase the photovoltage and improve the cell's output and stability.
- At the cathode, platinum was replaced by cobalt sulfide, which is far less expensive, more efficient, more stable and easier to produce in the laboratory.

Market introduction

Several commercial providers are promising availability of DSCs in the near future:

- Solaronix, a Swiss company specialized in the production of DSC materials since 1993, has extended their premises in 2010 to host a manufacturing pilot line of DSC modules.
- SolarPrint founded in 2008 by Dr. Mazhar Bari, Andre Fernon and Roy Horgan. SolarPrint is the first Ireland-based commercial entity involved in the manufacturing of PV technology. SolarPrint's innovation is the solution to the solvent based electrolyte which to date has prohibited the mass commercialisation of DSSC.
- G24innovations, founded in 2006, based in Cardiff, South Wales, UK. On October 17, 2007, claimed the production of the first commercial grade dye sensitised thin films.
- Hydrogen Solar is another company making dye-sensitized cells.
- Dyesol officially opened its new manufacturing facilities in Queanbeyan on the 7th of October 2008.
- Konarka, announced in 2002 that they were granted licensee rights to dye-sensitized solar cell technology from the Swiss Federal Institute of Technology (EPFL).
- Aisin Seiki has worked with Toyota Central R&D Labs to develop dye-sensitized solar cells (DSC) for applications in cars and homes.
- Sony Corporation has developed dye-sensitized solar cells with an energy conversion efficiency of 10%, a level seen as necessary for commercial use.

Chapter- 12

Cadmium Telluride Photovoltaics

A CdTe photovoltaic array

Cadmium telluride (CdTe) photovoltaics describes a photovoltaic (PV) technology that is based on the use of cadmium telluride thin film, a semiconductor layer designed to absorb and convert sunlight into electricity. Cadmium telluride PV is the first and only thin film photovoltaic technology to surpass crystalline silicon PV in cheapness for a significant portion of the PV market, namely in multi-kilowatt systems.

Background

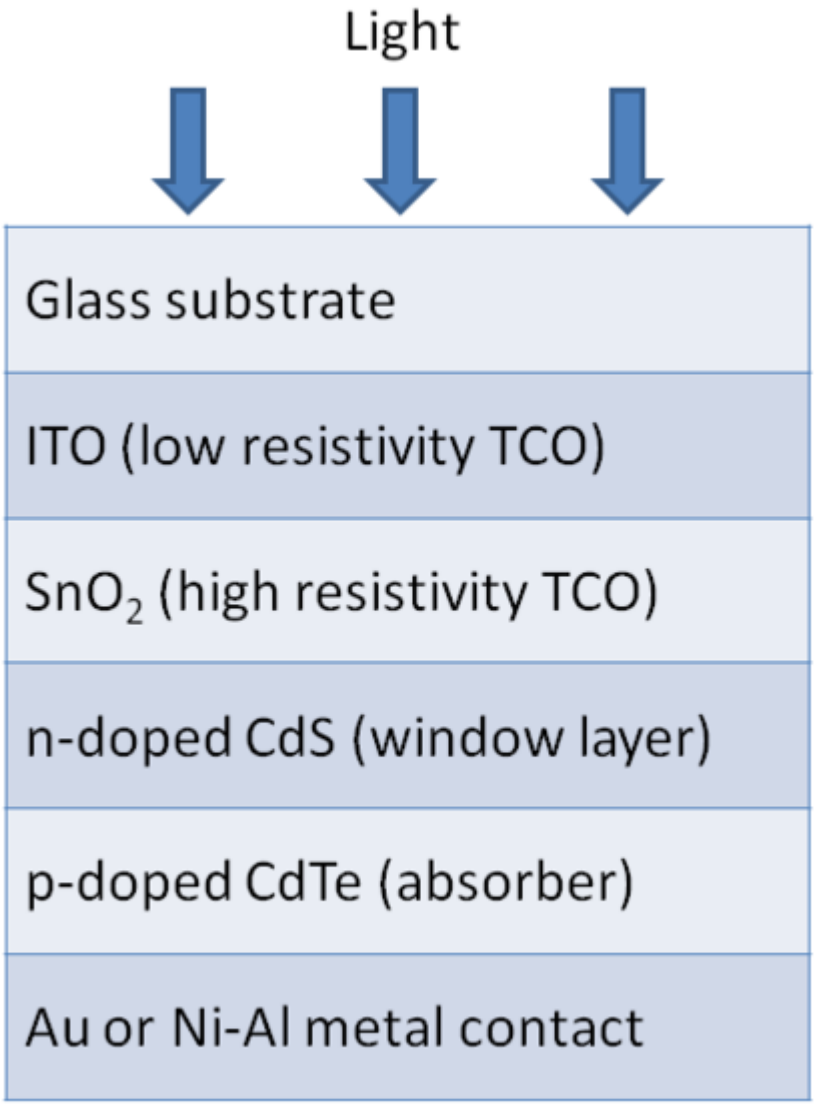

Cross-section of a CdTe thin film solar cell.

Since inception, the dominant solar cell technology in the marketplace has been based on wafers of crystalline silicon. During the same period, the idea of developing alternative, lower cost PV technologies led to the consideration of thin films and concentrators. Thin films are based on using thinner semiconductor layers to absorb and convert sunlight; concentrators, on the idea of replacing expensive semiconductors with lenses or mirrors. Both reduce cost, in theory, by reducing the use of semiconductor material. However, both faced critical challenges.

The first thin film technology to be extensively developed and manufactured was amorphous silicon. However, this technology suffers from low efficiencies and slow deposition rates (leading to high capital costs) and has not become a market leader. Instead, the PV market has grown to almost 4 gigawatts with wafer-based crystalline silicon comprising almost 90% of sales. Installation trails production by a slight time lag, and the same source estimates about 3 gigawatts were installed in 2007.

During this period, two other thin films continued in development (cadmium telluride, and copper indium diselenide or CIS-alloys). The latter is beginning to be produced in start-up volumes of 1–30 megawatts per year by individual companies and remains an unproven, but promising market competitor due to very high, small-area cell efficiencies approaching 20% in the laboratory.

History

40-MW CdTe PV Array, Waldpolenz, Germany

Research in CdTe dates back to the 1950s, because it was quickly identified as having a band gap (about 1.5 eV) almost perfectly matched to the distribution of photons in the solar spectrum in terms of optimal conversion to electricity. A simple heterojunction design evolved in which p-type CdTe was matched with n-type cadmium sulfide (CdS). The cell was completed by adding top and bottom contacts. Early leaders in CdS/CdTe cell efficiencies were GE in the 1960s, and then Kodak, Monosolar, Matsushita, and AMETEK.

By 1981, Kodak used close spaced sublimation (CSS) and made the first 10% cells and first multi-cell devices (12 cells, 8% efficiency, 30 cm^2). Monosolar and AMETEK used electrodeposition, a popular early method. Matsushita started with screen printing but shifted in the 1990s to CSS. Cells of about 10% sunlight-to-electricity efficiency were being made by the early 1980s at Kodak, Matsushita, Monosolar, and Ametek.

An important step forward occurred when cells were being scaled-up in size to make larger area products called modules. These products require higher currents than small cells and it was found that an additional layer, called a transparent conductive oxide (TCO), could facilitate the movement of current across the top of the cell (instead of a metal grid). One such TCO, tin oxide, was already being applied to glass for other uses (thermally reflective windows). Made more conductive for PV, tin oxide became and remains the norm in CdTe PV modules.

Professor Ting L. Chu of Southern Methodist University and subsequently of University of South Florida, Tampa, made significant contributions to moving the efficiency of CdTe cells to above 15% in 1992, a critical level of success in terms of potential commercial competitiveness. This was done when he added an intervening or buffer layer to the TCO/CdS/CdTe stack and then thinned the CdS to allow more light through. Chu used resistive tin oxide as the buffer layer and then thinned the CdS from several micrometres to under half a micrometre in thickness. Thick CdS, as it was used in prior devices, blocked about 5 mA/cm^2 of light, or about 20% of the light usable by a CdTe device. By removing this loss while maintaining the other properties of the device, Chu reached 15% efficiency in 1991, the first thin film to do so, as verified at the National Renewable Energy Laboratory(NREL). Chu used CSS for depositing the CdTe. For his achievements in taking CdTe from its status as “also-ran” to a primary candidate for commercialization, some think of Ting L. Chu as the key technologist in the history of CdTe development.

In the early 1990s, another set of entrants were active in CdTe commercial development, but with mixed results. A short-lived company, Golden Photon replaced Photon Energy, when it was bought by the Coors Company in 1992. Golden Photon, led by Scot Albright and John Jordan, actually held the record for a short period for the best CdTe module measured at NREL at 7.7% using a spray deposition technique. Meanwhile Matsushita, BP Solar, and Solar Cells Inc. were active. Matsushita claimed an 11% module efficiency using CSS and then dropped out of the technology, perhaps due to internal corporate pressures over cadmium. A similar efficiency and fate eventually occurred at BP Solar. BP used electrodeposition inherited from Monosolar by a circuitous route when it purchased SOHIO. SOHIO had previously bought Monosolar. BP Solar however never made a complete commitment to their CdTe technology despite its achievements and dropped it in the early 2000s. Another ineffective corporate evolution occurred at a European entrant, Antec. Founded by CdTe pioneer Dieter Bonnet (who made cells in the 1960s), Antec was able to make about 7%-efficient modules, but went bankrupt when it started producing commercially during a short, sharp downturn in the market in 2002. Purchased from bankruptcy, it never regained the technical traction needed to make further progress. However, as of 2008 Antec does make and sell CdTe PV modules.

There are a number of start-ups in CdTe today: Q-Cells' Calyxo (Germany), GE's PrimeStar Solar (Arvada, Colorado), Arendi (Italy), and Abound Solar (Fort Collins, Colorado). Including Antec, their total production represents less than 70 megawatts per year. In February 2009, Roth & Rau announced to develop turnkey CdTe production lines and launch the business before end of 2009.

There has been a lot of research on fabricating CdTe cells on flexible substrate since 1999. In 2009, EMPA, the Swiss Federal Laboratories for Materials Testing and Research, demonstrated a 12.4% efficient solar cell on flexible polyimide substrate.

SCI and First Solar

The major commercial success to emerge from the turmoil of the 1990s was Solar Cells Incorporated (SCI). Founded in 1990 as an outgrowth of a prior company, Glasstech Solar (founded 1984), led by inventor/entrepreneur Harold McMaster, it switched from amorphous silicon to CdTe as a better solution to the higher-cost crystalline silicon PV. McMaster championed CdTe for its high-rate, high-throughput processing. Technical leadership came from a team that included Jim Nolan, Rick Powell, Jim Foote, and Peter Meyers, with consulting help from Ting Chu and Al Compaan (U. Toledo). SCI started with an adaptation of the CSS method then shifted to a vapor transport approach, inspired by Powell. In February 1999, McMaster sold the company to True North Partners, an investment arm of the Walton family, owners of Wal-Mart. John T. Walton joined the Board of the new company, and Mike Ahearn of True North became the CEO of the newly minted First Solar.

In its early years First Solar suffered setbacks, and initial module efficiencies were modest, about 7%. Commercial product became available in 2002. But production did not reach 25 megawatts until 2005. The company built an additional line in Perrysburg, Ohio, then four lines in Germany, supported by the then substantial German production incentives (about 50% of capital costs). In 2006 First Solar reached 75 MW of annual production and announced a further 16 lines in Malaysia. The more recently announced lines have been operational ahead of schedule. As of 2008, First Solar is producing at nearly half a gigawatt annual rate, and in 2006 and 2007 was among the largest PV module manufacturers in the world.

Issues

Cell efficiency

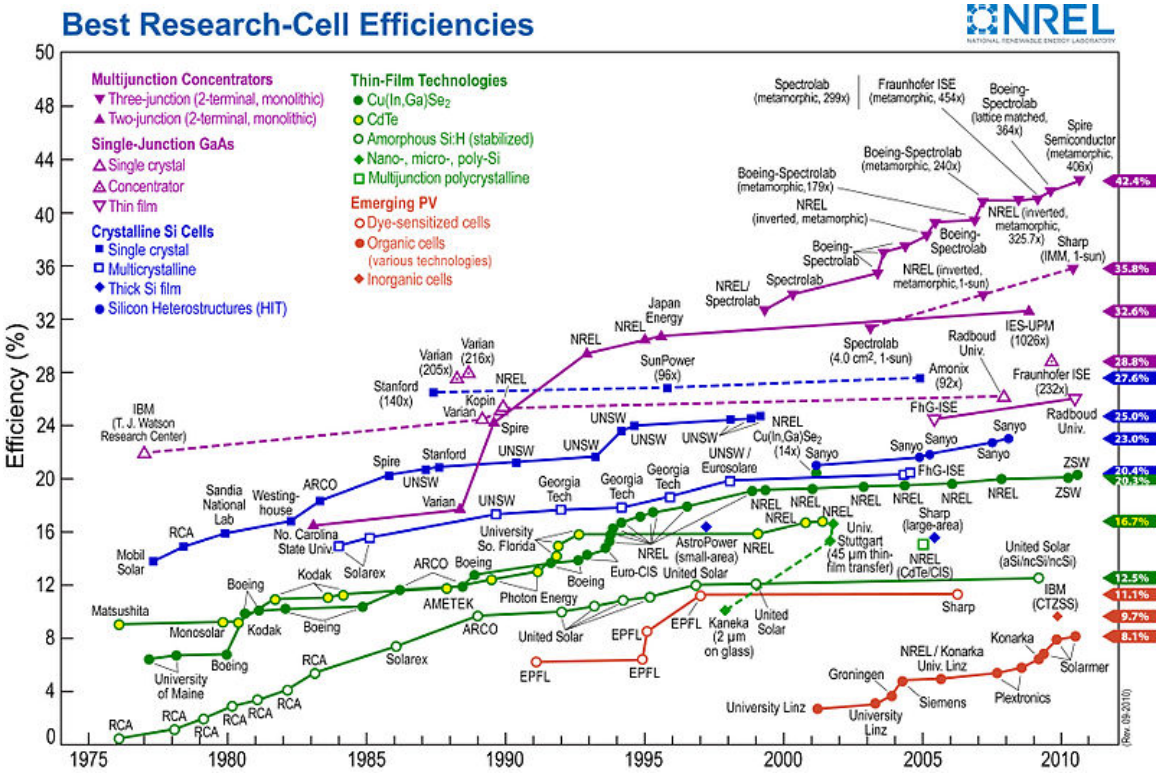

Solar Cell Efficiencies

Best cell efficiency has plateaued at 16.5% since 2001. The opportunity to increase current has been almost fully exploited, but more difficult challenges associated with junction quality, with properties of CdTe and with contacting have not been as successful. However, until recently the number of active scientists in CdTe PV was small. Improved doping of CdTe and increased understanding of key processing steps (e.g., cadmium chloride recrystallization and contacting) are key to progress. Since CdTe has the optimal band gap for single-junction devices, it may be expected that efficiencies close to exceeding 20% (such as already shown in CIS alloys) should be achievable in practical CdTe cells. Modules of 15% would then be possible.

Process optimization

Process optimization allows greater throughput at smaller cost. Typical improvements are broader substrates (since capital costs scale sublinearly, and installation costs can be reduced), thinner layers (to save material, electricity, and throughput time), and better material utilization (to save material and cleaning costs). Making components rather than buying them is also a traditional way for great manufacturers to shave costs. Today's CdTe module costs are about $\$110/m^2$ (normalized to a square meter). Costs are expected to reduce to $\$75/m^2$.

Thus a practical, long-term (10–20 year) goal for CdTe modules resulting from combining cost and efficiency goals would be $75 per 150 watts, or about $0.5 per watt. With commodity-like margins and combined with balance-of-system (BOS) costs, installed systems near $1.5/W seem achievable. With Southern California sunlight, this would be in the 6 to 8 US cents per kWh range (e.g., based on economic and other assumptions used in algorithms such as in the United States Department of Energy and NREL's Solar Advisory Model).

Tellurium supply

Perhaps the most subtle and least understood problem with CdTe PV is the supply of tellurium. Tellurium (Te) is an element not currently used for many applications. Only a small amount, estimated to be about 800 metric tons per year, is available. According to USGS, global tellurium production in 2007 was 135 metric tons. Most of it comes as a by-product of copper, with smaller byproduct amounts from lead and gold. One gigawatt (GW) of CdTe PV modules would require about 93 metric tons (at current efficiencies and thicknesses), so this seems like a limiting factor. However, because tellurium has had so few uses, it has not been the focus of geologic exploration. In the last decade, new supplies of tellurium-rich ores have been located, e.g., in Xinju, China. Since CdTe is now regarded as an important technology in terms of PV's future impact on global energy and environment, the issue of tellurium availability is significant. Recently, researchers have added an unusual twist – astrophysicists identify tellurium as the most abundant element in the universe with an atomic number over 40. This surpasses, e.g., heavier materials like tin, bismuth, and lead, which are common. Researchers have shown that well-known undersea ridges (which are now being evaluated for their economic recoverability) are rich in tellurium and by themselves could supply more tellurium than we could ever use for all of our global energy. It is not yet known whether this undersea tellurium is recoverable, nor whether there is much more tellurium elsewhere that can be recovered.

Other issues

Cadmium

Another issue frequently mentioned, is the use and recycling of the extremely toxic metal cadmium, one of the six most toxic materials banned by European Union's RoHS regulation. According to First Solar's annual report, the CdTe solar panel is not in RoHS compliance, not listed in the exemption product list, but not currently listed in the restricted product list either. So the product's future RoHS compliance status is uncertain. First Solar has a self-imposed recycling regimen that provides a deposited amount (<$0.05 a watt) that covers the costs of transport and recycling of the module at the end of its useful life. Recycling has been fully demonstrated on scrap modules although recent work has questioned the economic viability of recycling CdTe PV modules and called for producer responsibility policy to ensure all CdTe PV is recycled. In a validating test, Vasilis Fthenakis of the Brookhaven National Laboratory showed that the glass plates surrounding CdTe material sandwiched between them (as they are in all

commercial modules) seal during a fire and do not allow any cadmium release. All other uses and exposures related to cadmium are minor and similar in kind and magnitude to exposures from other materials in the broader PV value chain, e.g., to toxic gases, lead solder, or solvents (most of which are not used in CdTe manufacturing).

Price vulnerability

A subtle issue with CdTe and with all thin films in relation to greater efficiency PV module technologies is the potential impact of commodity inflation. Greater efficiency modules incur a better balance of system commodity cost per unit output. Thus such inflation can have a greater percentage impact on system cost. This is another reason that continued efficiency improvements are important.

Solar tracking

Almost all thin film photovoltaic module systems to-date have been non-solar tracking, because the output of modules has been too low to offset tracker capital and operating costs. But relatively inexpensive single-axis tracking systems can add 25% output per installed watt. This is climate-dependent. Tracking also produces a smoother output plateau around midday, allowing afternoon peaks to be met.

Market viability

Success of cadmium telluride PV has been due to the low cost achievable with the CdTe technology, made possible by combining adequate efficiency with lower module area costs. Direct manufacturing cost for CdTe PV modules reached $0.76 per watt in 2010, and capital cost per new watt of capacity is near $0.9 per watt (including land and buildings). However, module cost alone is not enough to assure the lowest installed system price. Thin films, including CdTe, are less efficient than most wafer silicon modules. Typical wafer silicon modules are 13% to 20% efficient, while the best CdTe modules were about 10.7% efficient; recent modules produced at First Solar and measured by NREL have shown CdTe modules with efficiencies at 12.5% or greater. Many components of an installed PV system (e.g., support structures, installation labor, land) scale with system area; and less-efficient modules require more area to produce the same output (all other things being equal). The impact of area-related costs on CdTe systems is about $0.5 per watt of extra cost.

Notable systems

Recent installations of large CdTe PV systems by First Solar confirm the competitiveness of CdTe PV with other forms of solar energy and how close it is to being competitive with conventional natural gas peakers:

1. A 40MW system being installed by juwi group in Waldpolenz Solar Park, Germany: at the time of its announcement, it was both the largest planned and lowest cost PV system in the world. The price of 3.25 euros translated then (when

the euro was equal to US$1.3) to $4.2/watt, much lower than any other known system.

2. A 7.5-megawatt system to be installed in Blythe, CA, where the California Public Utilities Commission has accepted a 12 US cent per kWh power purchase agreement with First Solar (after the application of all incentives). Defined in California as the "Market Referent Price," this is the price the PUC will pay for any daytime peaking power source, e.g., natural gas. Although PV systems are intermittent and not dispatchable the way natural gas is, natural gas generators have an ongoing fuel price risk that PV does not have.
3. A contract for two megawatts of rooftop installations with Southern California Edison, where the SCE program is designed to install 250 megawatts at a total cost of $875M (averaging $3.5/watt), after incentives.

Chapter- 13

Multi-junction Photovoltaic Cell

Multi-junction solar cells are solar cells containing several p-n junctions. This approach allows the cell to cover more of the light spectrum, but increases the complexity of cell design and manufacture.

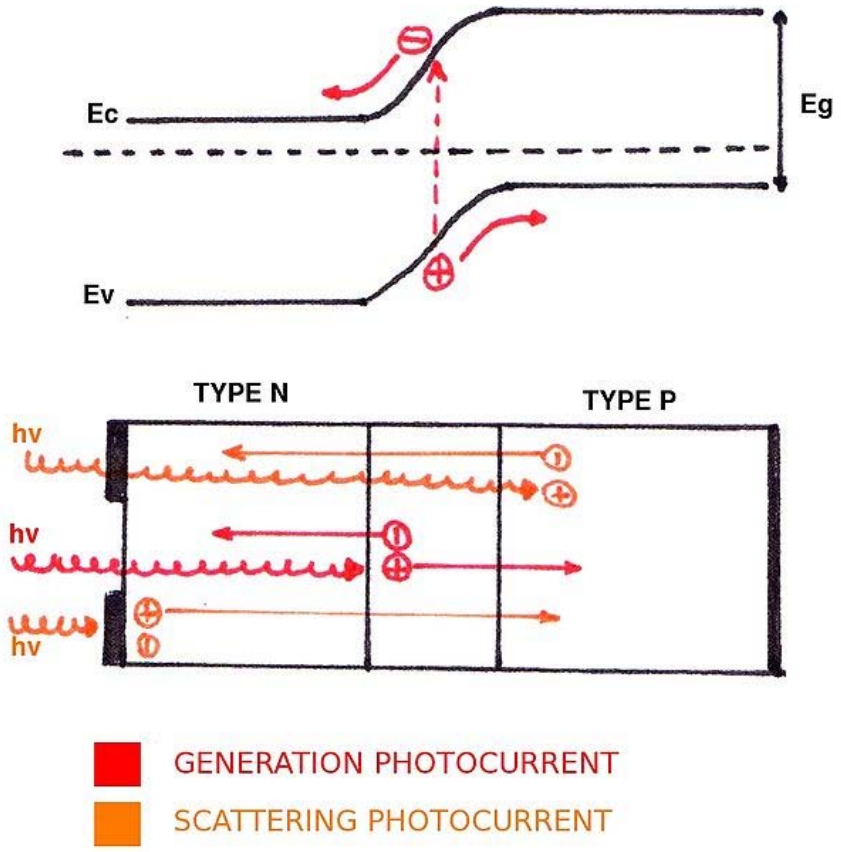

Figure A. Schematic illustration of the photovoltaic effect. Photons give their energy to electrons in the depletion or quasi-neutral regions. These move from conduction band to valence band. Depending of the location, electrons and holes are accelerated by E_{drift}, which gives generation photocurrent, or by E_{scatt}, which gives scattering photocurrent.

History

One of the most promising renewable energy technologies is photovoltaic solar panels which convert solar energy into electrical energy. The first solar cell was a crystalline silicon(c-Si) cell realised in 1954 by researchers at Bell Labs. It had an efficiency of 6%. The ensuing fifty years encompassed considerable progress photovoltaic technology and many different technologies emerged. As of 2010, commercial c-Si solar cells had reached a maximum efficiency of 24.7%. Multi-junction (MJ) solar cells had achieved 42.3% efficiency in laboratory settings as of October 2010 (with concentration at 406 suns.) MJ cells presents significant development potential because theoretical efficiency for an infinite number of pn junctions is 86.8%.

Basics of solar cells

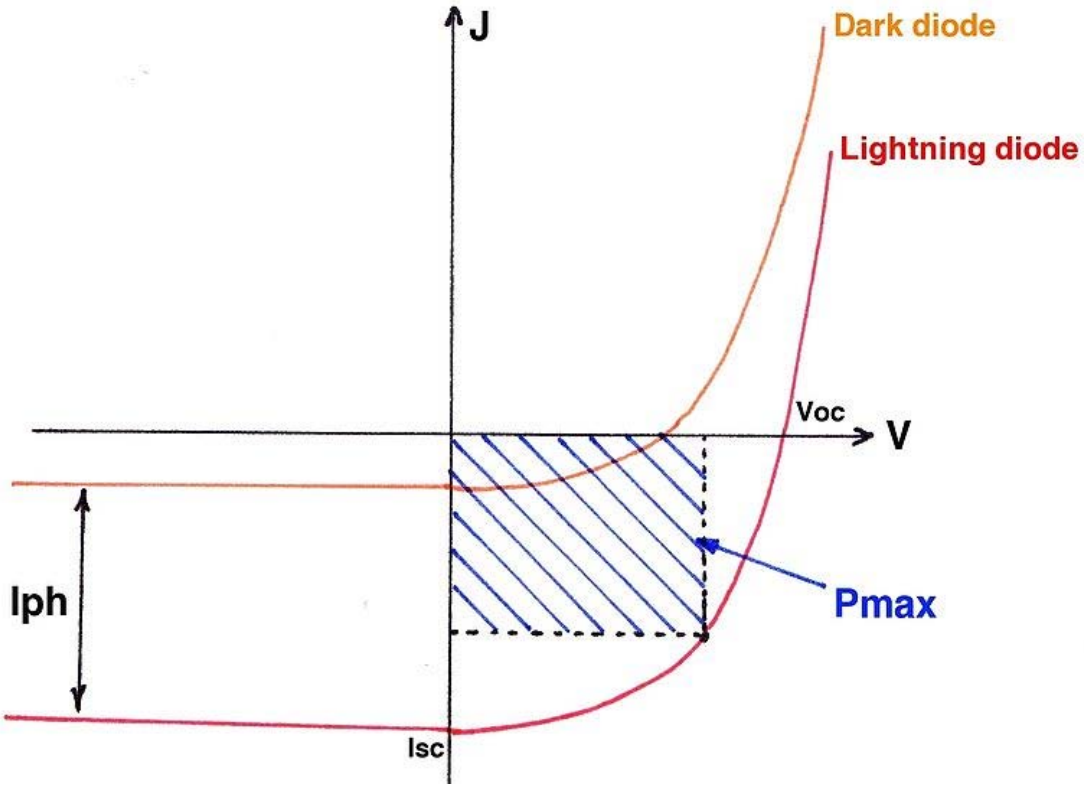

Figure B. Comparison between the J-V characteristics of a solar cell and a diode. The first one is obtained by moving downward the second one by the photocurrentI_{ph}.

Commercial photovoltaic panels are composed of several modules. Modules can be connected either inseries or in parallel and include numerous cells. These are composed of a pn junction made of doped silicon and metallic contacts. Photons that hit the top of the solar cell, are either reflected or transmitted. Transmitted photons give their energy hv to an electron. If $hv \geq E_g$, an electron/hole is generated. As shown in Figure A, electrons move from the valence band to the conduction band and holes appear in the valence band. In the depletion region, the drift electric field E_{drift}accelerates both electrons and holes

towards their respective n-doped and p-doped regions. The resultingcurrent I_g is called the generation photocurrent. In the quasi-neutral region, the scattering electric field E_{scatt} accelerates holes (electrons) towards the p-doped (n-doped) region, which gives a scattering photocurrent $I_{pscatt}(I_{nscatt})$. Consequently, due to the accumulation of charges, a potential V and a photocurrent I_{ph} appear. The expression for this photocurrent is obtained by adding generation and scattering photocurrents: $I_{ph} = I_g + I_{nscatt} + I_{pscatt}$.

The J-V characteristics (J is current density, i.e. current per area of pn junction) of a solar cell under illumination are simply obtained by shifting the J-V characteristics of a diode in the dark downward by I_{ph}, as shown in Figure B. Since solar cells are designed to supply power and not absorb it, the power $P = V \cdot I_{ph}$ must be negative. Hence, the operating point (V_m, J_m) is located in the region where $V>0$ and $I_{ph}<0$ are chosen so that they maximize the absolute value of the power $|P|$.

Physics

Single-junction cells

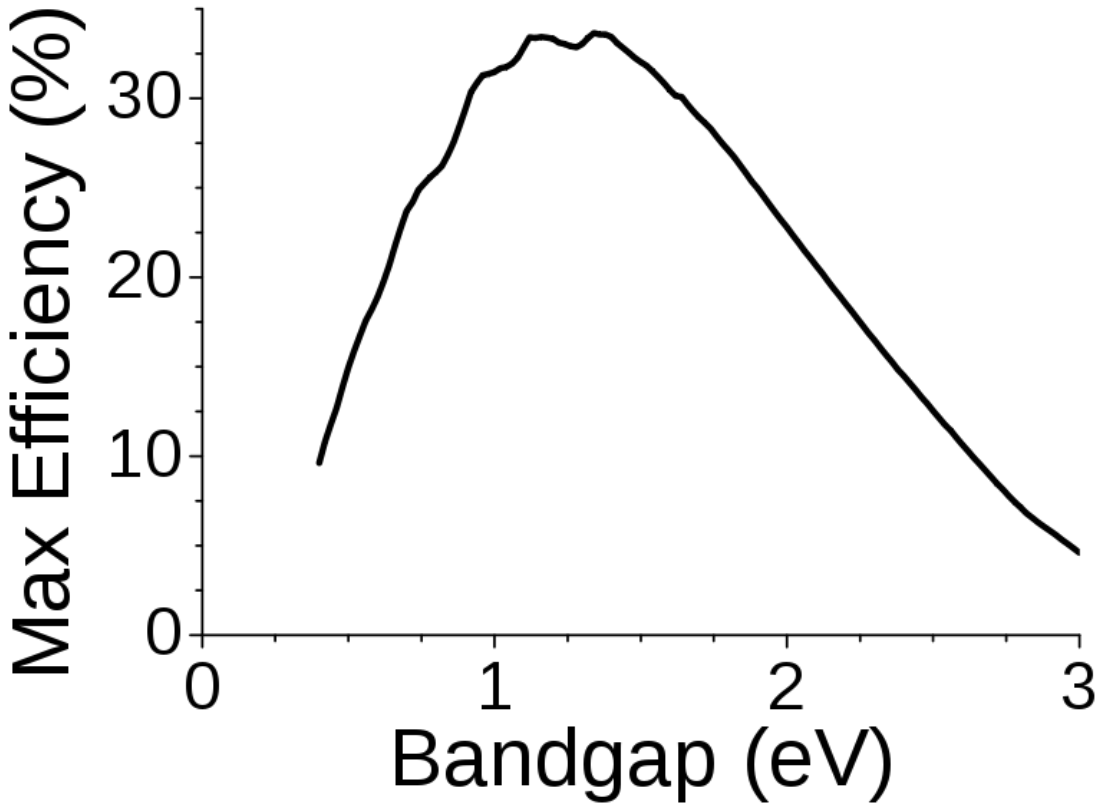

The Shockley-Queisser limit for the efficiency of a single-junction solar cell. It is essentially impossible for a single-junction solar cell, under unconcentrated sunlight, to have more than ~34% efficiency. A multijunction cell, however, can exceed that limit.

In a single band gap solar cell, efficiency is limited due to the inability to efficiently convert the broad range of energies that photons possess in the solar spectrum. Photons below the band gap of the cell material either pass through the cell or are converted to only heat within the material. Energy in the photons above the band gap energy is also lost, since only the energy necessary to generate the hole-electron pair is utilized, and the remaining energy is converted into heat.

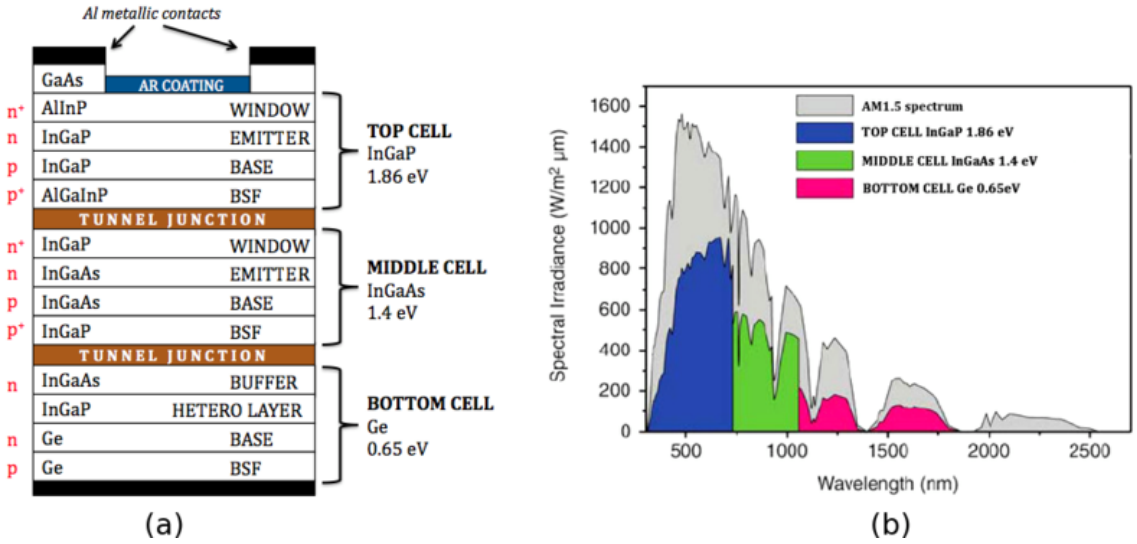

Figure C. (a) The structure of a MJ solar cell. There are six important types of layers: pn junctions, BSF layers, window layers, tunnel junctions, anti-reflective coating and metallic contacts. (b) Graph of spectral irradiance G vs. wavelength λ which shows the covering of the solar spectrum AM1.5.

Multi-junction cells

The fundamental difference between multi-junction solar cells and c-Si solar cells is the number of pn junctions connected in series, as illustrated on figure C(a). In order to better cover the solar spectrum AM1.5 (terrestrial reference spectrum for photovoltaic performance evaluation), suitable materials must be chosen for each pn junction.

The design must ensure that each material has a significantly different band gap E_g so that photons of different wavelength ($\lambda = hc/(eE_g) \approx 1.24\times10^{-6}/E_g$) are absorbed. The figure C(b) plots spectral irradiance $G(\lambda)$, which is the source power density at a given wavelength λ. Also, E_g must decrease from top cell to bottom cell so that the top cell does not absorb all the photons. Finally, the layers have to be electrically optimal for high performance and be stacked. This necessitates finding materials with better absorption coefficients $\alpha(\lambda)$, higher minority carrier lifetimes $\tau_{minority}$, higher mobilities μ and similar lattice constants *a*. The values in the table below justify the choice of the usual materials used for multi-junction solar cells: the top cell is generally made in InGaP (E_g = 1.86 eV), the middle cell in InGaAs (E_g= 1.4 eV) and the bottom cell in Germanium (E_g = 0.65 eV). The use of Ge is mainly due to its robustness, low cost and ease of production. In addition to the benefits listed above, the use of GaAs instead of Silicon allows higher

efficiencies because the efficiency of GaAs cells is 25.1% while the efficiency of c-Si cells is 24.7%.

Because the different layers are closely lattice-matched, the fabrication of the device typically employs metal-organic chemical vapor deposition (MOCVD). This technique is preferable to the molecular beam epitaxy (MBE) because it ensures high crystal quality and large scale production.

Material	E_g, eV	*a*, nm	absorption ($\lambda = 0.8$ µm), 1/µm	μ_n, cm²/(V·s)	τ_p, µs	Hardness (Mohs)	α, µm/K	*S*, m/s
c-Si	1.12	0.5431	0.102	1400	1	7	2.6	0.1–60
InGaP	1.86	0.5451	2	500	–	5	5.3	50
GaAs	1.4	0.5653	0.9	8500	3	4–5	6	50
Ge	0.65	0.5657	3	3900	1000	6	7	1000
InGaAs	1.2	0.5868	30	1200	–	–	5.66	100–1000

Structural elements

Metallic contacts

The metallic contacts in aluminium are low-resistivity electrodes that make contact with the semiconductor layer in GaAs. They are positioned on the two sides of the structure but mainly on the backwards face so that shadowing on the lightning surface is reduced.

Anti-reflective coating

Anti-reflective (AR) coating is generally composed of several layers in the case of MJ solar cells. The top AR layer has usually a NaOH surface texturation with several pyramids in order to increase the transmission coefficient *T*, the trapping of the light in the material (because photons cannot easily get out the MJ structure due to pyramids) and therefore, the path length of photons in the material. On the one hand, the thickness of each AR layer is chosen to get destructive interferences. Therefore, the reflection coefficient *R* decreases to 1%. In the case of two AR layers L_1 (the top layer, usually SiO_2) andL_2(usually [[TiO|2}}), there must be $n_{L2} = n_{AlInP}^{1/2} \cdot n_{L1}$to have the same amplitudes for reflected fields and $n_{L1}d_{L1} = 4\lambda_{min}$,$n_{L2}d_{L2} = \lambda_{min}/4$ to have opposite phase for reflected fields. On the other hand, the thickness of each AR layer is also chosen to minimize the reflectance at wavelengths for which the photocurrent is the lowest. Consequently, this maximizes J_{SC} by matching currents of the three subcells. As example, because the current generated by the bottom cell is greater than the currents generated by the other cells, the thickness of AR layers is adjusted so that the infrared (IR) transmission (which corresponds to the bottom cell) is degraded while the ultraviolet transmission (which corresponds to the top cell) is upgraded. Particularly, an AR coating

is very important at low wavelengths because, without it, *T* would be strongly reduced to 70%.

Tunnel junctions

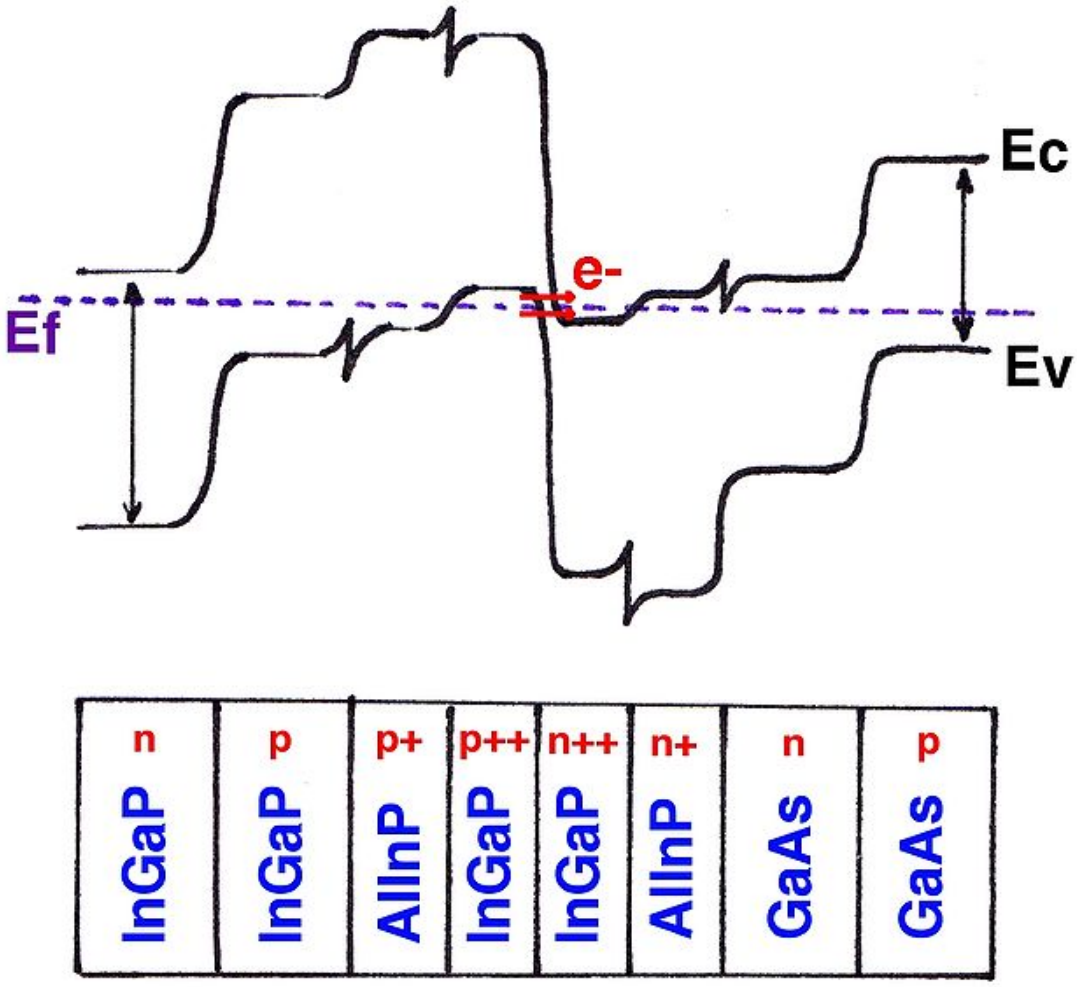

Figure D: Layers and band structure of the tunnel junction. Because the length of the depletion region is narrow and the band gap is high, electrons can tunneling.

The main goal of tunnel junctions is to provide a low electrical resistance and optically low-loss connection between two subcells. Without it, the p-doped region of the top cell would be directly connected with the n-doped region of the middle cell. Hence, a pn junction with opposite direction to the others would appear between the top cell and the middle cell. Consequently, the photovoltage would be lower than if there would be no parasiticdiode. In order to decrease this effect, a tunnel junction is used. It is simply a wide band gap, highly doped diode. The high doping reduces the length of the depletion region because

$$l_{depl} = \sqrt{\frac{2\epsilon(\phi_0 - V)}{q}\frac{N_A + N_D}{N_A N_D}}$$

Hence, electrons can easily tunnel through the depletion region. The J-V characteristic of the tunnel junction is very important because it explains why tunnel junctions can be used to have a low electrical resistance connection between two pn junctions. Figure D shows three different regions: the tunneling region, the negative differential resistance region and the thermal diffusion region. The region where electrons can tunnel through the barrier is called the tunneling region. There, the voltage must be low enough so that energy of some electrons who are tunneling is equal to energy states available on the other side of the barrier. Consequently, current density through the tunnel junction is high (with maximum value of J_P, the peak current density) and the slope near the origin is therefore steep. Then, the resistance is extremely low and consequently, the voltage too.. This is why tunnel junctions are ideal for connecting two pn junctions without having a voltage drop. When voltage is higher, electrons cannot cross the barrier because energy states are no longer available for electrons. Therefore, the current density decreases and the differential resistance is negative. The last region, called thermal diffusion region, corresponds to the J-V characteristic of the usual diode:

$$J = J_S(exp(\frac{qV}{kT}) - 1)$$

In order to avoid the reduction of the MJ solar cell performances, tunnel junctions must be transparent to wavelengths absorbed by the next photovoltaic cell, the middle cell, i.e. $E_{gTunnel} > E_{gMiddleCell}$.

Window layer and back-surface field

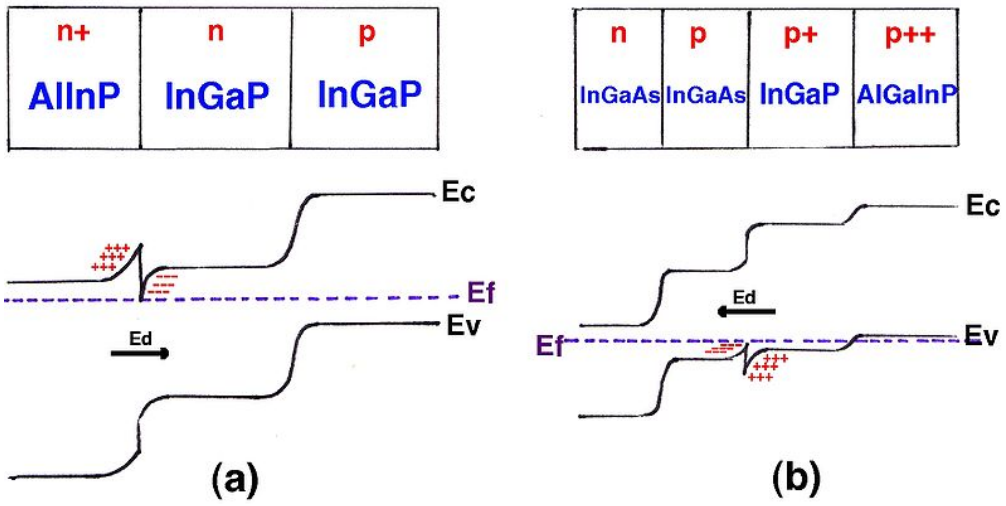

Figure E: (a) Layers and band structure of a window layer. The surface recombination is reduced. (b) Layers and band structure of a BSF layer. The scattering of carriers is reduced.

A window layer is used in order to reduce the surface recombination velocity *S*. Similarly, a back-surface field (BSF) layer reduces the scattering of carriers towards the tunnel junction. The structure of these two layers is the same: it is a heterojunction which catches electrons (holes). Indeed, despite the electric field E_d, these cannot jump above the barrier formed by the heterojunction because they don't have enough energy, as illustrated in figure E. Hence, electrons (holes) cannot recombine with holes (electrons) and cannot diffuse through the barrier. By the way, window and BSF layers must be transparent to wavelengths absorbed by the next pn junction i.e. $E_{gWindow} > E_{gEmitter}$ and $E_{gBSF} > E_{gEmitter}$. Furthermore, the lattice constant must be close to the one of InGaP and the layer must be highly doped ($n \geq 10^{18}$ cm^{-3}).

J-V characteristic

For maximum efficiency, each subcell should be operated at its optimal J-V parameters, which are not necessarily equal for each subcell. If they are different, the total current through the solar cell is the lowest of the three. By approximation, it results in the same relationship for the short-circuit current of the MJ solar cell: $J_{SC} = min\ (J_{SC1}, J_{SC2}, J_{SC3})$ where $J_{SCi}(\lambda)$ is the short-circuit current density at a given wavelength λ for the subcell *i*.

Because of the impossibility to obtain $J_{SC1}, J_{SC2}, J_{SC3}$ directly from the total J-V characteristic, the quantum efficiency $QE(\lambda)$ is utilized. It measures the ratio between the amount of electron-hole pairs created and the incident photons at a given wavelength λ. Let $\varphi_i(\lambda)$ be the photon flux of corresponding incident light in subcell *i*and$QE_i(\lambda)$ be the quantum efficiency of the subcell *i*. By definition, this equates to:

$$QE_i(\lambda) = \frac{J_{SCi}(\lambda)}{q\phi_i(\lambda)} \Rightarrow J_{SCi} = \int_0^{\lambda 2} q\phi_i(\lambda) QE_i(\lambda) d\lambda$$

The value of $QE_i(\lambda)$ is obtained by linking it with the absorption coefficient$\alpha(\lambda)$, i.e. the number of photons absorbed per unit of length by a material. If it is assumed that each photon absorbed by a subcell creates an electron/hole pair (which is a good approximation), this leads to :

$QE_i(\lambda) = 1 - e^{-\alpha(\lambda)d_i}$ where d_i is the thickness of the subcell *i* and $e^{-\alpha(\lambda)d_i}$ is the percentage of incident light which is not absorbed by the subcell *i*.

Similarly, because

$V = \sum_{i=1}^{3} V_i$ $\qquad$ $V_{OC} = \sum_{i=1}^{3} V_{OCi}$, the following approximation can be used: .

The values of V_{OCi} are then given by the J-V diode equation:

$$J_i = J_{0i}(e^{\frac{qV_i}{kT}} - 1) - J_{SCi} \Rightarrow V_{OCi} \approx \frac{kT}{q} ln(\frac{J_{SCi}}{J_{0i}})$$

Materials

Gallium arsenide substrate

Dual junction cells can be made on Gallium arsenide wafers. Alloys of Indium gallium phosphide in the range $In_{.5}Ga_{.5}P$ through $In_{.53}Ga_{.47}P$ serve as the high band gap alloy. This alloy range provides for the ability to have band gaps in the range of 1.92eV to 1.87eV. The lower GaAs junction has a band gap of 1.42eV.

Germanium substrate

Triple junction cells consisting of Indium gallium phosphide, Gallium arsenide or Indium gallium arsenide and Germanium can be fabricated on germanium wafers. Early cells used straight gallium arsenide in the middle junction. Later cells have utilized $In_{0.015}Ga_{0.985}As$, due to the better lattice match to Ge, resulting in a lower defect density.

Due to the huge band gap difference between GaAs (1.42eV), and Ge (0.66eV), the current match is very poor, with the Ge junction operated significantly current limited.

Current efficiencies for InGaP/GaAs/Ge cells are in the mid 30% range. Lab cells using additional junctions between the GaAs and Ge junction have demonstrated efficiencies above 40%.

Indium phosphide substrate

Indium phosphide may be used as a substrate to fabricate cells with band gaps between 1.35eV and 0.74eV. Indium Phosphide has a band gap of 1.35eV. Indium gallium arsenide($In_{0.53}Ga_{0.47}As$) is lattice matched to Indium Phosphide with a band gap of 0.74eV. A quaternary alloy of Indium gallium arsenide phosphide can be lattice matched for any band gap in between the two.

Indium phosphide-based cells have the potential to work in tandem with gallium arsenide cells. The two cells can be optically connected in series (with the InP cell below the GaAs cell), or in parallel through the use of spectra splitting using a Dichroic filter.

Performance improvements

Structure

All photovoltaic cells use III-V semiconductor materials. GaAsSb-based heterojunction tunnel diodes, instead of conventional InGaP highly doped tunnel diodes described above, have a lower tunneling distance. Indeed, in the heterostructure formed by GaAsSb and InGaAs, the valence band of GaAsSb is higher than the valence band of the adjoining p-doped layer. Consequently, the tunneling distance d_{tunnel} is reduced and so the tunneling current, which exponentially depends of d_{tunnel}, is increased. Hence, the voltage is lower than that of the InGaP tunnel junction. GaAsSb heterojunction tunnel diodes offer other advantages. The same current can be achieved by using a lower doping. Secondly, because the lattice constant is larger for GaAsSb than Ge, one can use a wider range of materials for the bottom cell because more materials are lattice-matched to GaAsSb than to Ge.

Chemical components can be added to some layers. Adding about one percent of Indium in each layer better matches lattice constants of the different layers. Without it, there is about 0.08 percent of mismatching between layers, which inhibits performance. Adding aluminium to the top cell increases its band gap to 1.96 eV, covering a larger part of the solar spectrum and obtain a higher open-circuit voltage V_{OC}.

The theoretical efficiency of MJ solar cells is 86.8% for an infinite number of pn junctions, implying that more junctions increase efficiency. The maximum theoretical efficiency is 37, 50, 56, 72% for 1, 2, 3, 36 pn junctions, respectively, with the number of junctions increasing exponentially to achieve equal effiency increments. The exponential relationship implies that as the cell approaches the limit of efficiency, the increase cost and complexity grow rapidly. Decreasing the thickness of the top cell increases the transmission coefficient T.

Finally, an InGaP hetero-layer between the p-Ge layer and the InGaAs layer can be added in order to create automatically the n-Ge layer by scattering during MOCVD growth and increase significantly the quantum efficiency $QE(\lambda)$ of the bottom cell. InGaP is advantageous because of its high scattering coefficient and low solubility in Ge.

Spectral variations

Solar spectrum at the Earth surface changes constantly depending on the weather and sun position. This results in the variation of $\varphi(\lambda)$, $QE(\lambda)$, $\alpha(\lambda)$ and thus the short-circuit currents J_{SCi}. As a result, the current densities J_i are not necessarily matched and the total current becomes lower. These variations can be quantified using the average photon energy (APE) which is the ratio between the spectral irradiance $G(\lambda)$ (the power density of the light source in a specific wavelength λ) and the total photon flux density. It can be shown that a high (low) value for APE means low (high) wavelengths spectral conditions and higher (lower) efficiencies. Thus APE is a good indicator for quantifying the effects

of the solar spectrum variations on performances and has the added advantage of being independent of the device structure and the absorption profile of the device.

Use of light concentrators

Light concentrators increase efficiencies and reduce the cost/efficiency ratio. The two types of light concentrators are refractive lenses like Fresnel lenses and reflective dishes. Thanks to these devices, light arriving on a large surface can be concentrated on a smaller cell. The intensity concentration ratio (or "suns") is the average intensity of the focused light divided by 0.1 W/m². If its value is *X* then the MJ current becomes *X* higher under concentrated illumination.

Comparison with other technologies

There are four main categories of photovoltaic cells: c-Si solar cells, thin film solar cells, MJ solar cells and new technologies (including organic solar cells).

Technology	**η (%)**	**V_{OC} (V)**	**I_{SC} (A)**	**W/m²**	**t (µm)**
u c-Si	24.7	0.5	0.8	63	100
p c-Si	20.3	0.615	8.35	211	200
a-Si	11.1	6.3	0.0089	33	1
CdTe	16.5	0.86	0.029	–	5
CIGS	19.5	–	–	–	1
MJ	40.7	2.6	1.81	476	140

MJ solar cells and other photovoltaic devices have significant differences. Physically, the main property of a MJ solar cell is having more than one pn junction in order to catch a larger photon energy spectrum while the main property of the thin film solar cell is to use thin films instead of thick layers in order to decrease the cost efficiency ratio. As of 2010, MJ solar panels are more expensive than others. These differences imply different applications: MJ solar cells are preferred in space and c-Si solar cells for terrestrian applications.

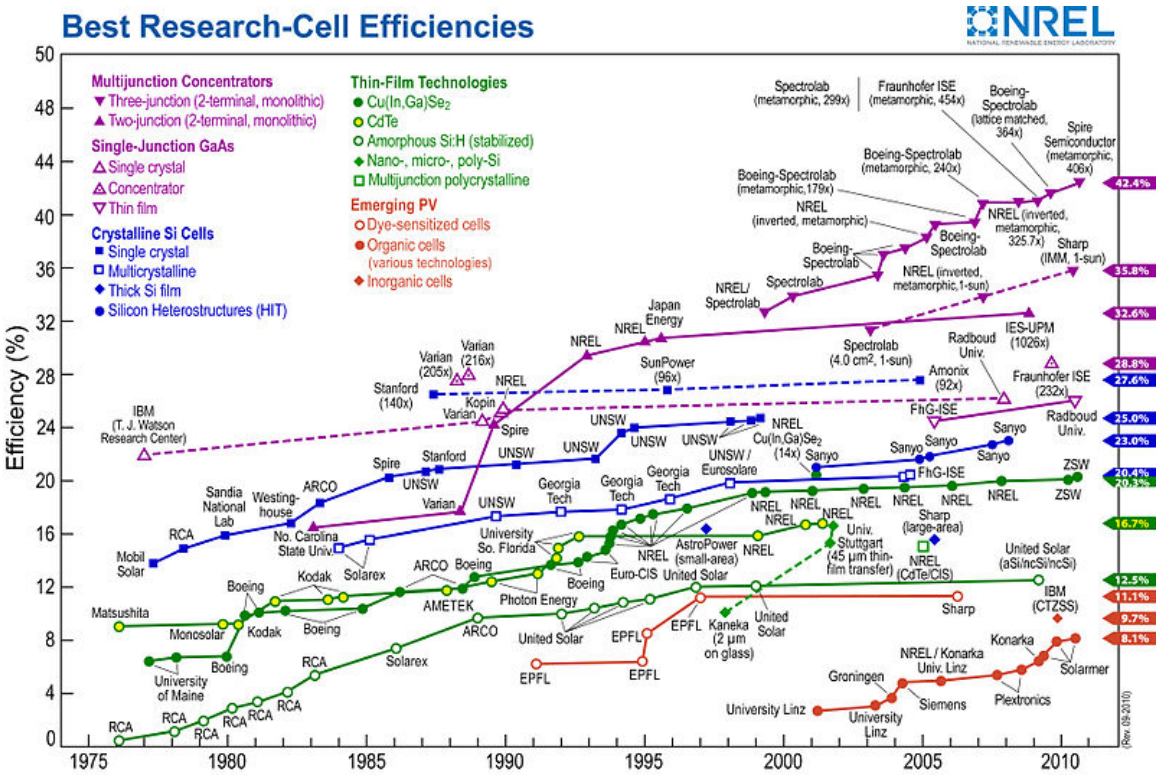

The efficiencies of solar cells and Si solar technology are relatively stable, while the efficiency of solar modules and multi-junction technology are progressing.

Measurements on MJ solar cells are usually made in laboratory, using light concentrators (this is often not the case for the other cells) and under standard test conditions (STCs). STCs prescribe, for terrestrial applications, the AM1.5 spectrum as the reference. This air mass (AM) corresponds to a fixed position of the sun in the sky of 48° and a fixed power of 833 W/m². Therefore, spectral variations of incident light and environmental parameters are not taken into account under STC.

Consequently, performance of MJ solar cells in terrestrial environment is inferior to that achieved in laboratory. Moreover, MJ solar cells are designed such that currents are matched under STC, but not necessarily under field conditions. One can use $QE(\lambda)$ to compare performances of different technologies, but $QE(\lambda)$ contains no information on the matching of currents of subcells. An important comparison point is rather the output power per unit area generated with the same incident light.

Applications

As of 2010, the cost of MJ solar cells was too high to allow use outside of specialized applications. The high cost is mainly due to the complex structure and the high price of materials. Nevertheless, with light concentrators under illumination of at least 400 suns, MJ solar panels become practical.

MJ cells are currently being utilized in the Mars rover missions.

The environment in space is quite different. Because there is no atmosphere, the solar spectrum is different (AM0). The cells have a poor current match due to a greater photon flux of photons above 1.87eV vs. those between 1.87eV and 1.42eV. This results in too little current in the GaAs junction, and hampers the overall efficiency since the InGaP junction operates below MPP current and the GaAs junction operates above MPP current. To improve current match, the InGaP layer is intentionally thinned to allow additional photons to penetrate to the lower GaAs layer.

In terrestrial concentrating applications, the scatter of blue light by the atmosphere reduces the photon flux above 1.87eV, better balancing the junction currents.Radiation particles that are no longer filtered can cause damage the cell. There are two kinds of damage: ionisation and atomic displacement. Still, MJ cells offer higher radiation resistance, higher efficiency and a lower temperature coefficient.

Chapter- 14

Quantum Dot Solar Cell

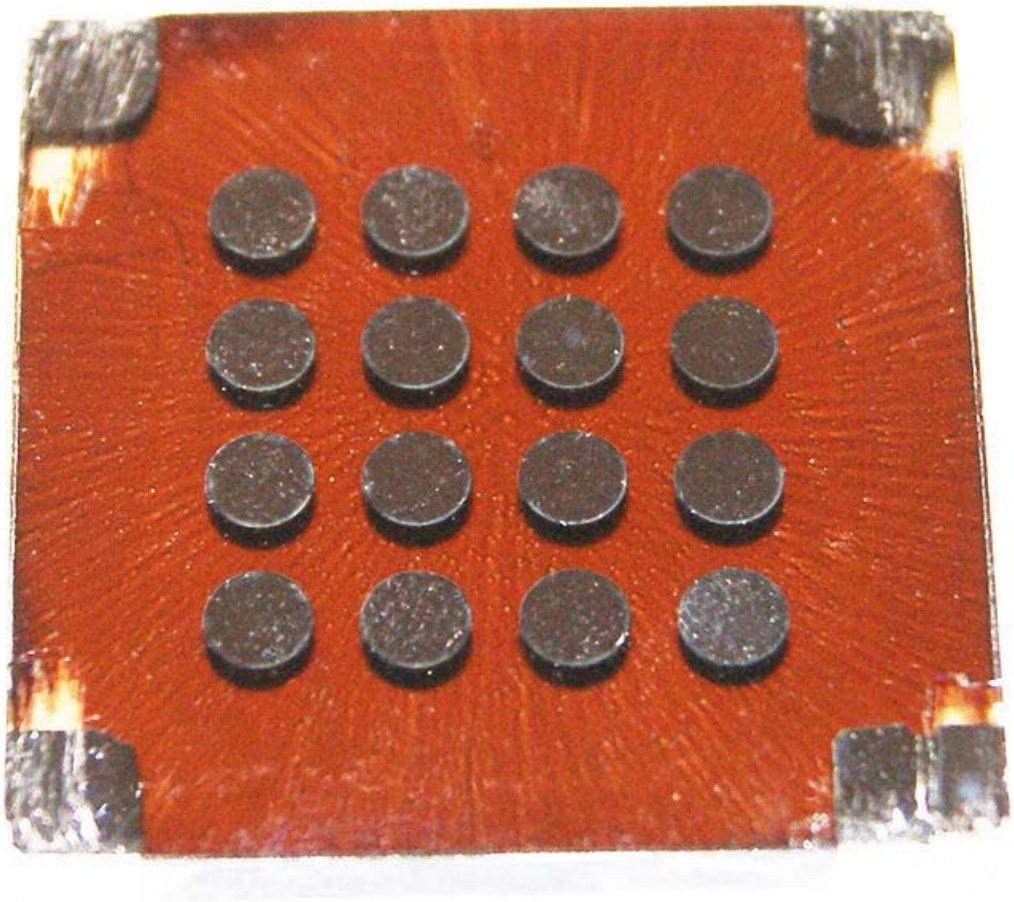

Spin-cast quantum dot solar cell built by the Sargent Group at the University of Toronto. The metal disks on the front surface are the electrical connections to the layers below.

Quantum dot solar cells are an emerging field in solar cell research that uses quantum dots as the photovoltaic material, as opposed to better-known bulk materials such as silicon, copper indium gallium selenide (CIGS) or CdTe. Quantum dots have bandgaps

that are tunable across a wide range of energy levels by changing the quantum dot size. This is in contrast to bulk materials, where the bandgap is fixed by the choice of material composition. This property makes quantum dots attractive for multi-junction solar cells, where a variety of different energy levels are used to extract more power from the solar spectrum.

The potential performance of the quantum dot approach has led to widespread research in the field. Early examples used costly molecular beam epitaxy processes, but alternative inexpensive fabrication methods have been developed. These attempts rely on quantum dot synthesis using wet chemistry (colloidal quantum dots – CQDs) and subsequent solution processibility of quantum dots. CQD solar cells currently hold the performance record for quantum dot solar cells. Their efficiency of 5.1% is yet low compared to that of commercial bulk silicon cells (about 17%), but it has a potential for improvement.

Background

Basic solar cell concepts

In a conventional solar cell, light is absorbed by a semiconductor producing an electron-hole (e-h) pair. This pair is separated by an internal electric field and the resulting flow of electrons and holes creates electric current. The internal electric field is created by doping one part of semiconductor with atoms which act as electron donors (n-type doping) and another with electron acceptors (p-type doping) that results in a p-n junction. Generation of e-h pair requires that the photons of light have energy exceeding the bandgap of the material. Whereas photons with lower energies produce negligible amount of e-h pairs, higher energy photons are relatively inefficient: they produce an energetic e-h pair which quickly (within about 10^{-13} s) loses its energy through collisions with the lattice ("thermalizes"). As a result, most photon energy is lost into heat that lowers the conversion efficiency of light into electricity. The detailed balance calculation shows that this efficiency can not exceed 31% if one uses a single material for a solar cell.

Numerical analysis shows that the 31% efficiency is achieved when the solar cell material has a bandgap of 1.13 eV, corresponding to light in the near infrared. This band gap nearly matches that of silicon (1.1 eV), one of the many reasons this material dominates solar cell production. It is possible to greatly improve on a single-junction cell by stacking extremely thin cells with different bandgaps on top of each other – the "tandem cell" or "multi-junction" approach. The same basic analysis shows that a two layer cell should have one layer tuned to 1.64 eV and the other at 0.94 eV, with a theoretical performance of 44%. A three-layer cell should be tuned to 1.83, 1.16 and 0.71 eV, with an efficiency of 48%. An "infinity-layer" cell would have a theoretical efficiency of 86%, with other loss mechanisms accounting for the rest.

Traditional silicon preparation methods do not lend themselves to this approach. There has been some progress using thin-films of amorphous silicon, but other issues have prevented these from matching the performance of traditional cells. Most tandem-cell structures are based on higher performance semiconductors, notably gallium arsenide

(GaAs). Three-layer InGaAs/GaAs/InGaP cells (bandgaps 1.89/1.42/0.94 eV) hold the efficiency record of 42.3% for experimental examples.

Quantum dots

Quantum dots are particles of semiconductor material with the size so small that, due to quantum mechanics considerations, the electron energies that can exist within them are limited. These energy levels, defined by the size of quantum dots, in turn define the bandgaps. The dots can be grown to any needed size, allowing them to be tuned across a wide variety of bandgaps without changing the underlying material or construction techniques. In typical preparations, the tuning is accomplished by varying the duration or temperature of synthesis

The ability to tune the bandgap is what makes them desirable for solar cell use. In this respect they are similar to the existing expensive GaAs tandem cells, and in theory have efficiencies on the same order. But CQDs can improve this further. In particular, lead sulfide (PbS) CQDs have bandgaps that can be tuned into the far infrared, energy levels that are normally unseen to traditional materials. Half of all the solar energy reaching the Earth is in the infrared, most of it in the near infrared region. With a quantum dot solar cell, IR-sensitive materials are just as easy to use as any other, opening the possibility of capturing much more energy cost-effectively.

Moreover, CQDs are far easier to make than GaAs materials, and in some cases even simpler than traditional silicon. When suspended in a colloidal liquid form they can be easily handled throughout production, with the most complex equipment needed being a fume hood while the solvents outgas. The entire production process takes place at room temperature or on a hotplate, dramatically reducing handling issues and energy input. Although the base semiconductor material might require a complex preparation before being made into dots, even then the material does not have to be produced in large blocks, significantly reducing operational costs. Although current production is limited and the materials are relatively expensive, the price should be significantly reduced in mass production. The dots can be distributed on a substrate through spin coating, either by hand or in an easily automated process. In large-scale production this technique could be replaced by spray-on or roll-printing systems, which dramatically reduces module construction costs.

Current research

Early concepts

The idea of using quantum dots as a path to high efficiency was first noted by Burnham and Duggan in 1990. At the time, the science of quantum dots, or "wells" as they were known, was in its infancy and early production examples were just becoming available.

DSSC efforts

Another modern cell design is the dye-sensitized solar cell, or DSSC. DSSCs use a sponge-like layer of TiO_2 as the semiconductor valve as well as a mechanical support structure. During construction, the sponge is filled with an organic dye, typically ruthenium-polypyridine, which provides the electrons. This dye is relatively expensive, and ruthenium is a rare metal. Another drawback of the design is that it requires direct contact between the dye molecules suspended in the film and the rear electrode to return electrons to the dye. In most designs, this is handled by a liquid electrolyte between the two, making the design susceptible to leakage and freezing. Finally, in order for the energy levels to work out, the front electrode has to be transparent. Such electrode is usually made of indium tin oxide (ITO), which is fragile and contains expensive indium metal.

Quantum dots as an alternative to the molecular dyes was considered from the earliest days of DSSC research. The ability to tune the bandgap means the designer can select a wider variety materials for other portions of the cell. The collaborating groups from the University of Toronto and École Polytechnique Fédérale de Lausanne developed a new design based on a rear electrode directly in contact with a film of quantum dots, eliminating the electrolyte and forming a depleted heterojunction. To date these cells have reached reached 5.1% efficiency, comparable to the best solid-state DSSC devices, but still below those based on liquid electrolytes.

Multi-junction efforts

During this period, other teams were working with nanocrystals of other semiconductors, notably cadmium telluride (CdTe). A colloidal suspension of these crystals is spin-cast onto a suitable substrate, often a thin glass slide, potted in a conductive polymer. These did not use quantum dots, but had a number of features in common with them. In particular, the method of casting a thin layer of crystals would work just as well as with quantum dots, and the use of a thin film conductor would both be applicable with few changes. In low scale production quantum dots are more expensive to form than mass producing of nanocrystals, but the crystals are based on rare metals that are already subject to major price swings, whereas a wide variety of materials can be used to make suitable dots.

Experiments using a variety of CQDs materials with spin-casting techniques started at the Sargent Group in the mid-2000s. In one noteworthy experiment, the group used lead selenide as an infrared-sensitive electron donor to produce the highest-efficiency IR solar cells ever built. The true advantage of this technique, however, is that it yields the prospect of combining the quantum dots inherent tunability with a simple manufacturing process to allow the construction of "tandem" cells of greatly reduced cost. The cells use a rear layer of gold as an electrode, but recent experiments have shown that nickel works just as well. This would greatly reduce the cost of the system in large-scale production.

Hot-carrier capture

Another way to improve efficiency is to capture the extra energy in the electron when emitted from a single-bandgap material. In traditional materials like silicon, the distance from the emission site to the electrode where they are harvested is too far to allow this to occur; the electron will undergo many interactions with the crystal materials and lattice, giving up this extra energy as heat. There was great hope in the 1980s that thin films of silicon or other materials would avoid this, and capture some of this extra energy. These films are amorphous, and in practice the defects that are inherent to these materials overwhelmed this advantage. Modern thin-film cells are generally less efficient than traditional silicon.

In the case of quantum dots, or other nanostructured donors, it is possible to cast cells as uniform films that avoid the problems with defects. These would still be subject to other issues inherent to quantum dots in general, notably resistivity issues and heat retention. It appears there has been little active development along these lines.

Multiple exciton generation

In 2005, the National Renewable Energy Laboratory in Golden, Colorado reported a spectroscopic evidence that several excitons could be efficiently generated upon absorption of a single, energetic photon in a quantum dot. This opens up the possibility of a different approach to the same problems that tandem cells attempt to solve, capturing more of the energy in highly energetic visible photons in sunlight. In this approach, known as "multiple exciton generation" (MEG), the quantum dot is tuned to release multiple electrons at a lower energy instead of one high-energy electron. This increases the cell efficiency. The dots in NRELs example where made from lead sulfide.

In 2010, a team at the University of Wyoming demonstrated similar performance using cells based on the DCCS design. In their examples, PbS quantum dots demonstrated two-electron ejection when the incoming photons had about three times the base bandgap energy.

NREL maintains an active research effort developing silicon-based quantum dots. In order to become cost effective, any new solar cell design will have to compete with the existing silicon industry. Silicon is plentiful and inexpensive in bulk form, it is only the processing that makes it expensive. If quantum dots with suitable properties can be made from silicon, they can compete on a cost basis. In 2007, NREL demonstrated that MEG occurs in silicon quantum dots as well as in the PbS dots.

Other issues

Although research is still at a pre-commercialization stage, in the future quantum dot based photovoltaics may offer advantages such as mechanical flexibility (as in quantum dot-polymer composite photovoltaics) as well as low cost, clean power generation and an efficiency of 65%.

One concern for any QD-based approach is the buildup of heat in the dots. A key to the dots operation is their natural isolation from the surrounding material, but this means that phonons are highly reflected off the interface. This process would lead to heat buildup within the dots.

Other third generation solar cells

- Photoelectrochemical cell
- Polymer solar cell

Chapter- 15

Polymer Solar Cell

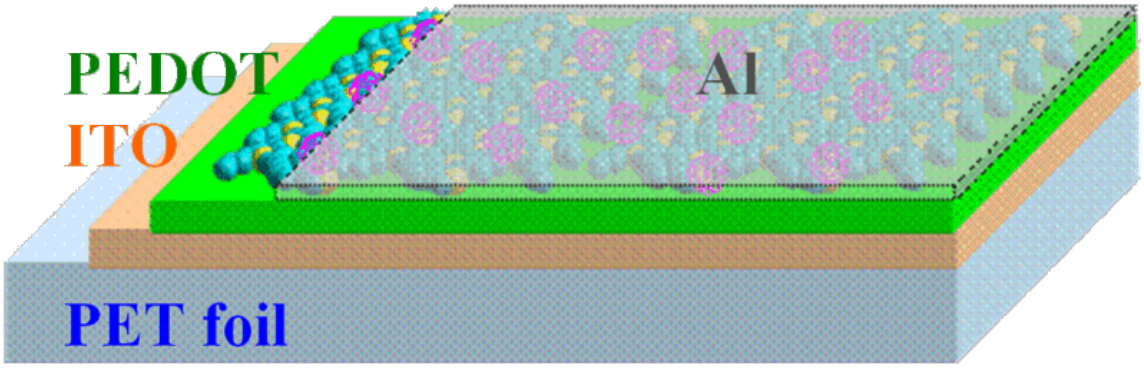

Polymer solar cells are a type of flexible solar cell. They can come in many forms including: organic solar cell (also called plastic solar cell), or organic chemistry photovoltaic cell that produce electricity from sunlight using polymers. There are also other types of more stable thin-film semiconductors that can be deposited on different types of polymers to create solar cells. This technology is relatively new, being actively researched by universities, national laboratories and several companies around the world.

Currently, commercial solar cells are made from a refined, highly purified silicon crystal, similar to the material used in the manufacture of integrated circuits and computer chips (wafer silicon). The high cost of these silicon solar cells, and their complex production process has generated interest in developing alternative photovoltaic technologies.

Compared to silicon-based devices, polymer solar cells are lightweight (which is important for small autonomous sensors), potentially disposable and inexpensive to fabricate (sometimes using printed electronics), flexible, and customizable on the molecular level, and they have lower potential for negative environmental impact. An example device is shown in Fig. 1. The disadvantages of polymer solar cells are also serious: they offer about 1/3 of the efficiency of hard materials, and they are relatively unstable toward photochemical degradation. For these reasons, despite continuing advances in semiconducting polymers, the vast majority of solar cells rely on inorganic materials.

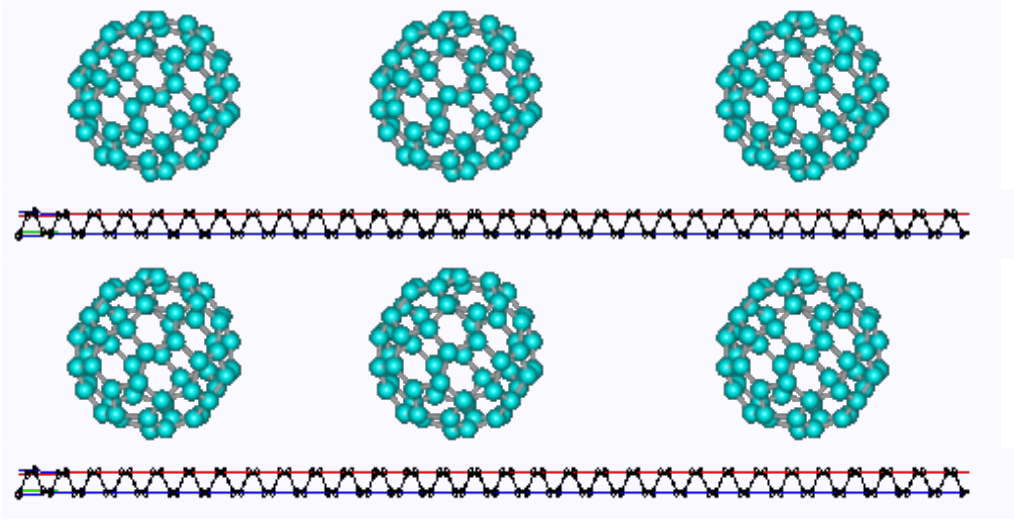

Fig. 2. Polymer chain with diffusing polaron surrounded by fullerene molecules

Device physics

The following discussion is based primarily on Mayer et al.'s review, cited below. Organic photovoltaics are made of electron donor and electron acceptor materials rather than semiconductor p-n junctions. The molecules forming the electron donor region of organic PV cells, where exciton electron-hole pairs are generated, are generally conjugated polymers possessing delocalized π electrons that result from carbon p orbital hybridization. These π electrons can be excited by light in or near the visible part of the spectrum from the molecule's highest occupied molecular orbital (HOMO) to the lowest unoccupied molecular orbital (LUMO), denoted by a π -π* transition. The energy bandgap between these orbitals determines which wavelength of light can be absorbed.

Unlike in an inorganic crystalline PV cell material, with its band structure and delocalized electrons, excitons in organic photovoltaics are strongly bound with an energy between 0.1 and 1.4 eV. This strong binding occurs because electronic wavefunctions in organic molecules are more localized, and electrostatic attraction can thus keep the electron and hole together as an exciton. The electron and hole can be dissociated by providing an interface across which the chemical potential of electrons decreases. The material that absorbs the photon is the donor, and the material acquiring the electron is called the acceptor. In Fig. 2, the polymer chain is the donor and the fullerene is the acceptor. After dissociation has taken place, the electron and hole may still be joined as a geminate pair and an electric field is then required to separate them.

After exciton dissociation, the electron and hole must be collected at contacts. However, charge carrier mobility now begins to play a major role: if mobility is not sufficiently high, the carriers will not reach the contacts, and will instead recombine at trap sites or remain in the device as undesirable space charges that oppose the drift of new carriers. The latter problem can occur if electron and hole mobilities are highly imbalanced, such

that one species is much more mobile than the other. In that case, space-charge limited photocurrent (SCLP) hampers device performance.

As an example of the processes involved in device operation, organic photovoltaics can be fabricated with an active polymer and a fullerene-based electron acceptor. The illumination of this system by visible light leads to electron transfer from the polymer chain to a fullerene molecule. As a result, the formation of a photoinduced quasiparticle, or polaron (P^+), occurs on the polymer chain and the fullerene becomes an ion-radical C_{60}^- Polarons are highly mobile along the length of the polymer chain and can diffuse away. Both the polaron and ion-radical possess spin S= ½, so the charge photoinduction and separation processes can be controlled by the Electron Paramagnetic Resonance method.

Architectures

This is derived largely from Mayer's review, referenced below. The simplest architecture that may be used for an organic PV device is a planar heterojunction, shown in Fig. 1. A film of active polymer (donor) and a film of electron acceptor are sandwiched between contacts in a planar configuration. Excitons created in the donor region may diffuse to the junction and separate, with the hole remaining behind and the electron passing into the acceptor. However, planar heterojunctions are inherently inefficient; because charge carriers have diffusion lengths of just 3-10 nm in typical organic semiconductors, planar cells must be thin to enable successful diffusion to contacts, but the thinner the cell, the less light it can absorb.

Bulk heterojunctions (BHJs) address this shortcoming. In a BHJ, the electron donor and acceptor materials are blended together and cast as a mixture that then phase-separates. Regions of each material in the device are separated by only several nanometers, a distance optimized for carrier diffusion. Although devices based on BHJs are a significant improvement over planar designs, BHJs require sensitive control over materials morphology on the nanoscale. A great number of variables, including choice of materials, solvents, and the donor-acceptor weight ratio can dramatically affect the BHJ structure that results. These factors can make rationally optimizing BHJs difficult.

The next logical step beyond BHJs are ordered nanomaterials for solar cells, or ordered heterojunctions (OHJs). This paradigm eliminates much of the variability associated with BHJs. OHJs are generally hybrids of ordered inorganic materials and organic active regions. For example, a photovoltaic polymer can be deposited into pores in a ceramic such as TiO_2. Holes still must diffuse along the length of the pore through the polymer to a contact, so OHJs do have thickness limitations. Mitigating the hole mobility bottleneck will thus be key to further enhancing OHJ device performance, but controlling morphology inside the confines of the pores is challenging.

Engineers at the University of California, San Diego (UCSD) have employed "nanowires" to boost the efficiency of organic solar cells.

Conclusion

At the moment, an open question is to what degree polymer solar cells can commercially compete with silicon solar cells and the other thin-film cells. The silicon solar cell industry has the important industrial advantage of being able to leverage the infrastructure developed for the computer industry. Besides, the present efficiency of polymer solar cells lies near 10 percent, much below the value for silicon cells. Polymer solar cells also suffer from environmental degradation. Good protective coatings are still to be developed.

Still, organic PV devices show great promise for decreasing the cost of solar energy to the point where it may become widespread in the decades ahead. While great progress has been made in the last ten years with respect to understanding the chemistry, physics, and materials science of organic photovoltaics, work remains to be done to further improve their performance. Specifically, novel nanostructures must be optimized to promote charge carrier diffusion; transport must be enhanced through control of order and morphology; and interface engineering must be applied to the problem of charge transfer across interfaces. Novel molecular chemistries and materials offer hope for revolutionary, rather than evolutionary, breakthroughs in device efficiencies in the future.

Current commercial status

For the reasons described above, polymer solar cells are not generally produced commercially today. One exception is the company Konarka Technologies, which in 2008 opened a factory with the capacity to produce a gigawatt's worth of polymer-fullerene solar cells each year. The initial cells from the factory are 3-5% efficient, and only last a couple years, but the company has stated that it would eventually be able to improve both the efficiency and durability. The company expects to initially sell the cells for a number of niche applications, such as in laptop-recharging briefcases; put into tents, umbrellas, and awnings; and as window tinting (since the cells can be made semi-transparent).

Other third generation solar cells

- Dye-sensitized solar cell
- Hybrid solar cell
- Nanocrystal solar cell
- Photoelectrochemical cell

Chapter- 16

Ellipsometry

A commercial ellipsometer

Ellipsometry is a versatile and powerful optical technique for the investigation of the dielectric properties (complex refractive index or dielectric function) of thin films.

It has applications in many different fields, from semiconductor physics to microelectronics and biology, from basic research to industrial applications. Ellipsometry is a very sensitive measurement technique and provides unequalled capabilities for thin

film metrology. As an optical technique, spectroscopic ellipsometry is non-destructive and contactless.

Upon the analysis of the change of polarization of light, which is reflected off a sample, ellipsometry can yield information about layers that are thinner than the wavelength of the probing light itself, even down to a single atomic layer. Ellipsometry can probe the complex refractive index or dielectric function tensor, which gives access to fundamental physical parameters and is related to a variety of sample properties, including morphology, crystal quality, chemical composition, or electrical conductivity. It is commonly used to characterize film thickness for single layers or complex multilayer stacks ranging from a few angstroms or tenths of a nanometer to several micrometers with an excellent accuracy.

The name "ellipsometry" stems from the fact that the most general state of polarization is elliptic. The technique has been known for almost a century, and has many standard applications today. However, ellipsometry is also becoming more interesting to researchers in other disciplines such as biology and medicine. These areas pose new challenges to the technique, such as measurements on unstable liquid surfaces and microscopic imaging.

Basic principles

Ellipsometry measures the change of polarization upon reflection or transmission. Typically, ellipsometry is done only in the reflection setup. The exact nature of the polarization change is determined by the sample's properties (thickness, complex refractive index or dielectric function tensor). Although optical techniques are inherently diffraction limited, ellipsometry exploits phase information and the polarization state of light, and can achieve angstrom resolution. In its simplest form, the technique is applicable to thin films with thickness less than a nanometer to several micrometers. **The sample must be composed of a small number of discrete, well-defined layers that are optically homogeneous and isotropic.** Violation of these assumptions will invalidate the standard ellipsometric modeling procedure, and more advanced variants of the technique must be applied.

Experimental details

Experimental setup

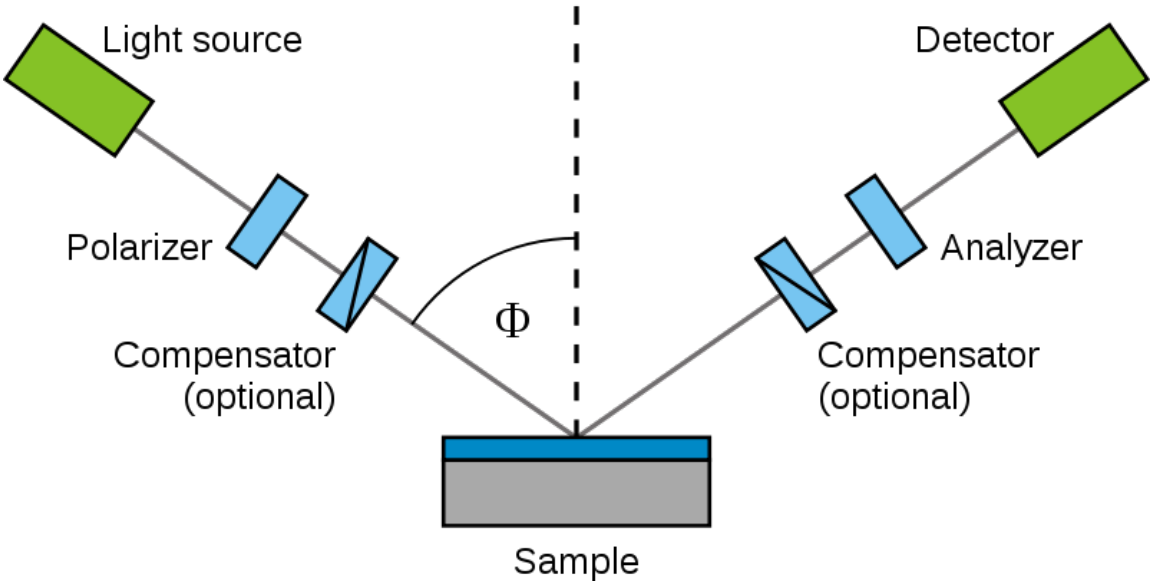

Schematic setup of an ellipsometry experiment.

Electromagnetic radiation is emitted by a light source and linearly polarized by a polarizer. It can pass through an optional compensator (retarder, quarter wave plate) and falls onto the sample. After reflection the radiation passes a compensator (optional) and a second polarizer, which is called an analyzer, and falls into the detector. Instead of the compensators some ellipsometers use a phase-modulator in the path of the incident light beam. Ellipsometry is a specular optical technique (the angle of incidence equals the angle of reflection). The incident and the reflected beam span the *plane of incidence*. Light which is polarized parallel to this plane is named *p-polarized* (p-polarised). A polarization direction perpendicular is called *s-polarized* (s-polarised), accordingly. The *"s"* is contributed from the German *"senkrecht"* (perpendicular).

Data acquisition

Ellipsometry measures the complex reflectance ratio, ρ, of a system, which may be parametrized by Ψ and Δ. The polarization state of the light incident upon the sample may be decomposed into an *s* and a *p* component (the *s* component is oscillating perpendicular to the plane of incidence and parallel to the sample surface, and the *p* component is oscillating parallel to the plane of incidence). The amplitudes of the *s* and *p* components, after reflection and normalized to their initial value, are denoted by r_s and r_p, respectively. Ellipsometry measures the complex reflectance ratio, ρ (a complex quantity), which is the ratio of r_p over r_s:

$$\rho = \frac{r_p}{r_s} = \tan(\Psi)e^{i\Delta}$$

Thus, tan(Ψ) is the amplitude ratio upon reflection, and Δ is the phase shift (difference). (Note that the right hand side of the equation is simply another way to represent a complex number.) Since ellipsometry is measuring the ratio (or difference) of two values (rather than the absolute value of either), it is very robust, accurate, and reproducible. For instance, it is relatively insensitive to scatter and fluctuations, and requires no standard sample or reference beam.

Data analysis

Ellipsometry is an indirect method, i.e. in general the measured Ψ and Δ cannot be converted directly into the optical constants of the sample. Normally, a model analysis must be performed. Direct inversion of Ψ and Δ is only possible in very simple cases of isotropic, homogeneous and infinitely thick films. In all other cases a layer model must be established, which considers the optical constants (refractive index or dielectric function tensor) and thickness parameters of all individual layers of the sample including the correct layer sequence. Using an iterative procedure (least-squares minimization) unknown optical constants and/or thickness parameters are varied, and Ψ and Δ values are calculated using the Fresnel equations. The calculated Ψ and Δ values which match the experimental data best provide the optical constants and thickness parameters of the sample.

Definitions

Single-wavelength vs. spectroscopic ellipsometry

Single-wavelength ellipsometry employs a monochromatic light source. This is usually a laser in the visible spectral region, for instance, a HeNe laser with a wavelength of 632.8 nm. Therefore, single-wavelength ellipsometry is also called laser ellipsometry. The advantage of laser ellipsometry is that laser beams can be focused on a small spot size. Furthermore, lasers have a higher power than broad band light sources. Therefore, laser ellipsometry can be used for imaging. However, the experimental output is restricted to one set of Ψ and Δ values per measurement. Spectroscopic ellipsometry (SE) employs broad band light sources, which cover a certain spectral range in the infrared, visible or ultraviolet spectral region. By that the complex refractive index or the dielectric function tensor in the corresponding spectral region can be obtained, which gives access to a large number of fundamental physical properties. Infrared spectroscopic ellipsometry (IRSE) can probe lattice vibrational (phonon) and free charge carrier (plasmon) properties. Spectroscopic ellipsometry in the near infrared, visible up to ultraviolet spectral region studies the refractive index in the transparency or below-band-gap region and electronic properties, for instance, band-to-band transitions or excitons.

Standard vs. generalized ellipsometry (anisotropy)

Standard ellipsometry (or just short 'ellipsometry') is applied, when no *s* polarized light is converted into *p* polarized light nor vice versa. This is the case for optically isotropic samples, for instance, amorphous materials or crystalline materials with a cubic crystal

structure. Standard ellipsometry is also sufficient for optically uniaxial samples in the special case, when the optical axis is aligned parallel to the surface normal. In all other cases, when *s* polarized light is converted into *p* polarized light and/or vice versa, the generalized ellipsometry approach must be applied. Examples are arbitrarily aligned, optically uniaxial samples, or optically biaxial samples.

Jones matrix vs. Mueller matrix formalism (Depolarization)

There are typically two different ways of describing mathematically, how an electromagnetic wave interacts with the elements within an ellipsometer (including the sample), the Jones matrix and the Mueller matrix formalism. In the Jones matrix formalism the electromagnetic wave is described by a Jones vector with two orthogonal complex-valued entries for the electric field (typically E_x and E_y), and the effect that an optical element (or sample) has on it is described by the complex-valued 2x2 Jones matrix. In the Mueller matrix formalism the electromagnetic wave is described by Stokes vectors with four real-valued entries, and their transformation is described by the real-valued 4x4 Mueller matrix. When no depolarization occurs both formalisms are fully consistent. Therefore, for non-depolarizing samples the simpler Jones matrix formalism is sufficient. If the sample is depolarizing the Mueller matrix formalism should be used, because it gives additionally access to the amount of depolarization. Reasons for depolarization are, for instance, thickness non-uniformity or backside-reflections from a transparent substrate.

Advanced experimental approaches

Imaging ellipsometry

Ellipsometry can also be done as imaging ellipsometry by using a CCD camera as a detector. This provides a real time contrast image of the sample, which provides information about film thickness and refractive index. Advanced imaging ellipsometer technology operates on the principle of classical null ellipsometry and real-time ellipsometric contrast imaging, using a single-wavelength ellipsometer setup with a laser as light source. The laser beam gets elliptically polarized after passing a linear polarizer (P) and a quarter-wave plate (C). The elliptically polarized light is reflected off the sample (S), passes an analyzer (A) and is imaged onto a CCD camera by a long working distance objective. In this PCSA configuration, the orientation of the angles of P and C is chosen in such a way that the elliptically polarized light is completely linearly polarized after it is reflected off the sample. The ellipsometric null condition is obtained when A is perpendicular with respect to the polarization axis of the reflected light achieving complete destructive interference, i.e., the state at which the absolute minimum of light flux is detected at the CCD camera. The angles of P, C, and A that obtained the null condition are related to the optical properties of the sample. Analysis of the measured data with computerized optical modeling leads to a deduction of spatially resolved film thickness and complex refractive index values.

In situ ellipsometry

In situ ellipsometry refers to dynamic measurements during the modification process of a sample. This process can be, for instance, the growth of a thin film, etching or cleaning of a sample. By in situ ellipsometry measurements it is possible to determine fundamental process parameters, such as, growth or etch rates, variation of optical properties with time. In situ ellipsometry measurements require a number of additional considerations: The sample spot is usually not as easily accessible as for ex situ measurements outside the process chamber. Therefore, the mechanical setup has to be adjusted, which can include additional optical elements (mirrors, prisms, or lenses) for redirecting or focusing the light beam. Because the environmental conditions during the process can be harsh, the sensitive optical elements of the ellipsometry setup must be separated from the hot zone. In the simplest case this is done by optical view ports, though strain induced birefringence of the (glass-) windows has to be taken into account or minimized. Furthermore, the samples can be at elevated temperatures, which implies different optical properties compared to samples at room temperature. Despite all these problems, in situ ellipsometry becomes more and more important as process control technique for thin film deposition and modification tools. In situ ellipsometers can be of single-wavelength or spectroscopic type. Spectroscopic in situ ellipsometers use multichannel detectors, for instance CCD detectors, which measure the ellipsometric parameters for all wavelength in the studied spectral range simultaneously.

Ellipsometric Porosimetry

Ellipsometric porosimetry measures the change of the optical properties and thickness of the materials during adsorption and desorption of a volatile species at atmospheric pressure or under reduced pressure depending on the application. The EP technique is unique in its ability to measure porosity of very thin films down to 10 nm, its reproducibility and speed of measurement. Compared to traditional porosimeters, Ellipsometer porosimeters are well suited to very thin film pore size and pore size distribution measurement. Film porosity is a key factor in silicon based technology using low-k materials, organic industry (encapsulated organic light-emitting diodes) as well as in the coating industry using sol gel techniques.

Magneto-optic generalized ellipsometry

Magneto-optic generalized ellipsometry (MOGE) is an advanced infrared spectroscopic ellipsometry technique for studying free charge carrier properties in conducting samples. By applying an external magnetic field it is possible to determine independently the density, the optical mobility parameter and the effective mass parameter of free charge carriers. Without the magnetic field only two out of the three free charge carrier parameters can be extracted independently.

Advantages

Ellipsometry has a number of advantages compared to standard reflection intensity measurements:

- Ellipsometry measures at least two parameters at each wavelength of the spectrum. If generalized ellipsometry is applied up to 16 parameters can be measured at each wavelength.
- Ellipsometry measures an intensity ratio instead of pure intensities. Therefore, ellipsometry is less affected by intensity instabilities of the light source or atmospheric absorption.
- No reference measurement is necessary.
- Both real and imaginary part of the dielectric function (or complex refractive index) can be extracted without the necessity to perform a Kramers–Kronig analysis.

Ellipsometry is especially superior to reflectivity measurements when studying anisotropic samples.